

Author Shantanu Ganesh Kulkarni

Title Adamantane based multitopic guests and their binding properties

Supervisor Mgr. Robert Vícha, PhD

Consultant Ing. Lenka Dastychová, PhD

Acknowledgement

I would like to express the deepest appreciation to my supervisor Dr. Robert Vícha, who has the attitude and the substance of a genius: he continually and convincingly conveyed a spirit of adventure in regard to research and scholarship. Without his guidance and persistent help this dissertation would not have been possible.

I take this opportunity to say thanks to Ing. Michal Rouchal, PhD, head of the department of chemistry for his consistent support throughout my tenure in UTB and prompt efforts in providing ESI-MS spectra. I am thankful to Ing. Zdenka Pruckova, PhD, for her efforts to perform isothermal titration calorimetry time to time. I would like to say thanks to Ing. Lenka Dastychova, PhD, for her help and support during my stay in UTB. I am grateful to the department of chemistry and the management of Tomas Bata University in Zlin for their consistent support during my stay in Zlin.

Without saying thanks to my lab mates it would not be impossible to conclude the acknowledgement. Their continuous help and friendship made my stay pleasant in Zlin. I will miss them all.

Last but not least, I want to say thanks to my father Prof. Ganesh Kulkarni and my younger sister Shweta, whose constant encouragement and support made everything possible.

The financial support of this work by Internal Funding Agency of Tomas Bata University (IGA/FT/2016/001, IGA/FT/2015/006, IGA/FT/2014/002, and IGA/FT/2013/008) is also appreciated.

Shantanu Ganesh Kulkarni
Zlin, Czech Republic

Table of Contents

Abstract.....	6
Abbreviations.....	6
1 General information.....	11
2 Brief historic overview of cyclodextrins.....	11
3 Industrial applications of cyclodextrins and toxicity studies.....	12
3.1 Inclusion and non-inclusion complexes.....	12
3.2 Solution behavior of cyclodextrin aggregates.....	13
3.3 Drug availability and cyclodextrins in dispersed systems.....	13
3.4 Toxicity study and regulatory affairs.....	13
3.5 Polyrotaxanes from cyclodextrins and linear polymers.....	14
4 Cucurbiturils.....	15
4.1 Synthesis and purification of CBs.....	15
4.2 Physical properties and cucurbituril cavity parameters.....	17
4.3 Catalysis using CB[n] cavity.....	17
4.3.1 1,3-dipolar cycloadditions.....	17
4.3.2 Oxidation.....	18
4.3.3 Hydrolysis.....	18
4.3.4 Metal ion assisted catalysis.....	19
4.3.5 Photochemical reactions with CB[n].....	20
4.4 Chiral applications.....	21
5 Supramolecular applications of cyclodextrins.....	23
5.1 Case binding studies.....	23
5.2 Advanced bioorganic systems.....	24
5.3 Biomedical applications of CD-drug complexes.....	25
5.3.1 Modified cyclodextrins.....	25
5.3.2 Delivery of insoluble drugs.....	26
5.3.3 Oral applications.....	26
5.3.4 Ophthalmic applications.....	27
5.3.5 Nasal applications.....	27
5.4 Supramolecular nanocarriers.....	27
5.4.1 Vesicles.....	28
5.4.2 Micelles.....	28
5.4.3 Supramolecular nanoparticles.....	29
5.4.3.1 Rotaxane and polyrotaxane based nanoparticles.....	29
5.4.3.2 Host-guest interaction induced nanoparticles.....	29
5.4.3.3 Host-guest nanohybrids.....	30
5.4.3.3.1 On-off switch on nanoparticles.....	30
5.4.3.3.2 Other nanohybrids.....	31
5.5 Supramolecular hydrogels.....	31
5.6 Gene delivery.....	32
5.6.1 Supramolecular nanoparticles for gene delivery.....	33
5.6.2 Rotaxanes/polyrotaxanes for gene delivery.....	34
5.6.3 Other host-guest gene delivery systems.....	34
5.7 Drug/gene delivery multifunctional nanoparticles.....	34
5.8 Bioimaging.....	35
6 Supramolecular applications of cucurbiturils.....	35
6.1 Analytical applications using fluorescence spectrometry.....	35
6.2 Biomedical applications.....	36

6.2.1	Supramolecular nanocarriers	36
6.2.1.1	Vesicles	36
6.2.1.2	Micelles.....	37
6.2.1.3	Supramolecular nanoparticles.....	37
6.2.1.3.1	On-off switch on nanoparticles.....	37
6.2.1.3.2	Other nanohybrids with host-guest interactions	37
6.2.1.3.3	Supramolecular hydrogels	38
6.3	Bioimaging.....	38
7	Adamantane: History, structure and binding properties	39
7.1	Historic overview of adamantane chemistry.....	40
7.2	Biological activity of 1-adamantanamine	40
7.3	Abundance of 1-monosubstituted and 2-monosubstituted adamantane.....	41
7.4	Binding ability of adamantane cage.....	41
8	Synthesis of desired guests	43
8.1	Apparatus and method	43
8.1.1	Chemicals and solvents.....	43
8.1.2	Instruments.....	43
8.1.3	Electrospray mass spectrometry	43
8.1.4	Isothermal titration calorimetry	44
8.2	Guests with trisubstituted centerpiece	44
8.2.1	Synthesis of compound 1.....	44
8.2.2	Synthesis of compound 2.....	44
8.2.3	Synthesis of compound 3.....	45
8.2.4	Synthesis of compound 4.....	45
8.2.5	Synthesis of compound 5.....	46
8.2.6	Synthesis of compound 6.....	46
8.3	Guests with disubstituted centerpiece.....	47
8.3.1	Synthesis of compound 7.....	47
8.3.2	Synthesis of compound 8.....	48
8.3.3	Synthesis of compound 9 from 8.....	48
8.3.4	Synthesis of compound 10.....	49
8.3.5	Synthesis of compound 11.....	49
8.3.6	Synthesis of compound 12.....	50
8.3.7	Synthesis of compound 13.....	50
8.3.8	Synthesis of compound 14.....	51
8.3.9	Synthesis of compound 9 from 14.....	51
8.3.10	Synthesis of compound 15.....	52
8.3.11	Synthesis of compound 16.....	52
8.3.12	Synthesis of compound 17.....	53
8.3.13	Synthesis of compound 18.....	54
8.3.14	Synthesis of compound 19.....	54
8.4	Synthesis of quaternary ammonium salts	55
8.4.1	Synthesis of compound 20.....	55
8.4.2	Synthesis of compound 21.....	56
8.4.3	Synthesis of compound 22.....	57
8.4.4	Synthesis of compound 23.....	58
8.4.5	Synthesis of compound 24.....	58
9	Tetratopic guests	61
9.1	Synthesis of tetratopic guests.....	61
9.1.1	Attempted synthesis by Ullmann or Suzuki coupling.....	61

9.1.2	Reduction first approach	62
9.1.3	Coupling via iodonium salt	63
9.1.4	Synthesis of tetratopic spacers 65 and 69	63
10	Tritopic guests.....	66
10.1	Synthesis of tritopic guests	66
10.1.1	Failed synthesis of quaternary ammonium salts from 25	66
10.1.2	Alternate strategy with different leaving group	66
10.1.3	Alternate strategy with quaternization in last step	67
10.1.4	Synthesis of tritopic guests with TBMB centerpiece.....	68
10.2	Supramolecular studies of tripod guests 4 and 6	68
10.2.1	Binary systems	69
10.2.2	Ternary systems	71
10.2.3	Mass spectrometry	73
11	Ditopic guests.....	74
11.1	Attempted synthesis of 1,2-diphenylethene and 1,2-diphenylethyne centerpieces ..	74
11.1.1	Synthesis of compound 42	75
11.1.2	Synthesis of compound 44	75
11.1.3	Synthesis of compound 45	76
11.2	Alternate strategy towards benzimidazolium derived centerpiece	77
11.3	Synthesis of imidazolium compounds	79
11.4	Synthesis of methyl and adamantyl salts from 17	81
11.5	Binding studies of the guests with stilbene centerpiece.....	83
11.5.1	Binding properties of (<i>Z</i>)- 20	83
11.5.2	(<i>E</i>)/(<i>Z</i>) interconversion of guests 20 and 21	87
11.6	Synthesis of 1,2-diphenylacetylene spacer	89
11.7	Synthesis of benzimidazolium salts with diphenylacetylene centerpiece.....	89
11.8	Binding studies of the guests with diphenylacetylene centerpiece	92
11.8.1	Binding properties of guest 22	92
11.8.2	Binding properties of guest 24	93
11.8.3	Binding properties of guest 23	97
Conclusion	101
References	103
Curriculum vitae	110

Abstract

Host-guest chemistry is very interesting phenomena in supramolecular chemistry. Inclusion complexes which are formed by non-covalent interactions between suitable hosts and guests have several applications. Formation of polymeric aggregates for drug storage, transport, and releasing is one of the most intriguing area. Properties of such systems, which components are bound together via supramolecular interaction, can be efficiently driven by chemical signals. Because of high application potential in pharmacology and/or medicine, new multitopic guest are needed for designing and formation of complex supramolecular systems. Seven new multitopic guests including two tritopic and five ditopic guests were prepared and studied. The main reason to make these guests was to study the ability of these compounds to form inclusion complexes with hosts such as cyclodextrins and cucurbiturils. In order to make these compounds, several synthetic approaches were used. The tritopic guest compounds were prepared in satisfactory yield by coupling 1,3,5-tris(bromomethyl)benzene with 1-(1-adamantylmethyl)-1*H*-benzo[*d*]imidazole and 1-(1-adamantylmethyl)-1*H*-imidazole, respectively. Ditopic guests were prepared by Wittig reaction of corresponding aldehydes with imidazole/benzimidazole substituent and benzimidazolium/imidazolium phosphorous ylides followed by quaternization with different alkyl halides. These guests were studied for their binding ability towards cucurbiturils and cyclodextrins. Two tritopic guests were able to form 1:3 inclusion complexes with β -CD and CB[7]. They also formed ternary aggregates with β -CD and CB[7] in ratios 1:1:2 and 1:2:1. The two families of ditopic guests were prepared differing in central part of the guest molecules. The first family was derived from 4,4'-disubstituted stilbene whereas the molecules of guests from the second family contained a 4,4'-disubstituted diphenylacetylene centerpiece. The stilbene guest with terminal methyl substituents **20** was obtained as (*E*)/(*Z*) isomeric mixture. It was separated into (*E*)-**20** and (*Z*)-**20** isomers by using their significantly different solubility in MeOH:CHCl₃ system. The geometry of the (*Z*)-**20** was confirmed by X-ray diffraction analysis. Binding study of ditopic guest molecule (*Z*)-**20** with β -CD showed inclusion of the guest in the β -CD cavity in such a way that the stilbene centerpiece is positioned inside the β -CD cavity and two benzimidazolium moieties occupy the opposite cyclodextrin portals. This complex displayed slow exchange mode on the NMR timescale. The positioning of one benzimidazolium core in the narrow β -CD caused locking of the rotation of the half of the molecule while the second half remained free in its rotating being positioned in the wider β -CD rim. The guests with diphenylacetylene centerpiece showed poor solubility but still two of the guests were studied for their binding ability. Finally, the complex of β -CD with the guest with terminal methyl substituents showed switching of the exchange mode from slow to fast in response to addition of non-polar solvents. The most important and interesting result was, that the influence of MeOH, DMSO, and AcMe was significantly different. Namely, MeOH did not influence the mode of the exchange whereas other two solvents did.

These interesting results justify further research on the new presented guests. Particularly, the behaviour in the complex supramolecular systems consisting of polymeric components will be studied.

Abbreviations

ABZ	abendazole
BER	berberine
BNEAH	<i>N</i> -benzyl-1-(1-naphthyl)ethylamine
Bu	butyl
CD	cyclodextrin
CMD	carboxymethyl dextran
CME- β -CD	<i>O</i> -carboxymethyl- <i>O</i> -ethyl- β -cyclodextrin
[C _n mim]Br	1-methyl-3-(C _n)alkylimidazolium bromide
[C ₄ mim]Br	1-butyl-3-methylimidazolium bromide
CPT	camptothecin
DCM	dichloromethane
DHA	1,4-dihydroxyanthraquinone
DIBAL-H	diisobutylaluminium hydride
DLS	dynamic light scattering
DMAE	dimethylaminoethyl
DM- β -CD	dimethyl- β -cyclodextrin
DMF	<i>N,N</i> -dimethyl formamide
DMSO	dimethyl sulfoxide
DNA	deoxyribose nucleic acid
Dox	doxorubicin
EMS	electromagnetic spectrum
ESI-MS	electrospray ionization mass spectrometry
Et	ethyl
FDA	food and drug administration
FITC	fluorescein isothiocyanate
GC-MS	gas chromatography mass spectroscopy
Glc	glucose
GFX	gemifloxin
HP- β -CD	hydroxylpropyl- β -cyclodextrin
HPG	hyperbranched polyglycerol
IR	infrared

IR RAS	infrared reflection-absorption spectroscopy
Me	methyl
mRNA	messenger ribose nucleic acid
MSNPs	mesoporous silica nanoparticles
MTT	3-(4,5-dimethylthiazol-2-yl)-2,5-diphenyltetrazolium bromide
MTX	methotrexate
NIPAAM	<i>N</i> -isopropylacrylamide
NMR	nuclear magnetic resonance
[Npmim]Br	1-methyl-3-(2-naphthyl)imidazolium bromide
PAL	palmitate
PAAm	polyacrylamide
PAA-C12-Azo	poly(acrylic acid)aminododecane- <i>p</i> - azobenzene aminosuccinic acid
PAAPBA	polyacrylamidophenyl boronic acid
PAMAM	polyamidoamine
PBLA	polybenzyl-L-aspartate
PDMAEMA	polydimethylaminomethyl methacrylate
PEI	polyethylenimine
PEG	polyethylene glycol
PMMA	polymethyl methacrylate
PNI-PAM	methylviologen terminated poly- <i>N</i> -isopropyl acrylamide
PNIPAAm	poly- <i>N</i> -isopropyl acrylamide
PPG	polypropylene glycol
PVA	polyvinyl alcohol
QCMD	quartz crystal microbalance with dissipation
QD	quantum dots
RNA	ribose nucleic acid
SBE- β -CD	sulfobutylether- β -cyclodextrin
SEM	scanning electron microscope
siRNA	small interfering ribose nucleic acid
TBMB	1,3,5-tris(bromomethyl)benzene
TBZ	thiabendazole
TEM	transmission electron microscopy

TLC	thin layer chromatography
THF	tetrahydrofuran
TMSPA	trimethylsilylpropargyl acrylate
UDCA	ursodeoxycholic acid

Introduction

1 General information

Within last few decades, scientific community has prepared complex supramolecular systems which have shown some interesting applications in various fields. Apart from micelles, dendritic polymers and membrane vesicles, hydrogels have been prepared for the purposes like storage and release of active compounds influenced by external conditions such as light, temperature, pH etc.¹⁻⁸ Construction of host-guest systems is one of the important aspect in this area.⁹ Insoluble compounds can be made more soluble by making their supramolecular host-guest complexes with compounds such as cyclodextrins and cucurbiturils. Cyclodextrins and cucurbiturils possess hydrophobic inner cavity and hydrophilic outer rim. The famous approach is to trap the water poorly soluble compound inside this cavity to deliver this complex inside the body so that drug molecule can easily reach to the target. Cavity size of each member of cucurbituril and cyclodextrin family is different. So, many compounds with different sizes can be selectively trapped inside their cavity.

I have tried to summarize the physical properties, synthesis, purification, and applications of the cucurbiturils and cyclodextrins in following text.

2 Brief historic overview of cyclodextrins

Cyclodextrins (CDs) are the cyclic molecules made up of glucose (Glc) units. The most important natural CDs are of the three types, namely α , β , and γ depending on the number of Glc units. Their structures are depicted in Figure 1.

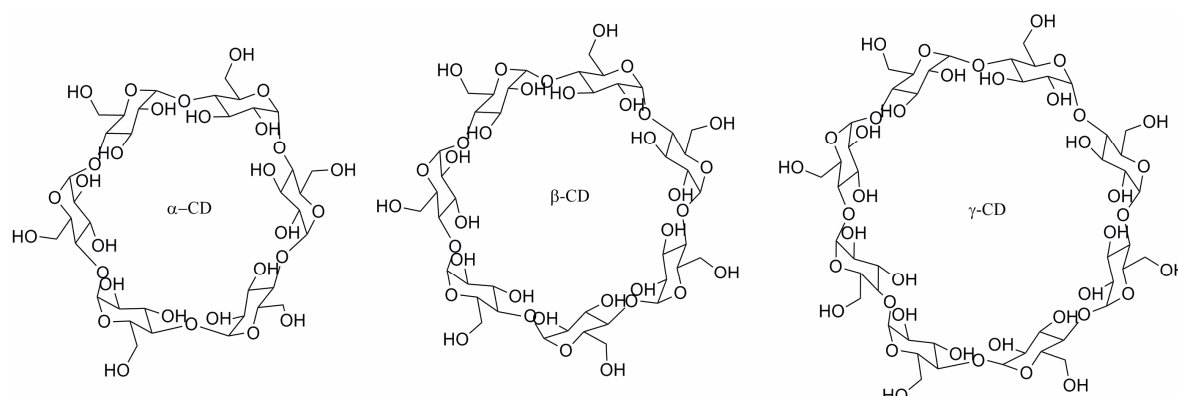


Figure 1: Naturally occurring forms of cyclodextrin

α -Cyclodextrin is the smallest ring whereas γ -Cyclodextrin is largest in the cavity size. CDs consist of 6–8 glucopyranoside units with an arrangement of that brings less hydrophilic groups in the cavity. This arrangement allows CDs to form host-guest complexes with hydrophobic compounds while outer part of cyclodextrins possesses of hydrophilic groups which makes it soluble in water. Thus, host-guest complexes of cyclodextrins are usually water soluble. Cyclodextrins were isolated by a French scientist A. Villiers in 1891 as a crystalline substance from bacterial digest of starch. This material was found to be resistant to acid hydrolysis. Later, Austrian microbiologist Schardinger separately isolated α and β -cyclodextrin in 1903. γ -Cyclodextrin was isolated in 1935 by Freudenberg and Jacobi. Cyclodextrins can be easily prepared from ordinary starch using enzymes *Cyclodextrin glycosyltransferase* and α -amylase. Despite this, cyclodextrin chemistry was quiet till 1980s because of problems with the isolation and purification. That time, some methods for

purification were developed. Enzymatic purification of CDs was carried out in 70s. Different types of enzyme CGTase were prepared by genetic engineering. They were found to be more active and specific towards the production of α -, β - and γ -cyclodextrins.¹⁰ Thereafter, lots of applications of cyclodextrins were developed. Nowadays, CDs are widely used in pharmaceutical and food industries. Apart from these industrial and commercial applications, they are used in research field especially in supramolecular host-guest studies and nanotechnology.

The solubility of α -, β - and γ -cyclodextrin is lower than that of linear dextrans because of binding of cyclodextrin molecules in crystal lattice. Intramolecular hydrogen bonds present in β -cyclodextrin makes it difficult to form hydrogen bonds with water molecules. In order to increase the solubility of cyclodextrins, semisynthetic approaches were used. This strategy ended up with synthesis of water soluble cyclodextrin derivatives. If any of the hydroxyl group is replaced by suitable hydrophobic functions such as methoxy, the solubility of corresponding cyclodextrin moiety increases. The highest solubility can be achieved by replacement of 2–3 OH groups by methoxy functions per glucose unit. However, the higher degree of substitution usually decreases the solubility.¹¹ Later, 2-hydroxypropyl derivatives of β - and γ -cyclodextrin, sulfobutylether derivative of β -cyclodextrin and branched β -cyclodextrin were prepared.¹²

3 Industrial applications of cyclodextrins and toxicity studies

In 70s, Japanese scientists worked on the industrial preparation of cyclodextrins. They introduced cyclodextrins as industrial raw material in 1980 for food and cosmetic industry. In 1976, first application of β -CD was made in pharmaceutical industry. Prostaglandin E₂@ β -CD was prepared by Ono Pharmaceuticals in Japan. After 12 years of this medicine, other drug named piroxicam@ β -CD was introduced to US market by Chiesi Farmaceutici from Italy.¹¹ Generally, cyclodextrins are used as solubilizers and sometimes stabilizers in pharmaceutical formulations. Many industrial applications of cyclodextrins were developed in food and cosmetic industry. CDs are used as flavoring agents and to reduce bad smell as well as taste in food industry. In cosmetic industry, CDs are used to stabilize chemically labile compounds so that their action can be prolonged.¹³

3.1 Inclusion and non-inclusion complexes

In aqueous solutions, cyclodextrins are capable of forming of inclusion complexes. High-energy water molecules from the lipophilic central cavity can be replaced by any size-compatible lipophilic guest while hydroxyl groups from outer surface of cyclodextrins form hydrogen bonds with water molecules. Thus, CDs form water soluble complex with water insoluble compounds.^{14–16} α -Cyclodextrin forms both inclusion and non-inclusion complexes with dicarboxylic acids which coexist in aqueous solution.¹⁷ In saturated aqueous solution of cyclodextrins, guest/CD complex can exist as a mixture of inclusion and non-inclusion complex. As a result of formation of such a complex system, the value of equilibrium constant is sometimes concentration dependent. However, in contrast to the so called specific binding inside the well-defined inner cavity with likely higher binding strength, the association constants of non-specific non-inclusion aggregates are usually rather small.¹⁸

3.2 Solution behavior of the cyclodextrin aggregates

Due to many reasons such as production cost, drug bioavailability and isotonicity, small amount of cyclodextrins are used in pharmaceutical formulations, food products and cosmetics. Many methods are used to increase complexation efficiency. Free guest molecules are in equilibrium with molecules in the complex. Solubility of guest can be increased by ionization, salt formation, by making metal complexes and addition of organic co-solvents.¹⁹ Cyclodextrins form complexes with various excipients such as water soluble polymers, organic acids and bases etc. In addition, cyclodextrins and their complexes can form nano-scale aggregates by associating with each other. These aggregates interact with excipients.¹⁹⁻²³ These structures cannot be detected easily. Only Cryo-TEM micrographs can detect their presence. The size and shape of cyclodextrin aggregates in water depends on cyclodextrin concentration and some other external factors. This makes it possible to have hydrodynamic radius of about 90 nm.²⁴ Some other studies have shown that this diameter is even smaller, from 3 to 5 nm.²³

3.3 Drug availability and cyclodextrins in dispersed systems

It was said that drug molecules would be released slowly from cyclodextrin cavity but it was proved later that the rates of formation and dissociation of drug/cyclodextrin complexes are almost the same as diffusion controlled limits with complexes being formed and broken down continually.²⁵ Thus, water soluble drug/cyclodextrin complexes increase availability of dissolved drug molecule. This strategy is more useful for the molecules with low aqueous solubility.²⁶ It has been proved that cyclodextrins increase oral bioavailability of FDA's class II (low solubility, more permeability) drugs but reduce the bioavailability of class I (more solubility and low permeability).²⁷

Cyclodextrins are used in vehicle systems such as emulsions, microcapsules, microspheres, nanospheres, nanocapsules, liposomes and niosomes. Inclusion complexes of glycerides or fatty acids have surface activity which together with their ability to form aggregates end up with formation of dispersed systems.^{28,29}

3.4 Toxicity studies and regulatory affairs

Some of the medicines that are presently available were made some decades ago when the toxicity norms were not so strict. When cyclodextrins were introduced to market in 80s, these norms were made strict by FDA's of many countries. Hence it took many years to prove that cyclodextrins are non-toxic. Initially, some experiments were carried out on rats in 1957 where rats died. But later it was proved that rats died because of impurities in α - and β -cyclodextrin.^{30,31} Structure of cyclodextrins, molecular weight (>972) and low octanol/water partition coefficient (between less than -3 and 0) shows that they cannot easily pass through biological membranes.^{32,33} Negligible amounts of hydrophilic cyclodextrins and drug/cyclodextrin complexes can pass through lipophilic gastrointestinal membrane and skin^{34,35}. When cyclodextrin is administered orally, it is non-toxic because it cannot be efficiently absorbed by gastrointestinal tract. Lipophilic methylated β -cyclodextrin is surface active and can be absorbed by gastrointestinal tract (approximately 10%). Accordingly, very few cyclodextrin derivatives can be used in oral formulations. β -Cyclodextrin cannot be used in parenteral formulations because of toxicity considerations while α -cyclodextrin have limited use even though it is non-toxic.³⁴ γ -Cyclodextrin is found to be non-toxic in animal

studies when delivered intravenously.³⁶ Toxicological studies of 2-hydroxypropyl- β -cyclodextrin³⁷ and sulfobutylether β -cyclodextrin³⁸ are completed and both of them are used in some formulations which are already in market.

The regulatory status of cyclodextrins is evolving continuously. Cyclodextrins are considered as safe by European, American pharmacopeia and Japanese Pharmaceutical codex. All three cyclodextrins (α , β and γ) are recognized food additives in Japan.

3.5 Polyrotaxanes from cyclodextrin inclusion complex and linear polymer

Rotaxanes are molecular assemblies in which macrocycles are mechanically interlocked on a dumbbell shaped molecular axle by bulky stoppers on its ends. Polyrotaxanes consist of an axle threaded more than one macrocycle. Sometimes, the macrocycle(s) is(are) not interlocked by bulky stoppers; i.e., the complex can dissociate under experimental temperature. Such systems are called as pseudo(poly)rotaxanes. Significant improvement in the synthesis of polyrotaxanes was observed after invention of cyclic molecules such as cyclodextrins.³⁹ Apart from low molecular weight substances, many linear polymers are able to form inclusion complexes with CDs to constitute aggregates in pseudorotaxane manner. For instance, an inclusion complex was prepared with polyethylene glycol and α -cyclodextrin to get polypseudorotaxanes.⁴⁰ Saturated aqueous solution of CDs and PEG were mixed at room temperature to form an inclusion complex. It was water insoluble white precipitate. In this inclusion complex, it was found that large number of CD units was threaded onto a PEG chain. The structure of this polypseudorotaxane was confirmed by X-ray analysis and ¹H NMR. Precipitation was not observed when solutions of CD and PEG carrying end groups which were too bulky for threading, such as 2,4-dinitrophenyl or 3,5-dinitrobenzoyl, was used.⁴⁰⁻⁴² The insolubility of polypseudorotaxanes can be explained by the formation of intermolecular and intramolecular aggregation of CDs through hydrophobic interactions and hydrogen bond formation. CDs aggregate to form channel like structure. These channels associate laterally with other polypseudorotaxanes. PEGs with molecular weights ranging from 10^3 to 10^5 can be included in the cavity of CDs. A gel was synthesized when CDs were complexed with PEG having a molecular weight of 2×10^4 . It showed channel structured CDs forming cross linking points⁴². Recrystallization of inclusion complex from water and phosphate buffer formed hexagonal microfibers. The cross section was reported to be *ca.* $2 \times 5 \mu\text{m}$.⁴³

Variety of different polymers was included into cyclodextrin cavity. Detailed study was carried out by Harada.^{44,45} Most of the inclusion complexes were obtained as water insoluble precipitate. Most notable observation was that every polymer could be included with specific CD whose cavity size is suitable for such inclusion. For example, PEG formed inclusion complex with α -CD, not with β or γ -CD. At the same time, PPG formed stable inclusion complex with β -CD only. The data is tabulated below for all the studied polymers and CDs.

Table 1: Polymers included in CDs

Polymer	CD type	M _r of included polymer
PEG (PEO)	α	< 10 ⁴
	α	> 10 ⁴
	β, γ	Not described
	γ	Not described
PPG (PPO)	β	400–4000
Polytetrahydrofuran	α (methylated)	<10 ⁶ (1400)
Poly-ε-caprolactone	α	
	α	4–6.5 × 10 ⁴
	α, γ	Star polymer
Poly (L- lactic acid)	α	2.85 × 10 ⁵
Poly (vinyl alcohol)	γ	94000
Poly (vinyl acetate)	γ	12800, 1.67 × 10 ⁵
Polycarbonate	γ	28800
PMMA	γ	15000
Polyethyleneterephthalate	γ	1.80 × 10 ⁴
Polyisobutylene	β, γ	
Polybutadiene	α, β, γ	2.0 × 10 ³ –3.1 × 10 ⁴
Polydimethyl siloxane	γ (β)	
Polylysine	α	4090
Silk fibroin	γ	Not described
Nylon 6	-	Approximately 1.2 × 10 ⁴
Poly(bola-amphiphiles)	α	2.8 × 10 ³ and 3.5 × 10 ⁴
Polyaniline	β	6.2 × 10 ⁴
PEG-PPG-PEG block copolymer	α	
	β	10650
PEG-PPG-PEG random	α	2500
PEG-PEI-PEG-block	α	4100
PEG-octanedicarboxylic acid	α, β, hydroxyl-propylated	14400 and 11700

4 Cucurbiturils (CBs)

4.1 Synthesis and purification of CBs

Cucurbiturils are highly symmetric barrel-like shaped macrocycles made from glycoluril monomers bridged by methylene groups. Oxygen atoms are located on the two opposite rims and are tilted inward. Accordingly, a partly enclosed cavity is formed. The name cucurbiturils is related to the similar shape of CBs to the pumpkin from cucurbitaceae family. They are written as cucurbit[n]urils where n is number of glycoluril units. They are abbreviated as CB_n or CB[n]. Three of the smallest cucurbiturils are as shown in Figure 2.

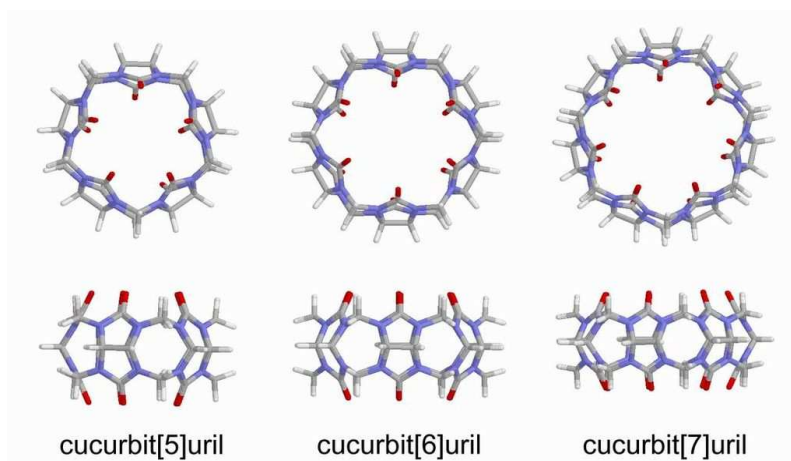


Figure 2: Some basic cucurbiturils

Parent cucurbituril CB[6] was prepared by Behrend in 1905. Till today, CBs are prepared by the original method reported by Behrend with minor modifications. Synthesis of cucurbiturils is carried out in two steps. In the first step, monomer glycoluril is prepared from glyoxal and urea. The next step is polymerization of glycoluril in presence of a mineral acid such as sulfuric or hydrochloric acid. Reaction is as shown in the Figure 3. The reaction gives mixture of many cucurbiturils such as CB[6], CB[5], CB[7], CB[8], CB[5]@CB[10], *nor-seco*-CBs, inverted CBs, etc. Complex purification techniques are required to purify CBs. Majority of the product is CB[6]. One of the recent procedure for the purification of CBs is mentioned by Dezhi Jiao and Oren Scherman. It includes formation of [C_nmim]Br, [Npmim]Br. Isolation of CB[5] and CB[7] (both are soluble in water) is carried out using washing and filtering with water. Insoluble solid (CB[6] and CB[8]) is removed. Then [C₄mim]Br is added to the filtrate to form complex with CB[6] selectively. Subsequently, bromide ion is exchanged with NH₄PF₆ to precipitate the [C₄mim]PF₆@CB[7] complex. CB[5] remains in aqueous solution. Upon evaporation, washing by methanol followed by recrystallization from water gives pure CB[5]. Complex containing CB[7] is then mixed with [C₄mim]Br in water. Solution is heated to 80°C till the solid dissolves. Counter ion exchange takes place in this reaction from PF₆⁻ to bromide. Now [C₄mim]Br@CB[7] complex is precipitated by methanol. Finally, CB[7] is purified by SSM decomplexation method.⁴⁶

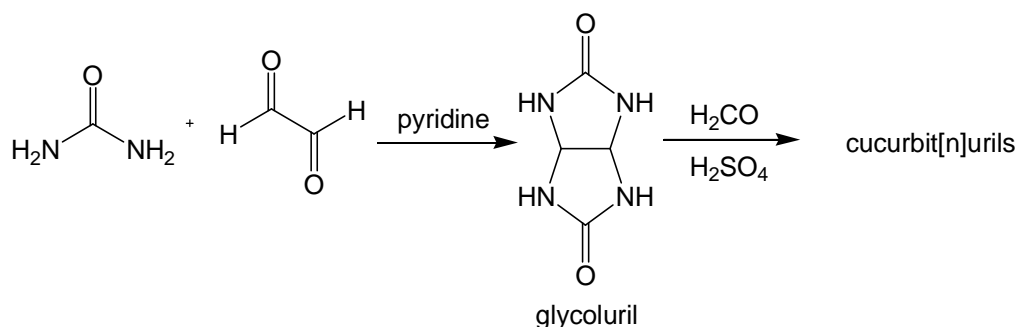


Figure 3: Synthesis of cucurbit[n]uril

CB[6]/CB[8] mixture can also be purified. The mixture of CB[6]/CB[8] along with [Npmim]Br is treated with water. Insoluble CB[6] is separated by filtration. Aqueous solution contains ([Npmim]Br)₂@CB[8] complex. To this aqueous solution is added NH₄PF₆ to exchange the counter ion from Br to PF₆. This complex is precipitated out from the aqueous

solution. $([\text{Npmim}]\text{PF}_6)_2@\text{CB}[8]$ is re-dissolved in aqueous solution along with $[\text{Npmim}]\text{Br}$. Obtained mixture is heated for 2 hours at 80°C to exchange the counter ion to Br. After cooling, extraction is carried out with DCM to remove $[\text{Npmim}]\text{PF}_6$. Methanol is added to the aqueous solution to precipitate out $([\text{Npmim}]\text{Br})_2@\text{CB}[8]$. This complex is again purified by SSM decomplexation method to get pure $\text{CB}[8]$.⁴⁶

4.2 Physical properties and cucurbituril cavity parameters

All CBs are highly symmetric structures with carbonyl rims and a hydrophobic cavity. Presence of electron density on carbonyl oxygen makes them cation receptor functionality. Inner cavity does not have any functional group and electron pair pointing inside. Thus absence of hydrogen bonding interactions makes the cavity completely hydrophobic. When a guest is incorporated into the cucurbituril cavity then absorption, fluorescence and NMR spectra change completely.

Table 2: Geometrical parameters of basic cucurbiturils

Macrocycle	Internal diameter [nm]	External diameter [nm]	Height [nm]
CB[5]	0.44	0.24	0.91
CB[6]	0.58	0.39	0.91
CB[7]	0.73	0.54	0.91
CB[8]	0.88	0.69	0.91

4.3 Catalysis using CBn cavity

CBns are proved to be good catalysts for many reactions such as cycloadditions, oxidations, hydrolysis, photochemical reactions and metal ion assisted catalysis reactions.

4.3.1 1,3-dipolar cycloadditions

Dipolar [3+2] cycloaddition using $\text{CB}[6]$ was reported between acetylenes and azides as shown in Figure 4.⁴⁷ Later, these reactions became popular as *in situ* click reactions.^{48,49}

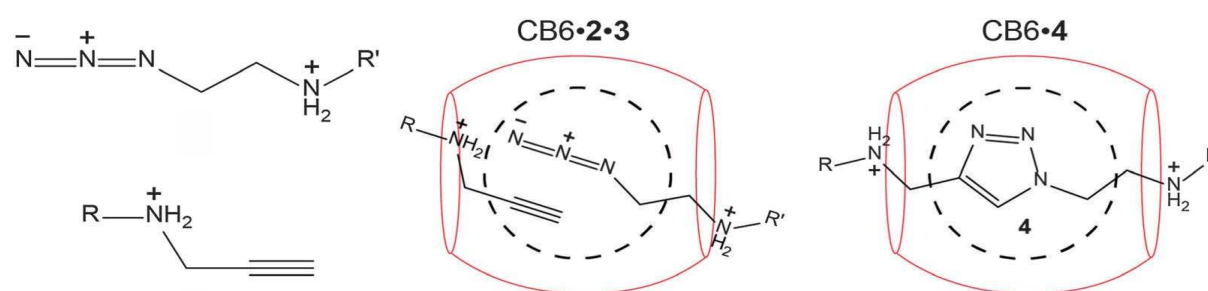


Figure 4: Click reaction of azide and alkyne catalyzed by $\text{CB}[6]$.

The reaction was 6×10^4 times faster in the presence of $\text{CB}[6]$. Ion dipole interactions between ammonium ions and $\text{CB}[6]$ carbonyl rim stabilized the complex formed. According to Mock,⁴⁷ the rate of reaction was increased due to overcoming of entropic constraints and strain activation of the bound substrate.

4.3.2 Oxidation

As Figure 5 shows, alcohols were oxidized to their corresponding aldehydes using *o*-iodoxybenzoic acid in presence of CB[8].^{50,51} Most of the reactions took place at neutral pH. Role of CB[8] is not yet completely clarified. Reddy et al carried out some known reactions with molecular halogens and their complexes with CB[6]. These stable complexes were prepared by diffusion of gaseous halogen into CB[6] cavity. Iodine catalyzed Prins cyclization was studied using free iodine as well as iodine@CB[6] complex. The rate of reaction was much faster in case of pre-complexed iodine.⁵² Tao and coworkers studied aerobic oxidation of furan and thiophene. In aqueous medium, oxidation took place with hemiCB[6] but no reaction took place without host.⁵³

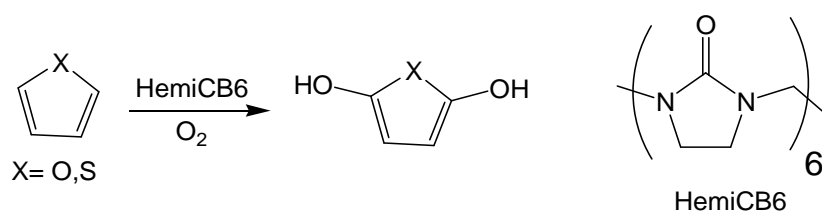


Figure 5: Aerobic oxidation of heterocyclic substrates mediated by hemicucurbit[6]uril

4.3.3 Hydrolysis

Garcia-Rio et al. performed hydrolysis reactions on substituted benzoyl chlorides in presence of CB[7] and DM- β -CD (Figure 6). When benzoyl chloride was substituted with electron donating group, the reaction was catalyzed by CB[7] and terminated by DM- β -CD and vice versa when benzoyl chloride had an electron withdrawing substituent. Inhibition of hydrolysis of 4-nitrobenzoyl chloride was accelerated by 100 times with CB[7] while hydrolysis of 4-methoxybenzoyl chloride was accelerated by 5 folds.⁵⁴

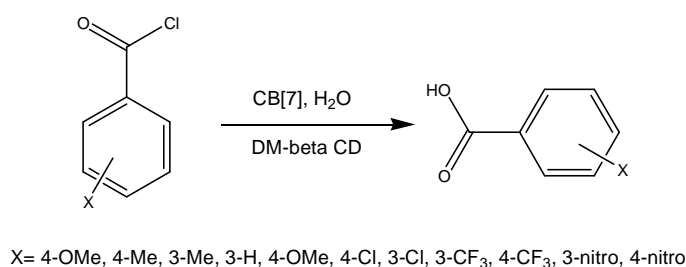


Figure 6: Hydrolysis of benzoyl chloride

Hydrolysis of carbamates (2) and amides (1) were reported in presence of CBs. CB[6] and CB[7] acted as catalysts. Hydrolysis of carbamates with cadaverine (which binds strongly to CB[6] because of its length dependent selectivity for CB[6] and CB[7]) was enhanced by the factor 5 for CB[6] while for CB[7], it was 11.6.⁵⁵ The schematic representation is as shown in Figure 7.

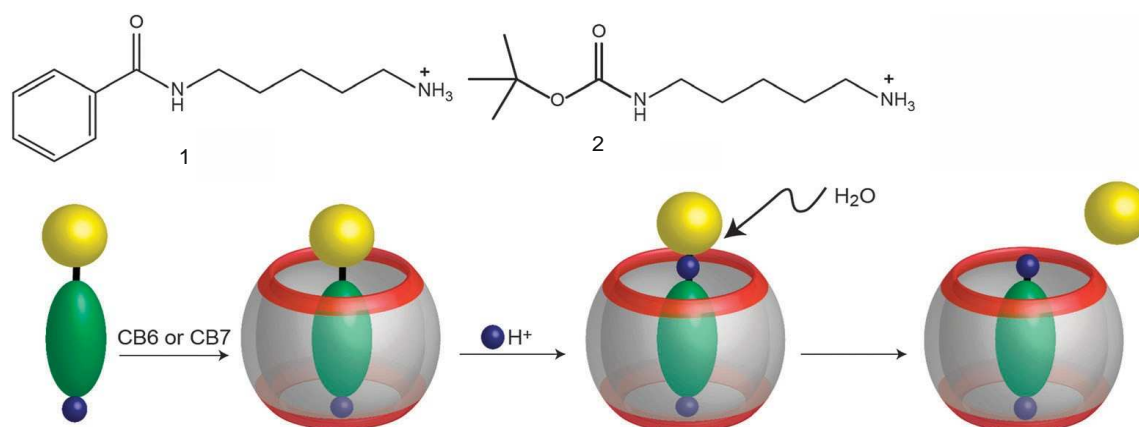


Figure 7: Acidic hydrolysis of *N*-benzoyl-cadaverine (**1**) and mono-*N*-(*tert*-butoxy)carbonyl cadaverine (**2**) mediated by *CBn*.⁵⁵

4.3.4 Metal ions assisted catalysis

As mentioned above, CBs have electronegative carbonyl rims. So, they can bind metal cations.^{56–64} This property has been used to catalyze organic reactions using metal ions.^{65–67} In addition, oxidation of unbranched alkanes was reported in presence of CB[6]/oxovanadium complex.⁶⁵ Cyclic alkanes did not undergo any oxidation as they do not form any inclusion complex with CB[6]. Masson and Lu reported desilylation of trimethylsilylalkynyl derivatives (**3**) catalyzed by *CBn* in presence of Ag(I) salts.⁶⁶ A silver complex $\text{Ag}^+\cdot\text{CB}[7]\cdot\text{trimethylsilylalkynyl}$ converted to trimethylsilanol (**5**) and an alkynylsilver complex. The reaction is shown in Figure 8.

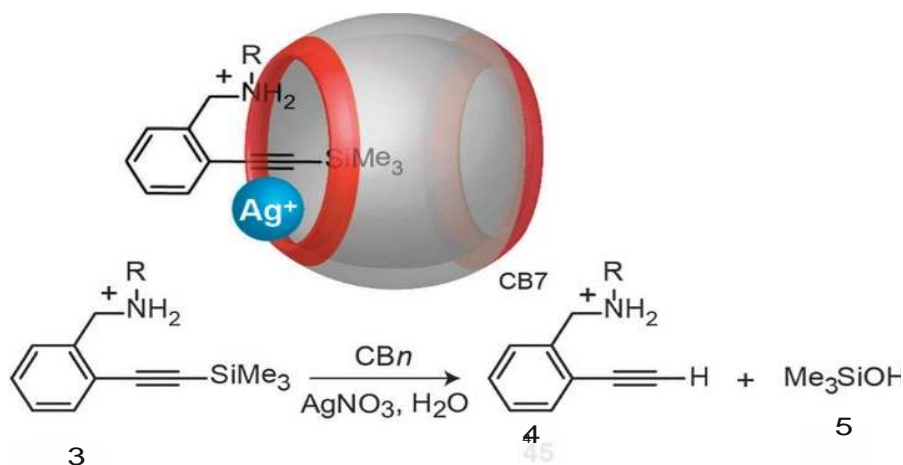


Figure 8: *CBn*-catalyzed desilylation of trimethylsilylalkynyl derivatives (**3**) in the presence of Ag(I) salt; shown on top is the postulated ternary complex.⁶⁶

Nau et al reported phase selective photolysis of bicyclic azoalkanes, 2,3-diazabicyclo[2.2.1]hept-2-ene (**6**) and 2,3-diazabicyclo[2.2.2]octa-2-ene (**9**) catalyzed by transition metal ions which are coordinated with CB[7] rim (Figure 9). The photoproduct was supposed to have a reduced affinity with host and high solubility in organic solvents. Upon UV irradiation of 2,3-diazabicyclo[2.2.1]hept-2-ene, bicyclo[2.1.0]pentane (**7**) and cyclopentene (**8**) were obtained as products. Irradiation of 2,3-diazabicyclo[2.2.2]octa-2-ene yielded 70:30 mixture of 1,5-hexadiene (**10**) and bicyclo[2.2.0]hexane (**11**). Subsequently

performed photolysis with CB[7] and transition metal ions such as Fe^{3+} , Co^{2+} , or Ni^{2+} gave 5 to 10 fold more diene product.⁶⁷

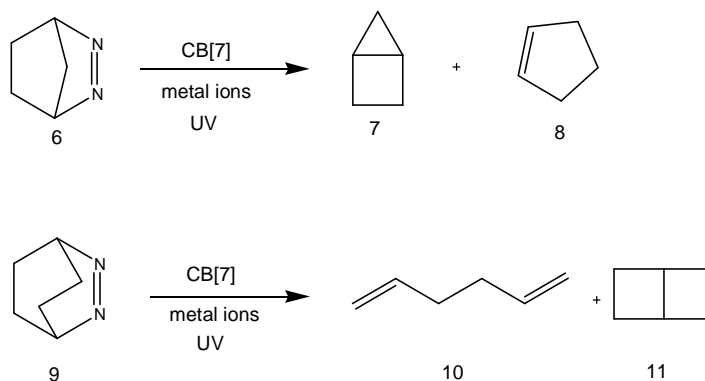


Figure 9: Photolysis of bicyclic azoalkanes

4.3.5 Photochemical reactions using CBn

Photophysical properties of guests can be influenced by CBn.^{68–72} Usually CBn are optically transparent in near UV and visible region.^{73–75} More interesting CBn are CB[7] and CB[8] because of their large cavity size that can accommodate two guests to form binary 1:2 or ternary 1:1:1 supramolecular complexes.

Two equivalents of (*E*)-diaminostilbene was treated with CB[8] to form 1:2 complex which undergone 2+2 cycloaddition upon UV irradiation giving *syn* adduct as a major product while *anti* adduct was minor product. In strong contrast, (*Z*) isomer formation took place in absence of CB[8].⁷⁶

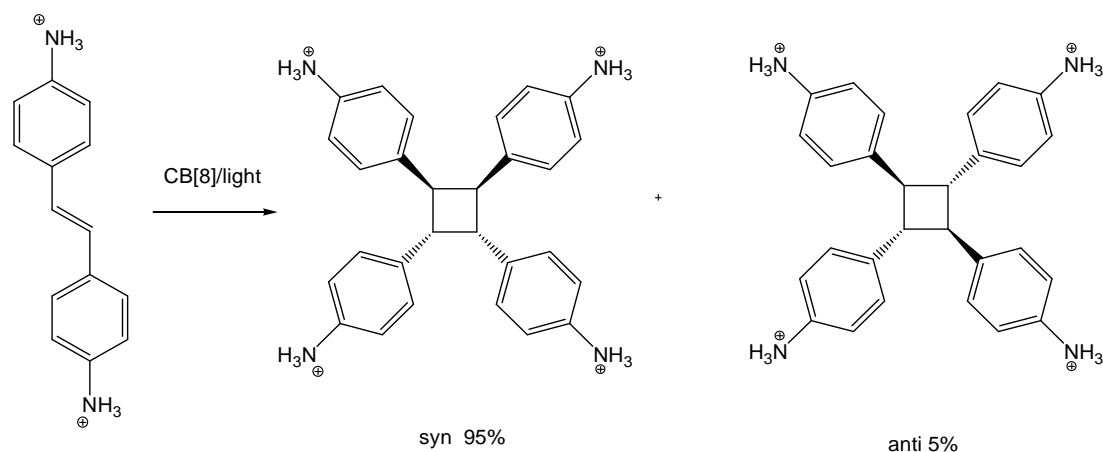


Figure 10: UV light promoted 2+2 cycloaddition in the presence of CB[8]

Similar experiment was carried out by Ramamurthy and coworkers (Figure 11). They encapsulated different olefins in CB[8] in aqueous solution. This 1:2 host-guest complex was irradiated to get 90% *syn* dimer while no dimerization was reported without CB[8]. With CB[7], this reaction did not work out. Without CB[8], phenanthroline, *cis*-isomer and hydration product were isolated (see the Figure 11 for the structures).^{76–80}

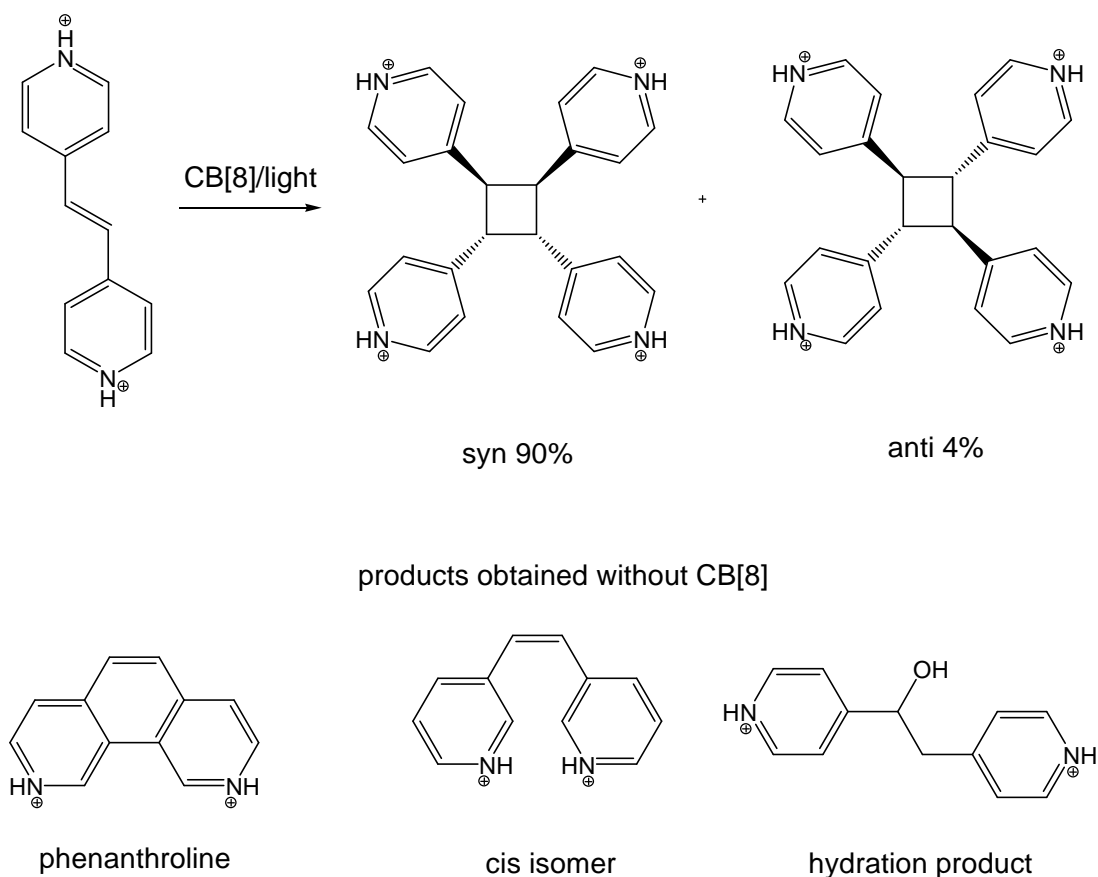


Figure 11: Experiment carried out by Ramamurthy and coworkers

In another experiment, cycloaddition of coumarin derivatives was carried out in presence of CB[8] (Figure 12). In absence of CB[8], reaction yields four products including syn-HH (head-to-head), syn-HT (head-to-tail), anti-HH and anti-HT. Upon UV irradiation of the 1:2 complex, HH regioisomer was formed as a major product. Whether syn or anti adduct is going to form depends upon nature of the substituents at positions 4 (R_3), 6 (R_2), and 7 (R_1). Coumarins with $R_1 = \text{Me}$, R_2 and $R_3 = \text{H}$ form only syn-HH adduct.⁸¹⁻⁸⁴

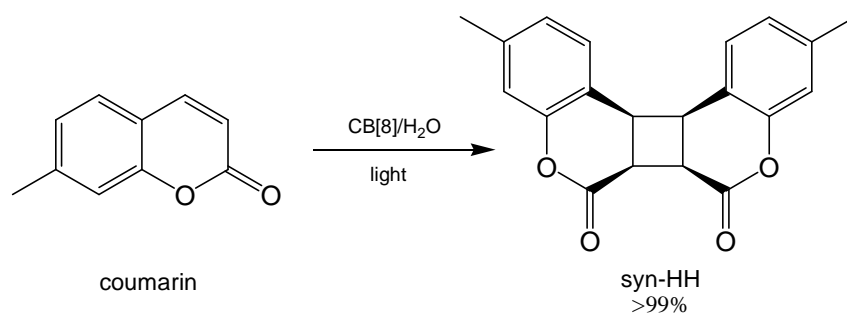


Figure 12: CB[8]-promoted cycloaddition of coumarin

4.4 Chiral applications

Contrary to cyclodextrins, CBs are achiral. Still they can contribute in the fields such as asymmetric synthesis and catalysis. Lot of work has been carried out recently on CBs that showed their use in above mentioned areas.⁸⁵⁻⁹⁰

Kim and coworkers described a structure of helical polyrotaxane in which CB[6] units were threaded with *N,N'*-bis(3-pyridylmethyl)-1,5-diaminopentane and locked as Ag⁺ complex. Each CB[6] unit was present at the center of repeating thread units through combination of hydrophobic chain encapsulation within cavity and dipole interactions between CB[6] and protonated amines.⁹¹

(±)-Bis-ns-CB[6] was identified as first chiral cucurbituril. It has a chiral cavity where enantio- and distereoselective recognition was possible by cavity selection. Chiral auxiliary was not needed in this case.^{92,93} Moderate chiral recognition was observed by using enantiomerically pure (+)-1-phenylethanamine to form the mixture of (±)-1-phenylethanamine in the ratio of 72:28. Absence of two bridging methylene groups in (±)-Bis-ns-CB[6] provides slightly larger cavity than CB[6]. The volume of cavity lies between CB[6] and CB[7]. It can accommodate methyl viologen. Some other guest molecules were also examined by Issacs and coworkers and (±)-2-amino-3-phenylpropanoic acid (88:12) showed highest diastereoselectivity. Phenyl ring acquires chiral space with better fit and amine binds with electronegative portal.⁹⁴

Wagner et al. encapsulated fluorescent 8-(phenylamino)naphthalene-1-sulfoinic acid and 6-(phenylamino)naphthalene-2-sulfonic acid. Fluorescence was increased by CBn cavity association.⁹⁵ This phenomenon of fluorescence enhancement was subsequently used by Nau and coworkers. They developed efficient supramolecular tandem enzyme assay. This method was dependent on differential binding strengths between fluorescent dye, amino acid and the product which is amine of enzymatic decarboxylation. Binding strength of dye is higher than that of amine (substrate) but lower than that of product. So, the dye has high fluorescent intensity when bound with CB[7] but when displaced with amine which binds more strongly the fluorescence intensity is reduced.^{96,97} This method has been used in determining of the enantiomeric excess of D and L amino acids.⁹⁷ The amino acid specific enzyme (decarboxylase) is required to differentiate comparative D and L amino acid. Only one leads to product by displacing fluorescent dye from CB[7].

In another study carried out by Macartney and coworkers, interrelationship between achiral CB[7] and chiral protonated enantiomers (*R*) and (*S*)-*N*-benzyl-1-(1-naphthyl)ethylamine (BNEAH⁺) was studied. Both (*R*) and (*S*) enantiomers form stable 1:1 complex with CB[7] in aqueous solution. Phenyl group of BNEAH⁺ binds into CB[7] molecule while naphthyl group remains outside. This inclusion increased the molecular rotation from -208 to -940 deg cm² in case of free to bound (BNEAH⁺). (*S*) isomer gave opposite sign with equal magnitude. The circular dichroism spectra showed a difference between free and CB[7] complexed BNEAH. The two peaks were of opposite signs, (-) for (*R*) isomer (275–285 nm) and (+) for (*S*) isomer (225–230 nm) were recorded. When these isomers were bound to CB[7] cavity, magnitude for (*S*) isomer was reduced from 225–230 nm while magnitude for (*R*) isomer was increased from 275–280 nm. This change was seen because of benzyl group of BNEAH⁺ in the hydrophobic cavity of CB[7] and naphthyl group had restricted rotation which caused change in optical rotation spectra.⁹⁸

Recently, an example of chiral open CB-based host was introduced by Issacs and coworkers. They prepared enantiomerically pure acyclic cucurbit[n]uril-based containers by condensing enantiomerically pure (2*S*,2'*S*)-1,1'-(1,4-phenylenebisoxo)bis(2-propanol) and (2*R*,2'*R*)-1,1'-(naphthalene-1,4-diylbisoxo)bis(2-propanol) with glycoluril tetramer.⁹⁹

Some other example of chiral recognition inside a chiral cucurbituril derivative bis-nor-seco-CB[6] was reported by Huang et al.¹⁰⁰ This chiral member of the cucurbituril family was isolated from crude mixture after glycoluril/formaldehyde condensation. However, its wider application is limited by low yield and time-consuming isolation procedure.

5 Supramolecular applications of cyclodextrins

Cyclodextrins are used in supramolecular studies because of their ability to form inclusion complexes with guest molecules. Inner part of cyclodextrin is hydrophobic. Hence, water insoluble compounds can be trapped to form inclusion complex. Such inclusion complexes are used for various purposes such as drug delivery, analytical study of inclusion complexes etc. Some recent approaches are summarized in this section.

5.1 Case binding studies

Inclusion complex of gemifloxacin (GFX) and hydroxypropyl- β -cyclodextrin (HP β -CD) was prepared by Ali Dsugi et al. The complex was examined by techniques such as ESI-MS, UV-VIS, FTIR and fluorescence spectroscopy. Inclusion complex formation was confirmed by observing changes in spectroscopic properties. Molecular modeling approaches supported 1:1 host-guest inclusion complex. From increase in the fluorescence intensity of GFX produced through complex formation, more accurate and sensitive spectrofluorometric method for GFX determination was identified. This method is used in the determination of GFX in pharmaceutical formulations. The linear relationships between intensity and GFX concentration were observed in the limit of 20–140 ng/cm³. Correlation coefficient obtained was 0.9997 with detection limit of 4 ng/cm³. This method has been successfully checked in the analysis of GFX in pharmaceutical formulations.¹⁰¹

Similar study was carried out by Ali Dsugi et al on moxifloxacin. An inclusion complex between moxifloxacin and β -cyclodextrin was prepared in the stoichiometric ratio of 1:1. A similar method was used to detect the amount of moxifloxacin in commercial pharmaceutical formulations.¹⁰²

Bo Tang et al studied supramolecular interactions between gemfibrozil and β -cyclodextrin by flow injection spectrofluorimetry. β -CD forms 1:1 complex with gemfibrozil with association constant K_a of 7.57×10^2 dm³/mol. Fluorescence intensity was increased after complexation. Flow injection spectrofluorimetric method was developed to detect gemfibrozil in bulk solution in presence of β -cyclodextrin. This method was successfully tested for gemfibrozil capsules and serum.¹⁰⁵ Bo Tang et al extended their research to study of the interactions between β -CD dimer and berberine hydrochloride by spectrofluorimetry. Association constant K_a obtained was 1.53×10^4 dm³/mol. Similar procedure as mentioned in the previous case was developed for berberine hydrochloride. It was used to detect berberine hydrochloride in tablets and serum. This approach was found to be useful in drug monitoring pharmacokinetics and clinical applications.¹⁰⁶ In another study, Bo Tang et al studied supramolecular interactions of disulfide linked β -cyclodextrin dimer and dimethomorph by spectrofluorimetry. Similar method was employed as mentioned in mentioned references^{104,105} to determine the amount of dimethomorph in commercial capsules and serum. Association complex obtained had a K_a value 2.25×10^4 dm³/mol.¹⁰⁷

Binding of cyclodextrins in aqueous media are useful studying host-guest chemistry. CDs are used in sensing and controlled release systems as well. Siripornnoppakhun et al prepared

a water soluble tricationic compound ($3N^+$) with three branches of phenyleneethylene fluorescent moieties and related amphiphilic compounds ($3C^-$, N^0N^+ , N^+ , and $2N^+$). Structures of these compounds are showed in Figure 13. These compounds were used as molecular probes for determining supramolecular interactions with cyclodextrins. Formation of 1:1 inclusion complex was confirmed by increase in fluorescence, circular dichroism and 1H NMR. The highest binding strength was observed for γ -Cyclodextrin with association constant of 3×10^4 dm^3/mol . Moderate fluorescence enhancement and shifting in chemical shift values confirmed the exchange of β -CD with guest compound.¹¹⁰

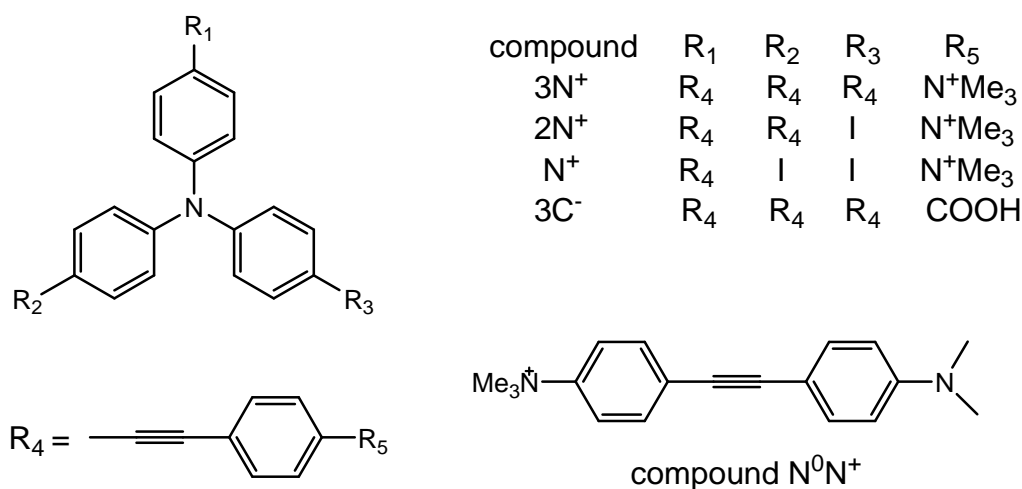


Figure 13: Structures of compounds $3N^+$, $3C^-$, N^0N^+ , N^+ , and $2N^+$

Vícha et al studied the binding properties of 4,4'-biphenylene bisimidazolium (BiPh) salts with β -CD and obtained the association constant approximately 10^{3-4} dm^3/mol . BiPh site was combined with two symmetrically equivalent adamantyl sites showing high affinity towards CB[7]. These guests were used to prepare binary 1:2 and 1:3 pseudorotaxanes with β -CD and ternary rotaxane-like aggregates with CB[7] and β -CD. The observed stoichiometry was 1:1:1 and 1:2:1.¹¹¹

5.2 Advanced biorganic systems

Carborane-peptide bioconjugates were prepared by Neiryneck et al to study supramolecular functionalization of β -cyclodextrin coated surfaces. Formation of β -cyclodextrin-carborane-cRGD surfaces was confirmed by IR-RAS and WCA. High affinity of these surfaces was observed by QCM-D. Cells placed on β -CD+Cb-cRGD showed more elongated morphology and stronger cell adhesion as compared to β -CD and β -CD+Cb-cRAD substrate. It confirmed the functionality of the supramolecular immobilization strategy on macroscopic level.¹⁰³

Gd(III) complexes are used in magnetic resonance imaging as contrast agents as they increase the relaxation rate of water protons of tissues where they are distributed. This effect increases if paramagnetic material is a part of macromolecular system. In molecular imaging more and more molecules of contrast agent are supposed to be directed to the desired site. Silvio Aime et al synthesized a polymer from chitosan with β - and γ -cyclodextrins. This polymer is capable of forming high affinity adduct with suitable Gd(III) complexes. They treated cyclodextrins with maleic anhydride to get 6-monosubstituted derivatives. These derivatives reacted regioselectively with the amino groups present in chitosan. Yields were

high as the reactions were carried out using either microwave or ultrasound technique. β - and γ -CD-chitosan adducts showed increase in binding affinity for Gd(III) complexes as compared to cyclodextrin monomers. They found to be good carriers for in vivo transport of Gd(III) complexes.¹⁰⁴

Controlled self-assembly of amphiphilic cyclodextrin provides generation of well-defined aggregation with host sites. It has many potential applications in drug-carrier systems. Tao Sun et al prepared β -CD modified anthraquinone moiety which was able to self-assemble to vesicles. This species was characterized by TEM, SEM, EFM and DLS. The formation of vesicles was suggested from 2D NMR ROESY and UV studies. The vesicles were found to be able to load paclitaxel within the membrane with macrocyclic cavities.¹⁰⁸

Supramolecular interactions between biotin and β -cyclodextrin were studied by Michael Holzinger et al. Association constant K_a of $3 \times 10^{12} \text{ dm}^3/\text{mol}$ was obtained by studying NMR shift differences of β -cyclodextrin protons at various biotin concentration. To find new alternative for immobilization of bioreceptors, biotin and β -cyclodextrin containing biomolecules were immobilized on transducer surface. This affinity system was studied by enzymes glucoseoxidase and polyphenoloxidase. This inclusion complex showed 7 fold increase in maximum current density and 20 times more sensitivity was observed by the immobilized biological layer.¹⁰⁹

5.3 Biomedical applications of CD-drug complexes

5.3.1 Modified cyclodextrins

Ability of cyclodextrins to form inclusion complexes with organic compounds has given rise to the concept of using them in drug delivery. Many compounds cannot be used practically because of their poor solubility in biological fluids. CDs have fascinated chemists because of their unique properties such as low toxicity and high solubility in water. However, natural α - and β -cyclodextrins are considered to be unsafe because of their nephrotoxicity.^{38,112,113} γ -Cyclodextrin has much lower toxicity, however, the binding properties are significantly different compared to that of α - and β -CD. In addition, the pure γ -CD is much more expensive than β -CD. Thus scientific community focused on preparing of modified cyclodextrin derivatives which have low toxicity and their capability of forming inclusion complexes is not affected. Two such modified cyclodextrins are hydroxypropyl- β -cyclodextrin (HP- β -CD) and sulfobutylether- β -cyclodextrin (SBE- β -CD). SBE- β -CD is also called as (SBE)_{7M}- β -CD. 7M indicates total number of oxygen atoms that connects each cyclodextrin unit. (SBE)_{7M}- β -CD possess 7 β -CD units.

HP- β -CDs have higher aqueous solubility than parent β -CD. Binding constant between drug and HP- β -CDs is usually less than that for parent cyclodextrin. More the hydroxypropyl groups, less is the drug binding. In case of (SBE)_{7M}- β -CDs, the solubility in aqueous medium is higher with higher number of sulfomethyl groups. (SBE)_{7M}- β -CDs cannot form any 1:2 complex with cholesterol and other membrane lipids causing no membrane disruption. This behavior makes (SBE)_{7M}- β -CDs more safe for applications in the drug delivery than parent cyclodextrins.^{114,115} Most of the modified cyclodextrins are expected to be complex mixtures. Some of the important in vivo applications of cyclodextrins are described in following part.

5.3.2 Delivery of insoluble drugs

Release of drugs from cyclodextrin complexes is considered to be rapid since it is based upon simple dissociation and/or competitive displacement mechanisms. Nevertheless, the question remains whether drug pharmacokinetics would be disturbed because of presence of cyclodextrin or not. Loscher et al checked the pharmacokinetics of carbamazepine and found out that HP- β -CD does not change this important property.¹¹⁶ Similar results were obtained for thiopental when it was administered orally as a γ -CD complex.¹¹⁷ The pharmacokinetic properties of propofol (2,6-diisopropylphenol) remained almost identical when it was delivered through HP- β -CD and commercial oil in water emulsion.¹¹⁸ Stella et al studied *in vivo* bolus pharmacokinetics in rats of methylprednisolone from an (SBE)_{4M}- β -CD solution (0.075M) and a co-solvent solution (60% PEG400, 12% ethanol, and 28 % water (% vol)). Results showed no significant difference in any pharmacokinetic parameter.¹¹⁹ Jarvinen et al. was able to administer water insoluble cinnarizine orally by forming its inclusion complex with (SBE)_{4M}- β -CD.¹²⁰

In some cases, pharmacokinetic properties have seen to be changed by cyclodextrins. Frijilink et al administered naproxen and flurbiprofen to rats in form of their inclusion complexes with HP- β -CD. The drugs got dissolved in rat plasma. Tissue distribution remained unaffected after administering naproxen but higher levels of flurbiprofen were observed in brain, kidney, spleen and liver. It was explained by Frijilink that protein binding was affected by HP- β -CDs.¹²¹

5.3.3 Oral applications

The purpose of using cyclodextrins in oral formulations is to increase bioavailability with increased rate and extent of drug dissolution. One such example was reported by Panini et al. They used HP- β -CD to increase the availability of ursodeoxycholic acid (UDCA) which prescribed for cholesterol gallstone. Panini prepared tablets that contained HP- β -CD complex of UDCA, starch and cellulose. The dissolution was much faster and complete as compared to commercial tablets.¹²²

Bioavailability effect of increased drug dissolution rate in presence of cyclodextrin is clearer in cases when drug-cyclodextrin complex is present in either solid or in solution phase. Jarvinen et al. used HP- β -CD and (SBE)_{4M}- β -CD to improve bioavailability of cinnarizine in dogs. Cinnarizine is weak base and availability issues have been seen in case of high stomach pH. The drug was administered by forming suspension of drug-HP- β -CD or (SBE)_{4M}- β -CD solution with phosphate buffer or as solid through capsules. The bio availabilities of suspension, neat capsule and (SBE)_{4M}- β -CD complex capsule were observed to be 8 \pm 4%, 0.8 \pm 0.45%, and 38 \pm 12%, respectively. The HP- β -CD and (SBE)_{4M}- β -CD gave bio availabilities of 55 \pm 11% and 60 \pm 13%.¹²⁰

Atovaquone was completely insoluble in water. It used to be available as microfluidized suspension Mepron^R. Studenberg et al. administered this drug to dogs by making atovaquone·(SBE)_{4M}- β -CD or HP- β -CD complex in gelatin capsule. Absolute bio availabilities were increased by 2–3 folds as compared to commercial Mepron^R formulation.¹²³

Cyclodextrins affect oral absorption of drugs by increasing mucosal membrane permeation. Haerberlin et al. found out that permeability of calcitonin and octapeptide

octreotide (Sandostatin^R) was increased using cyclodextrins. Experiments revealed that β -CD and HP- β -CD showed increased octreotide absorption. In situ absorption of calcitonin was also increased when administered by forming inclusion complexes with β -CD, γ -CD, HP- β -CD and DM- β -CD. Non modified cyclodextrins showed highest increase in peptide permeation in Caco-2 cell model.¹²⁴ Many cyclodextrin derivatives have been prepared that exhibit pH dependant solubility for selective dissolution of drug-CD complex. *O*-carboxymethyl-*O*-ethyl- β -CD (CME- β -CD) has pK_a of 3.7 and exhibits pH-dependent solubility. CME- β -CD has low solubility in acidic environment such as stomach. Studies were carried out on diltizen and molsidomine in gastric acidity controlled dogs. Molsidomine was complexed with CME- β -CD. The results showed that the absorption of drug was significantly lower in high acidic areas as compared to those in low acidic areas of small intestine.¹²⁵

5.3.4 Ophthalmic applications

The primary concern about CDs was if it could cause some damage to the cornea. Jensen et al showed that dimethyl- β -cyclodextrin (DM- β -CD) was not suitable for such purpose but 12.5% HP- β -CD did not cause any irritation to cornea.¹²⁶ In addition, Jarvinen et al showed that α -CD, β -CD, and DM- β -CD cannot be used as they cause irritation to cornea. It is said that only pure drug, not a complex with β -CD penetrates pre corneal area.¹²⁷ Ophthalmic solution containing complex must contain low concentration of CD. Thus, drug dissociation from complex will be dependent on drug binding to pre-corneal proteins. If concentration of cyclodextrin is high then drug would not be delivered. (SBE)_{4M}- β -CD and HP- β -CD did not affect corneal permeability for polar drug such as pilocarpine. It was noticed that high concentration of CD reduced miotic response to pilocarpine.¹²⁸ 4M in (SBE)_{4M}- β -CD indicates 4 cyclodextrin units connected with each other by 4 oxygen atoms. Similar observation was obtained by Reer et al. for in vitro corneal permeability of diclofenac in presence of HP- β -CD.¹²⁹

Major application of inclusion complexes of drug-CD comes for solubilizing poor water soluble drugs. Best example is steroid dexamethasone and its acetate ester.^{130,131} Usayapant prepared an inclusion complex of dexamethasone and dexamethasone acetate with HP- β -CD. This complex showed better ophthalmic delivery of both the drugs.¹²⁹ Inclusion complexes of HP- β -CD with carbonic anhydrase inhibitors acetazolamide and ethoxzolamide also showed improved ophthalmic delivery.¹³²

5.3.5 Nasal applications

Application of cyclodextrins can improve the nasal mucosa permeability, drug solubility or can change metabolism rate at the site of delivery. High concentration of DM- β -CD have shown some adverse effect on nasal mucosa in both in vitro and in vivo studies but the toxicity is still less than surfactants such as sodium glycocholate and laureth-9, phospholipid, L- α -lysophosphatidylcholine.¹³³

5.4 Supramolecular nanocarriers

Nowadays attention has been given on nano-sized delivery systems like enhanced cellular uptake, controlled drug release and targeted drug delivery.¹³⁴⁻¹³⁶ Many supramolecular nanocarriers have been prepared such as micelles, vesicles and supramolecular nanoparticles. Host-guest interactions played a vital role in their preparation process.

5.4.1 Vesicles

Supramolecular chemistry approaches are commonly used to synthesize artificial vesicles. They have uniform nanoscale size, ease of fabrication and empty hollow cores for drug storage. Vesicles are prepared by using noncovalent interactions like polar/non-polar interactions provided by amphiphilic surfactants.^{137,138} Drug materials are loaded inside the core of vesicles. Generally amphiphilic molecules are required to make vesicles. The role of inclusion complex in the formation of vesicles is to act as fabrication of supramolecular amphiphiles which acts as a driving force to form vesicles. Ravoo and coworkers fabricated long hydrophobic alkyl tails on one side of β -CD which can form vesicles. The alkyl groups were directed inwards, i.e., to the inner side of the vesicle cavity and hydrophilic OH groups of β -CD were present on the outer side in contact with aqueous environment. Sugar units such as maltose/lactose were modified on the surface of vesicle by host-guest inclusion between β -CD and adamantyl group from sugars.¹³⁹⁻¹⁴¹

Hydrophilic hyperbranched polyglycerol (HPG) was conjugated on β -CD covalently to form CD-HPG complex. The hydrophobic alkyl chain of HPG was coupled with adamantyl group. Supramolecular amphiphiles were prepared by making inclusion complex between β -CD and adamantyl group from HPG. It was able to self-assemble on core-shell structured vesicles.¹⁴²

5.4.2 Micelles

Micelle is one of the important type of supramolecular self-assembly system. They are formed from amphiphilic surfactant that carries hydrophilic heads facing outside and hydrophobic tails going towards the center of micelle. Amphiphilic block copolymers with hydrophilic and hydrophobic ends are widely used in micelle preparation.¹⁴³

Dong and coworkers prepared micelles based on biodegradable block copolymer. The inclusion complex was formed between β -CD and polymer chain which led to the formation of hydrogels. Hydrogels are popular for drug delivery and tissue engineering (see chapter 5.4). This micelle-hydrogel drug delivery system showed reduction responsive doxorubicin release in the block copolymer main chain.¹⁴⁴ Apart from redox responsive drug release from micelle, thermal responsive micelles were prepared on temperature sensitive block copolymer made up of *N*-isopropylacrylamide (NIPAAm) and trimethylsilylpropargylacrylate (TMSPA) for abendazole (ABZ) delivery. β -CD ring was made to form pendant on NIPAAm so that the block copolymer would show hydrophilic nature leading to micelle formation in aqueous medium by self-assembly. In this complex system, β -CD served to encapsulate ABZ.¹⁴⁵

In another approach, supramolecular capsules were prepared from polymers which were covalently conjugated to α -CD as a pendant. α -CD grafted with carboxymethyl dextran (CMD-g- α -CD) and poly(acrylic acid)aminododecane *p*-azobenzene aminosuccinic acid (PAA-C12-Azo) was prepared. The inclusion complex formation was assisted by α -CD and azobenzene unit on the surface of solid CaCO_3 nanoparticles. Supramolecular hollow capsules were obtained after removal of CaCO_3 . Capsules were found to be responsive for UV irradiation which led to dissociation of α -CD-azobenzene complex.¹⁴⁶

5.4.3 Supramolecular nanoparticles

Nanoparticles have attracted scientific community because of their unique properties. Supramolecular particles within nanoscale size have been prepared which are proved to be suitable devices in drug delivery. Thiele and coworkers prepared inclusion complex between starch and cyclodextrin. Pteric acid was conjugated with nanoparticles to target cancer cells. Similarly, 1,4-dihydroxyanthraquinone (DHA) was loaded into above supramolecular nanoparticles prepared from starch and cyclodextrin.¹⁴⁷

5.4.3.1 Rotaxane and polyrotaxane based nanoparticles

In early research, polypseudorotaxanes were prepared by threading α -CD on PEG polymer chains to deliver anticancer drugs Dox and CPT (camptothecin). Cell penetrating peptides were conjugated on polypseudorotaxane drug delivery system. This system was able to penetrate cancer cells which enhanced efficiency of chemotherapy.^{148,149} Another approach is self-assembly of polypseudorotaxanes which forms supramolecular nanoparticles. α -CD/PEG polypseudorotaxane based nanoparticles were prepared by self-assembly phenomenon with size of 200 nm. Anticancer drug methotrexate (MTX) was loaded into them by hydrogen bonding. In vitro study indicated that the nanoparticles were nontoxic to human body. Anticancer strength of MTX was increased after forming supramolecular nanocomplex as compared to free MTX.¹⁵⁰ Das and coworkers prepared a polymer complex from polyacrylamide (PAAm) and polyvinylalcohol (PVA). Cyclodextrin were grafted on polyacrylamide. The complex formed was polypseudorotaxane and it was able to form supramolecular nanoparticles by self-assembly.¹⁵¹

5.4.3.2 Host-guest interaction induced nanoparticles

Supramolecular nanoparticles can be prepared by host-guest complexation between macrocyclic molecules and guest molecules. These guest molecules are conjugated on different polymer chains or building blocks. While preparing supramolecular nanoparticle, anticancer drug can be encapsulated in the nanoparticle. It is then released in two ways, either sustained release or controlled release by dissociation of nanoparticle. Zhao and coworkers synthesized supramolecular nanoparticles that contained β -CD conjugated polyacrylic acid (PAA-CD), adamantyl conjugated PAA (PAA-Ad) and adamantyl conjugated PEG (PEG-Ad). Inclusion complex was formed between adamantyl group and β -CD to form nanoparticles with uniform size of 35 nm. Subsequently, Dox can load to these nanoparticles. Folic acid, a ligand that targets cancer cell and fluorescence probe FITC were introduced via an inclusion complex with β -CD and Ad-functionalized folic acid and FITC (FITC-Ad). Selective drug delivery as well as killing of two cancer cells strains MDA-MB231 (breast cancer cells) and B16F10 (skin cancer cells) were observed. Nanoparticles showed good inhibition activity against tumor when tested in vivo in mice having tumor.¹⁵²

Ma and coworkers developed another kind of supramolecular nanoparticles. They also conjugated β -CD onto the polymer chain as pendant for drug delivery. However, the synthesized block copolymer contained hydrophilic PEG segment and β -CD with polyaspartamide group. Anticancer drug formed inclusion complex with β -CD cavity and block co-polymer self-assembled into core-shell nanoparticles.¹⁵³ Authors prepared temperature-responsive nanoparticles from a block copolymer with β -CD containing segment and PEG segment. Host-guest interactions were observed between CD and isopropyl group of

poly(*N*-isopropylacrylamide). These interactions led to the formation of supramolecular nanoparticles which were able to carry hydrophobic drug such as indomethacin and the drug release rate could be controlled by the temperature.¹⁵⁴ Not much attention was paid towards *in vitro* and *in vivo* drug delivery. Tseng and coworkers synthesized a series of supramolecular nanoparticles which were based on the interactions between CD and adamantane conjugated with polymers or dendrimers. They prepared supramolecular nanoparticles with CD/Ad host-guest interactions using Ad-modified polyamidoamine dendrimer (Ad-PAMAM), β -CD grafted on branched polyethylenimine (CD-PEI), and Ad-functionalized PEG (Ad-PEG). Supramolecular nanoparticles were self-assembled and their size ranged from 30–450 nm. These nanoparticles were studied for stability, disassembly, size tenability, and whole body misdistribution. Study revealed the critical role of the size of the nanoparticles.¹⁵⁵ Addition of CPT grafted PEG (CPT-PEG) to previous three building blocks made CPT containing supramolecular nanoparticles with two different sizes. Positron emission tomography (PET) revealed the body distribution and tumor accumulation of the nanoparticles. The antitumor effect of CPT containing supramolecular nanoparticles was enhanced.¹⁵⁶

5.4.3.3 Host-guest nanohybrids

5.4.3.3.1 On-off switch on nanoparticles

The host-guest inclusion complexes arise and decompose reversibly. It can lead to the design of controlled drug delivery where the supramolecular systems are integrated with inorganic nanoparticles such as mesoporous silica nanoparticles (MSNPs). These MSNPs have several advantages in drug delivery application such as high specific surface area, large pore volume, uniform pore size, ease of functionalization, and good biocompatibility.^{157–159} Lot of systems containing MSNPs were developed. Loaded drug release was triggered by external stimuli like variation of pH^{160–162}, temperature,¹⁶³ and redox reactions in the body.^{164,165} Many drug delivery systems were prepared from MSNP where host-guest complex played the role of nano-gate which were able to respond to the external stimuli. Some nanoparticles were prepared by combining magnetic nanocrystals with MSNP. The surface of MSNP was modified with pseudorotaxanes which acted as nano-gate. The employing of the external magnetic field on magnetic nanocrystals generated heat which caused destruction of host-guest inclusion complex of pseudorotaxanes causing drug release.¹⁶⁶ Zink et al developed a snap-top stopper using β -CD and coumarin derivative covalently linked to MSNP surface. The bond between coumarin and MSNP was easily cleaved with UV or two-photon-NIR light.¹⁶⁷

Some systems were synthesized for dual responsive drugs and selective cargo release. Hoechst 33342, a nucleic acid stain 2'-(4-ethoxyphenyl)-5-(4-methylpiperazin-1-yl, 2,5'-Bi-1H-benzimidazole) was loaded to β -CD which was anchored to mesopores via disulfide linkage. In the similar way, small sized molecule like *p*-coumaric acid was trapped into β -CD cavity and the cavity was blocked by using guest molecule like methyl orange (MO). Under acidic conditions, methyl orange gets protonated and drug trapped inside the cavity was released. In case of Hoechst 33342, the release took place due to cleavage of disulfide linkage causing removal of β -CD ring.¹⁶⁸ Series of controlled drug delivery systems were prepared in which β -CD was used as capping agent. Controlled drug release property of some systems was studied by *in vivo* as well as *in vitro* methods. Azobenzene can undergo UV-mediated

(*E*)/(*Z*) isomerization which controls the movement of α -CD on the surface of MSNP. Thus drug can be released on demand at the site. Such systems were studied in vivo on zebrafish models. The results showed effective heart failure therapy as compared to the free drug.¹⁶⁹ Zhao and coworkers attached α -CD based rotaxane on hollow MSNPs. Here folic acid served as targeting ligand as well as terminal group of the thread. The disulfide bond caused redox controlled drug release in vitro and in vivo.¹⁷⁰ Folic acid containing stalk group was engineered over MSNPs and β -CD ring was threaded on the stalk. Addition of bioactive molecules such as porcine liver esterase caused cleavage of stalk and the drug was released. The studies were further extended into in vitro methodology by delivering anticancer drugs like CPT into U2OS cells.¹⁷¹

5.4.3.3.2 Other nanohybrids

Some functional nanomaterials like quantum dots (QDs), gold nanoparticles, magnetic nanoparticles and graphene oxide are tested in biomedicine. Mulder and co-workers prepared polymer-lipid nanoparticles on gold nanocrystal. Anticancer drug Dox formed an inclusion complex with the β -CD cavity on polymer-lipid nanoparticle. This system was used in the drug delivery.¹⁷² In another study, inclusion complex was formed between β -CD and anticancer drug CPT which was attached to the surface of magnetic nanoparticle by disulfide linkage. This drug delivery system was capable of giving response to reducing agents and external magnetic field. The above mentioned system allows study the in vivo application by magnetic resonance imaging technique.¹⁷³

5.5 Supramolecular hydrogels

Hydrogels (HG) are three dimensional cross-linked molecular network that are capable of holding water by surface tension or capillary effects. The first synthetic polymeric hydrogels were prepared in 1950s. Since then they have been used in variety of applications. Depending on their molecular basis, they can have good biocompatibility and mechanical properties similar to human tissues. So, HGs are used a lot in biomedical applications like carriers for chemotherapeutic reagents or biomolecules.¹⁷⁴⁻¹⁷⁸

Supramolecular hydrogels are prepared by host-guest inclusion. They are divided into two groups. First type is based on polypseudorotaxanes by threading macrocyclic molecules on polymer chain. Polymer cross-linking takes place via hydrogen bond formation between macrocyclic molecules. Such hydrogel was initially developed by Harada et al in 1994 and they continued their work.^{179,180} HGs of the second type are formed from macrocyclic hosts and guest molecules that are conjugated on polymer as a side chains. The host-guest complexation can form cross links between two polymer chains as shown in the Figure 14.¹⁸¹⁻¹⁸⁴

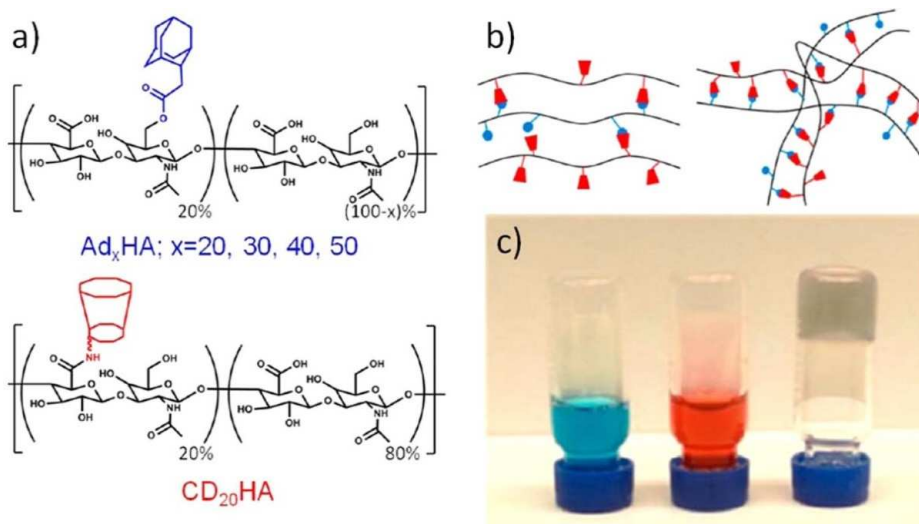


Figure 14: (a) Chemical structure of the host-guest components. (b) Schematic representation of weak network junction (left) and multifold junction (right). (c) Qualitative inversion tests: Ad20HA 5 wt % (blue, left), CD20HA 5 wt % (red, middle), and CD20HA with Ad20HA 5 wt % (purple, right).¹⁸¹⁻¹⁸⁴

Nielsen and coworkers prepared a hydrogel that contained poly vinylpyrrolidone/polyethylene glycol-dimethacrylate (PVP/PEG-DMA) and CDs covalently conjugated with polymer chain. This system was able to deliver the drug ibuprofenate (IBU) slowly.¹⁸⁵ Other researchers loaded lysozyme, β -estradiol and quinine into CD-PEG hydrogel. The drug release rate was found to be dependent upon its interaction with hexamethylated β -CD inside the hydrogel.¹⁸⁶ As it was mentioned above, the host-guest complexes are reversible. This fact was used in the production of stimuli-responsive hydrogels. Stoddart and coworkers prepared a hydrogel which was light sensitive by complexation between azobenzene and β -CD. Zhang and coworkers prepared supramolecular hydrogel from α -CD to form 3D polymer network. Polymer side chain poly(ethyleneglycol)methylether was made to conjugate with heparin polymer main chain. α -CD was mounted on PEG side chains to connect the polymers to form cross-linked polymer networks. This hydrogel was capable of forming an inclusion complex with model drug bovine serum albumin. Release properties were studied with different amounts of α -CD or heparin-PEG conjugate used. Another supramolecular hydrogel was prepared with α -CD and prodrug; PEGylated indomethacin. The properties such as gelation kinetics, mechanical strength, shear thinning behavior, and thixotropic response were studied. Sustained release of drug was observed.¹⁸⁷ Peng and coworkers synthesized a light responsive hydrogel using β -CD and azobenzene. They coupled dextrans separately with both azobenzene and β -CD and mixed together to get inclusion of *trans*-azobenzene with β -CD. This mixture was irradiated at 365 nm to convert (*E*) isomer to (*Z*) form. Consequently, β -CD/azobenzene complex was dissociated causing dissolution of hydrogel. This dissolution made sure the release of protein inside the hydrogel.¹⁸⁸

5.6 Gene delivery

Gene therapy has attracted the researchers in biomedical field. Successful gene delivery depends upon the gene carrier. Supramolecular chemistry for gene therapy has become a hot topic in recent years. Cyclodextrins were extensively studied as gene carriers in this field.

5.6.1 Supramolecular nanoparticles for gene delivery

Davis and coworkers were the first who prepared supramolecular nanoparticles for therapeutic delivery of siRNA. Supramolecular nanoparticles were consisted of cyclodextrin-based linear polymer, Ad-terminated hydrophilic polymer PEG (PEG-Ad), a human transferring (hTf) protein targeting ligand containing PEG-Ad (Ad-PEG-hTf), and siRNA duplex. Non covalent self-assembly interactions between CD and adamantane formed the desired nanoparticles. Targeting ligand hTf was fixed on the surface of these nanoparticles by CD/Ad complexation. The results showed comparable reduction in specific mRNA and target protein level in the tissue after delivery of siRNA which indicated the good efficiency of the system against cancer cells.¹⁸⁹ Thompson and coworkers reported similar supramolecular nanoparticle based gene delivery system containing polyvinylalcohol (PVA) polymer main chain bearing PEG carrying cholesterol pendant by benzylidene acetal linkage. Supramolecular nanoparticles were formed by interaction between β -CD derivative and cholesterol unit. siRNA can be introduced into this nanoparticle either before or after self-assembly process. siRNA was delivered in vitro by using green fluorescence protein (GFP) expressed cell lines. Gene silencing study was carried out by anti-GFP siRNA. After getting into the target cells, cleavage of acid sensitive linkage took place which resulted into the dissociation of supramolecular nanoparticles and release of siRNA. This complex showed better capability of gene silencing as compared to the traditional transfection agents such as PEI or lipofectamine 2000. This gene delivery system was also tested in plasmid DNA (pDNA) delivery as shown in the Figure 15.¹⁹⁰

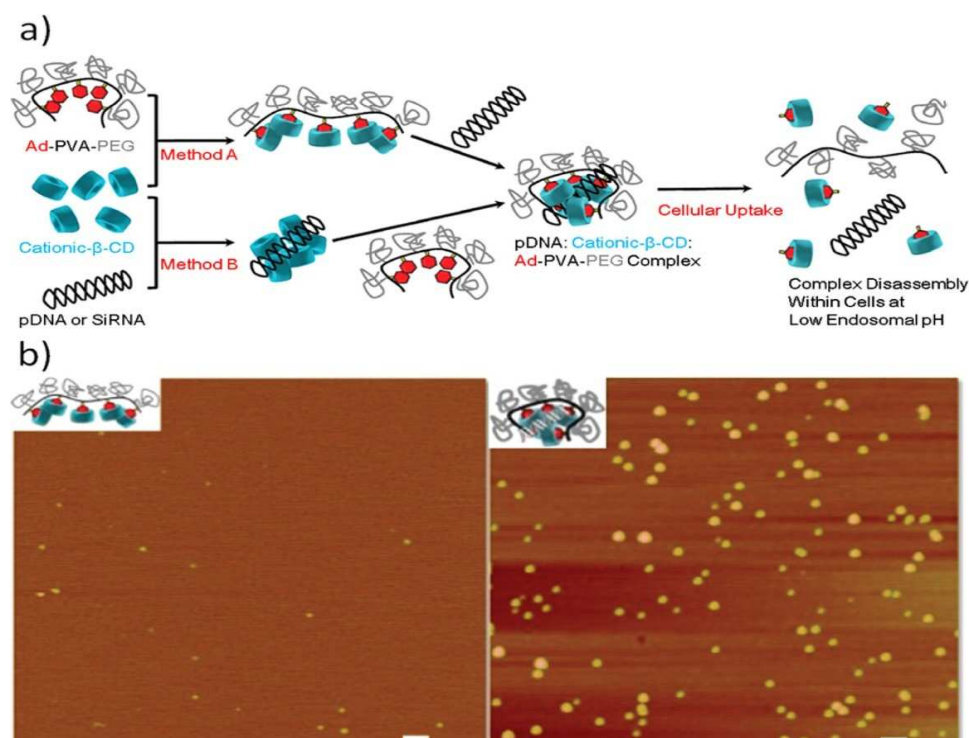


Figure 15: (a) pDNA delivery system prepared based on non-covalent assembly of bioresponsive amino- β -CD/Ad-PVA-PEG complex. (b) AFM images of (left) Chol-PVA-PEG:3 and (right) Chol-PVA-PEG:3:siRNA at N/P = 10. Scale bar = 100 nm.¹⁹⁰

5.6.2 Rotaxanes/polyrotaxanes for gene delivery

Yui and coworkers used polyrotaxanes for siRNA delivery. They studied the relationship between the structure of polyrotaxane and its ability to deliver siRNA efficiently. High amount of dimethylaminoethyl (DMAE)- α -CD mounted on PEG polymer forms better complex with siRNA and intracellular uptake of siRNA is also high. Successful attempt in siRNA transfection caused removal of luciferase expression in HeLa cells. Apart from this success, polyrotaxanes with biocleavable disulfide group showed increased gene silencing as compared to that of without disulfide groups.¹⁹¹ Harashima and coworkers synthesized a non-viral gene vehicle from polyrotaxanes. Initially, they synthesized dimethylaminoethyl-modified α -CD (DMAE- α -CD) mounted on PEG. Both the terminals of PEG were blocked with benzyloxycarbonyl tyrosine via disulfide linkage. The positive charge from DMAE- α -CD interacted with negative charge from pDNA forming polyrotaxane/pDNA complex. Once the complex is entered in target cell, glutathione cleaved disulfide bond and supramolecular complex got dissociated causing release of pDNA which further entered into cell nucleus for treatment.^{192,193}

5.6.3 Other host-guest gene delivery systems

Zhu and coworkers prepared a charge tunable dendritic polycation as gene carrier. Adamantane derivative was coupled onto hyperbranched polyglycerol (HPG) dendrimer to get HPG-Ad. Two types of cationic β -CD derivatives were prepared carrying different amino groups. The host-guest interaction between Ad and β -CD or its derivative stabilized supramolecular dendritic polymer (SDP). They also provide the facility of tuning the surface charge of SDP by changing the ratio of β -CD derivatives with different amino groups. This method was used for development of series of SDPs with different surface charge properties. Their gene transfection efficacy was studied in COS-7 cell line by using luciferase assay and the gene transfection efficiency was obtained. Use of only β -CD caused decrease in surface-charge density of SDPs and the obtained transfection efficiency was dramatically reduced. These results were confirmed by using pDNA-encoding GFP as gene transfection model. The obtained efficacy was comparable with traditional gene delivery system.¹⁹⁴

5.7 Drug/gene delivery multifunctional nanoparticles

Therapeutic efficacy of chemotherapy drugs is sometimes hampered by drug resistance effect. In order to increase this efficacy, anticancer drugs and therapeutic genes are co-delivered to increase the effect of chemotherapy via synergetic treatment. Cyclodextrins have been used in such treatments to co-deliver drug and gene. Ma and coworkers have contributed a lot in the field of drug or gene delivery. They also have contribution in drug/gene co-delivery. Core-shell structure of the co-delivery vehicle was formed by the host-guest interactions between cationic PEI polymer bearing α -CD and a hydrophobic material poly (benzyl L-aspartate) (PBLA) carrying flanking benzyl groups. This nanoparticle had hydrophobic internal core which acted as nanocontainer for hydrophobic drug. The outer surface had strong positive charge which could condense pDNA to achieve transfection/expression efficiency in osteoblast cells. This multifunctional nanoparticle was capable of delivering anticancer drugs and genes like DNA and siRNA.¹⁹⁵

Tang and coworkers prepared a series of drug/gene co-delivery systems which were based on supramolecular nanoparticles. They used host-guest interactions between β -CD and Ad to

make co-delivery nanocarrier. Instead of encapsulating anticancer drug Dox inside β -CD cavity, Ad-conjugated Dox (Ad-Dox) was attached to β -CD which was in conjugation with PEI to load Dox by complexation of CD and adamantane. Then addition of pDNA formed the desired nanoparticle with size of about 140–200 nm. Positively charged nanoparticles prevented the decay of pDNA. Apart from delivering the anticancer drug, this co-delivery system successfully transfected EGFP plasmid on B16F10. In vivo studies were carried out using mice but synergetic effects of chemotherapy and gene therapy were not studied. In further studies, a human tumor necrosis factor-related apoptosis inducing ligand (TRAIL) encoding plasmid gene, pTRAIL was also loaded in above mentioned co-delivery systems.¹⁹⁶

5.8 Bioimaging

Biological images have been proved useful in the diagnosis of diseases. Bioimaging agent must fulfill several criteria such as good biocompatibility, high stability against biochemical degradation, photo bleaching and strong signal generation capacity. Use of supramolecular chemistry improves the properties mentioned above. Host guest complexes are formed between fluorescence dyes and hosts such as CDs. Tseng and coworkers identified a new technique to produce fluorescent supramolecular nanoparticles by forming host-guest complex between β -CD and Ad which were present separately on PEI and PAMAM. Fluorescent dye Cy5 was present onto CD-PEI part. Cellular uptake and targeted fluorescence imaging were studied on U87 and MCF7 cell lines.¹⁹⁷ Other type of supramolecular nanoparticles were prepared by Xu and co-workers who used self-assembly of β -CD modified fluorine copolymer called as PFC6CD. Inclusion complexes were formed between β -CD and many other guest molecules. Different fluorescent spectra were recorded which could be used in organic molecule sensing and cell labeling. Study of MTT (3-(4,5-dimethylthiazol-2-yl)-2,5-diphenyltetrazolium bromide) cytotoxicity assay and in vitro fluorescence imaging using KB cells (Initially derived from an epidermoid carcinoma of the mouth. They contain HeLa marker chromosome) showed good biocompatibility and better cellular uptake of the prepared supramolecular nanoparticles.¹⁹⁸

6 Supramolecular applications of cucurbiturils

6.1 Analytical applications using fluorescence spectrometry

Fluorescence spectrometry is used in the determination of inorganic, bioactive materials and pharmaceutical compounds. In recent years, scientific community has started to show interest in the systems that contained CB[n] and their fluorescent properties have been studied along with their potential applications. CBs can be used in either increasing or quenching fluorescence. Wagner et al reported the 5 folds increase in the fluorescence of 2,6-aminophenyl naphthalene-6-sulfonate in the presence of CB[6].¹⁹⁹ Similar results were observed in case of pesticide carbendazim²⁰⁰, curcumin²⁰¹, 4-aminobipyridine derivatives²⁰² when CB[6] was present. Li et al identified the interactions of CB[n] (n=5,6,7,8) with coptisine and sanguinarine. Upon dropwise addition of CBs to the aqueous solution of coptisine and sanguinarine, increase was observed in the fluorescence. CB[7] exhibits more binding capability as compared to other CBs. Depending on the enhancement observed, spectrofluorometric method was developed for above mentioned two compounds to find their presence in human urine and serum.^{203,204}

Zhou and coworkers developed a method to detect the melamine concentration in tainted milk. They used CB[7] for development of this method. CB[7] forms 1:1 complex with melamine which was detected by fluorescence.²⁰⁵ In similar way, CB[7] forms inclusion complex with carbendazim to allow using of matrix solid-phase dispersion approach for carbendazim determination.²⁰⁶ Pyrene (PYR) is commonly found in tap water in developing and poor countries. CB[6] was used to identify its amount by Sueldo Ocelllo.²⁰⁷ Haung et al studied complex formation between thiabendazole (TBZ) and CB[6], CB[7] and symmetric tetramethyl-cucurbit[6]uril by UV/VIS fluorescence measurement.²⁰⁸ Berberine chloride is capable of making supramolecular interactions with CB[7] in aqueous solution. Increase in the fluorescence of berberine chloride was observed.^{209,210} Wang et al developed a fluorescent probe method for carbachol based on the competitive reaction between carbachol and BER to occupy the CB[7] cavity.²¹¹ Similar study was carried out by Wu et al to develop a fluorometric method for determining the amount of ethambutol by studying the competition between ethambutol and berberine chloride to occupy the CB[7] cavity. This method is useful for determination of ethambutol in bulk and biological fluids.²¹²

CBs are used in quenching of the fluorescence as well. Fluorescent probes such as methylene blue, berberine (BER) and palmatine (PAL) are used. Nicotine possessed low fluorescence which could be detected from cigarettes. It is achieved by quenching methylene blue@CB[7] complex. When nicotine forms inclusion complex with CB[7], it displaces methylene blue and thus fluorescence intensity of the complex is reduced.²¹³ BER and PAL show low fluorescence in aqueous solutions. They react with CB[7] in acidic medium at room temperature to form stable complexes. The fluorescence intensity of these complexes is higher than that of free guests in aqueous solutions.²¹⁴ Highly sensitive and selective quantitative analytical method was developed to determine the amount of herbicide paraquat (PQ). It is based on quenching of the fluorescence intensity of CB[7]-coptisine fluorescent probe when paraquat is added to this system.²¹⁵

6.2 Biomedical applications

6.2.1 Supramolecular nanocarriers

6.2.1.1 Vesicles

As mentioned earlier, vesicles are made from lipid bilayer membrane inside the cell. They are of uniform size, comparatively easy to prepare and possess hollow pores to store the drugs. In 2005, Kim and coworkers prepared vesicles from amphiphilic CB[6] derivative that had triethylene glycol groups at its periphery. The vesicles were modified with molecular tags by host-guest complexation between hydrophobic CB[6] cavity and polyamine.²¹⁶ Reduction sensitive vesicles were formed by introducing redox-responsive disulfide unit into the functional groups present at the periphery of CB[6]. Polyamine conjugated folic acid or fluorescence molecule was attached to the vesicle surface by host-guest complexation for cancer targeted drug delivery. Dox, an anticancer drug was loaded into vesicles and it was effectively delivered into HeLa cancer cells.²¹⁷ Kim and coworkers connected thiols directly with CB[6] derivative carrying alkoxy group at periphery by 'click' reaction to get robust polymer nanocapsule. They embedded disulfide bond into functional groups present at the rim of CB[6] derivative to obtain reduction responsive polymer capsules.²¹⁸ Cancer cell targeting ligand conjugated with polyamine was introduced on the capsule surface by host-guest

interactions. The polymer capsules delivered carboxyfluorescein towards HepG2 liver cancer cells.²¹⁹

6.2.1.2 Micelles

One macrocyclic molecule and two guest compounds interact with each other forming ternary system which can act as an amphiphile for micelles construction. Ji and coworkers used CB[8] to form inclusion complex HPHEEP-CB[8]-PLA with two host amphiphilic units methyl viologen containing hyperbranched polyphosphate (HPHEEP-MV) and indole terminated poly(D,L-lactide) (PLA-IPA). In this system, micelles were formed with PLA facing inside and HPHEEP from outside aqueous medium. When adamantane or Na₂S₂O₄ were added, the micelles were destroyed by binding with CB[8] cavity and previously loaded hydrophobic drug coumarin 102 was released.²²⁰ CB[8], PLA-IPA and methyl viologen terminated polyethylene oxide formed a supramolecular amphiphilic complex which self-assembled into micelles of nano size. Anticancer drug Dox was loaded into these nanoparticles and its release was triggered by adding Na₂S₂O₄. Na₂S₂O₄ forms inclusion complex with CB[8] which can replace PLA-IPA and PEO-MV causing dissociation of supramolecular micelles. Micelles showed good biocompatibility towards cell lines, human umbilical vein endothelial cell line (HUVEC) and human liver cancer HepG2 cell line when studied in vitro. Dox showed higher toxicity for human liver cancer HepG2 cells.²²¹ Loh and coworkers prepared a ternary complex between CB[8], naphthalene-terminated poly(dimethylaminomethyl methacrylate) (PDMAEMA) and methylviologen terminated poly(*N*-isopropylacrylamide) (PNI-PAM). The latter two were responsible for pH and temperature. This complex was able to form micelles which encapsulated anticancer drug Dox. Along with temperature and pH control, the micelles were active towards guest like adamantane. This system showed triple stimuli-responsive drug releasing capacity. The same authors prepared another complex from CB[8] and temperature as well as glucose responsive materials poly(isopropylacrylamide) (PNIPAAm) and poly(acrylamidophenylboronic acid) (PAAPBA). After forming micelles, this system was able to deliver insulin.²²²

6.2.1.3 Supramolecular nanoparticles

6.2.1.3.1 On-off switch on nanoparticles

Basic information about on-off switches is mentioned in section 4.3.3.3.1. Utilization of CBs has gained attention of scientific community in recent years but not much work has been carried out yet. For instance, gold particles were embedded in MSNPs. The gold particles acted as heat generating cores. In addition, nano-gate was formed by host-guest interactions between CB[6] and *N*-(6-aminoethyl)-aminomethyltriethoxysilane. This nano-gate was opened by external laser source causing controlled release of drug.²²³

6.2.1.3.2 Other nanohybrids with host-guest interactions

Jung and coworkers prepared theranostic system by using host-guest interactions between CB[6] and molecules with various functional groups. CB[6] was conjugated on the backbone of hyaluronic acid by host-guest interactions. Various moieties like FITC for bio imaging, anticancer drugs were tied with spermidine which can form inclusion complex with CB[6] in aqueous solution. There are too many good results at laboratory level but its practical application is still too far from the reality.²²⁴ Rotello and coworkers prepared a host-guest system which was anchored on ultra-small gold nanoparticles. Diaminohexane which was

present on the surface of nanoparticles acted as a thread for CB[7]. Addition of diaminohexane to attach CB[7] reduced the cytotoxicity. Subsequently, 1-adamantyl amine was added to replace diaminohexane. This addition caused uncapping of CB[7] inside the living cells thus cytotoxicity of AuNP-NH₂ was activated. This strategy provides new approach for developing theranostic platforms.²²⁵

6.2.1.3.3 Supramolecular hydrogels

Not much work on supramolecular hydrogels has been carried out by using cucurbiturils probably due to lack of effective method for CBs monofunctionalization. Scherman and coworkers reported a multiresponsive supramolecular hydrogel that contained CB[8] which formed an inclusion complex with a guest carrying polyvinyl alcohol. This hydrogel was found to be sensitive for temperature change, chemical potential and competing guests.²²⁶

6.3 Bioimaging

Biological images are useful in diagnosis of diseases. As discussed earlier in cyclodextrins, bioimaging agent must have properties such as good biocompatibility, high stability for biodegradation, and photobleaching and strong signal generation capability. Supramolecular vesicles provide a way to study the fluorescence labeling in biological systems. Some attempts were made to prepare the supramolecular complexes using cucurbiturils. Host-guest complex was formed between CB[7] and Hoechst dye (used for fluorescence enhancement) and studied for external pH change as shown in Figure 16a. In vitro bioimaging was carried out on breast cancer MCF-7 cell line. The fluorescence intensity of CB[7]·Hoechst dye inclusion complex was more than that of free Hoechst dye as shown in Figure 16b and 16c. Apart from this result, the inclusion complex showed good photostability and reduction in DNA binding capability.²²⁷

Finally, Scherman and coworkers synthesized supramolecular vesicles via host-guest inclusion that contained amphiphilic pyrene·viologen·CB[8] ternary complex. Viologen functionalized lipids (Figure 16d) acted as hydrophobic segment in this complex. Supramolecular micelles entered in HeLa cancer cells and successfully delivered the peptide intracellularly. When competitive guest molecules were added, the peptide was released into the cells simultaneously causing switch on of the fluorescence and cytotoxic effects.²²⁸

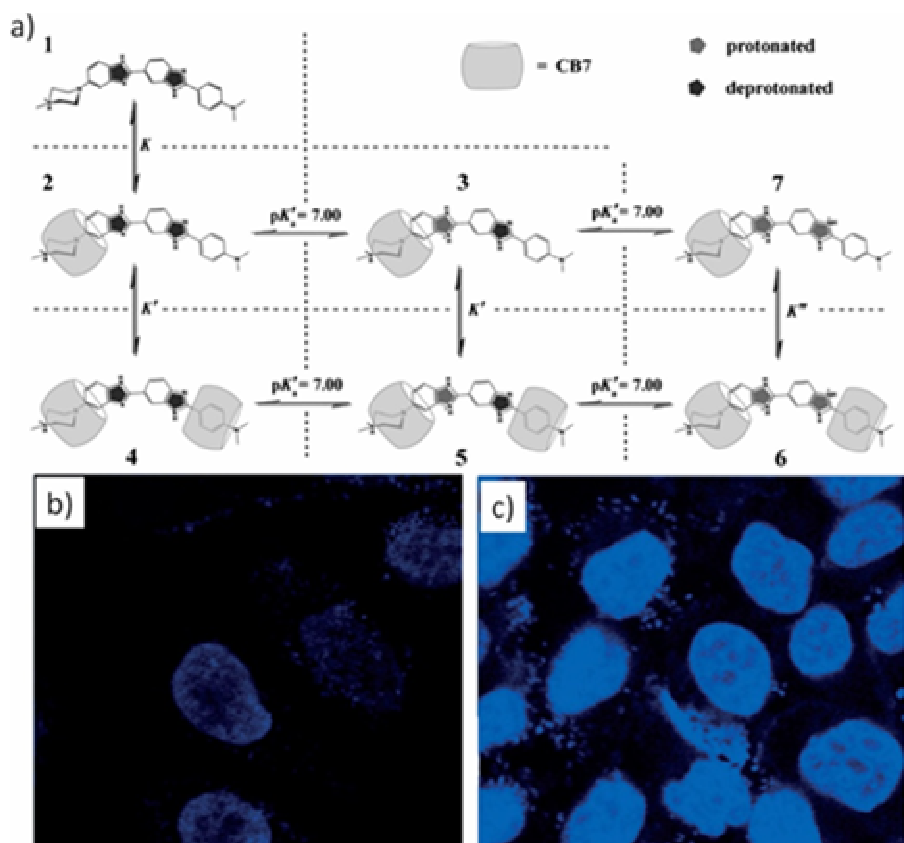
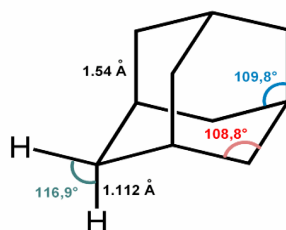


Figure 16: (a) Six major complexes formed between Hoechst 34580 and CB[7] in PBS solution (5 mM, pH 7.0) showing the protonation equilibrium and the host–guest complexation equilibrium. Confocal microscopy images of MCF-7 cells incubated with (b) 5 mM Hoechst 34580 alone or (c) 5 mM Hoechst 34580 and 50 mM CB[7] (d) Structure of viologen functionalized lipid. (e) Structure of the guest Hoechst 34580.²²⁸

7 Adamantane: history, structure, and binding properties

Adamantane is a C₁₀H₁₆ hydrocarbon with three-dimensional cage-like structure. Such cycloalkanes are sometimes referred as diamondoids because their carbon cages fit the crystal lattice of diamond. Adamantane consists of three fused cyclohexane rings with armchair configuration. It is a rigid structure but still strain free as all the C–C–C angle values are close to common tetrahedral angle; i.e., 109.5°. Structure and some geometrical parameters are shown in Figure 17.

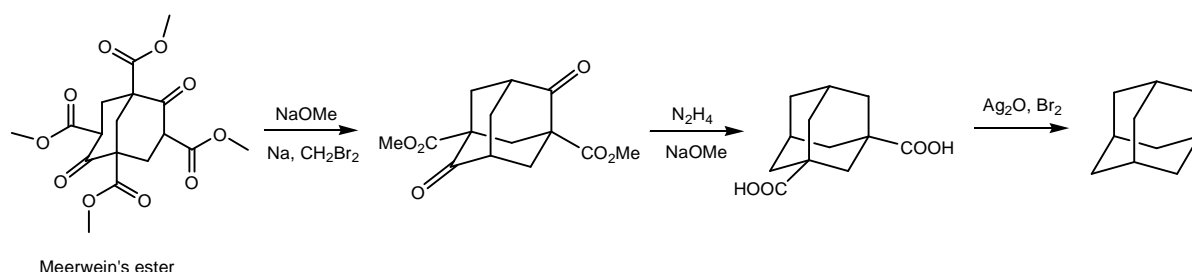
Figure 17: Structure of Adamantane



7.1 Historic overview of adamantane chemistry

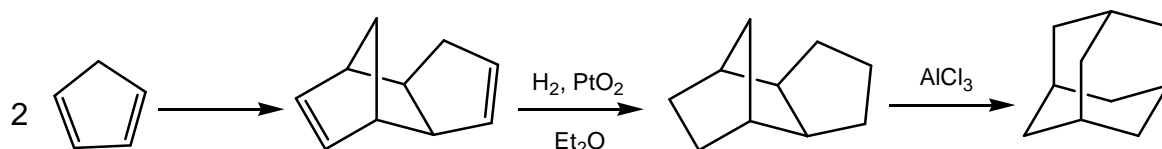
For the first time, adamantane was isolated from the petroleum pool from Hodonin in Czech Republic in 1932 by Landa, Macháček and Mžourek.²²⁹ The first synthesis of adamantane was reported by Vladimir Prelog in 1941. He used Meerwein's ester as a starting compound.^{230, 231} The synthetic approach is as shown in figure 17.

Figure 18: The first synthesis of adamantane



Unfortunately, the overall yield of adamantane was not so only 0.16 %. This yield was improved to 6.5 % by refining Prelog process. The yield of decarboxylation was increased by Heinsdecker reaction and then by Hoffman reaction. However, this improved yield was still very low and synthetic procedure remained too complicated to provide enough of adamantane for extensive studies. The situation was completely changed in late fifties of twentieth century. The first synthesis of adamantane applicable in industrial scale was given by Schleyer in 1957. He hydrogenated dicyclopentadiene and then the hydrogenated product was converted to adamantane by thermal treatment with AlCl₃ (Figure 18).²³²

Figure 19: Synthetic approach from cyclopentadiene towards adamantane



The yield was improved to 30 % to 40 %. Later, the yield of adamantane was increased to 98% by ultrasound and super acid catalysts. Nevertheless, the present method used for industrial production is based on the cheap Lewis acid AlCl₃ to provide adamantane in app. 20% in last rearrangement step.

7.2 Biological activity of 1-adamantanamine (adamantine)

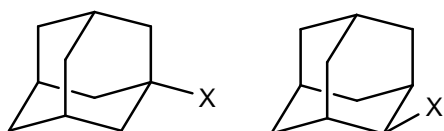
Although the adamantane is intriguing structure, its chemistry was quiet up to sixties with no more than ten papers per year. Very important milestone was reached in 1964 when

antiviral activity of 1-aminoadamantane (adamantine) against influenza virus was reported.²³³ Tissue culture studies have shown that adamantine hydrochloride was capable of blocking the penetration of the host cells by virus. Similar results were observed in the studies with mice and chick embryo. Since then, many adamantane-based compounds with biological activity have been prepared.

7.3 Abundance of 1-monosubstituted and 2-monosubstituted adamantane

Although the adamantane has sixteen hydrogen atoms, there are only two different positions to provide monosubstituted derivatives. The abundance of 1-adamantyl and 2-adamantyl (see Figure 18) in scientific papers is significantly different. The Chemical Abstracts (CAPLUS, SciFinder) returns 5.584 and 1.733 hits for 1- and 2-adamantyl, respectively. This difference can be most likely attributed to the different availability of key adamantane precursors. Since the adamantane is non-polar hydrocarbon, the most important reactions for its cage modification are based on the free radical chemistry. Thus, it is not surprising that more stable radical in bridgehead position is formed and subsequently transformed into 1-adamantyl derivatives. Similarly, carbocation chemistry on adamantane cage prefers the formation of tertiary cation at bridgehead position.

Figure 20: 1-monosubstituted and 2-monosubstituted adamantanes



The synthetic approaches towards 2-substituted adamantane derivatives including 2-adamantanol, 2-haloadamantanes, 2-alkyladamantanes, adamantane-2-carboxylic acid, esters and amides, 2-substituted aldehydes and ketones begin with oxidising adamantane to 2-adamantanone and its subsequent transformation towards required compounds.²³⁴⁻²³⁷ Chemistry of 2-adamantyl derivatives is not as rich as that of 1-adamantyl likely due to longer and less convenient synthetic procedures and lower yields of 2-regioisomers in radical reactions.

7.4 Binding ability of adamantane cage

Since adamantane cage adopts almost sphere shape and is lipophilic, derivatives of adamantane can form inclusion complexes with hydrophobic cavities of macrocyclic hosts; e.g., CDs and CBs. This happens likely due to hydrophobic effect and Van der Waals interactions between adamantane hydrogens and internal cavity surface of these host compounds. Since diameter of the adamantane scaffold is complementary to the internal dimensions of β -CD cavity, the adamantane derivatives are the most suitable guest for inclusion complexes with β -CD. In addition, guests with extraordinary binding strength towards CB[7] can be designed and prepared combining adamantane core with adjacent cationic moiety. Such ultra-affinity guests attack the affinity of biotin towards avidine; i.e., values of association constants are in order of 10^{12} M^{-1} . These properties make adamantane containing compounds very special as they can be used in many purposes and applications. Some of them are summarized in early parts of the Introduction section.

Experimental

8 Synthesis of desired guests

8.1 Apparatus and Methods

8.1.1 Chemicals and Solvents

All solvents, reagents and starting compounds were of analytical grade, purchased from commercial sources without further purification unless mentioned elsewhere. 1,3,5-Tris(bromomethyl)benzene and sodium hydride were purchased from Sigma-Aldrich chemical company. Adamantane-1-carboxylic acid, imidazole and benzimidazole were commercially purchased from Lachema s.r.o. 4-Tolulnitrile was purchased commercially from Mikrochem chemical company. All other reagents such as *N*-bromosuccinimide (NBS), *t*-BuOK and Br₂ were purchased from Merck. DIBAL-H was purchased from Acros Organics. All the solvents used for the reactions were distilled before using.

8.1.2 Instruments

Melting points were measured on a Kofler block and are uncorrected. Elemental analyses (C, H, and N) were determined with a Thermo Fischer Scientific Flash EA 1112. NMR spectra were recorded at 30°C on Bruker Advance III 500 spectrometer operating at frequencies of 500.11 MHz (¹H) and 125.77 MHz (¹³C) and on a Bruker Advance III 300 spectrometer operating at frequencies of 300.13 MHz (¹H) and 75.77 MHz (¹³C). ¹H and ¹³C NMR shifts were referenced to the signal of the solvent [¹H: δ (residual HDO) = 4.70 ppm; ¹H: δ (residual DMSO-*d*₅) = 2.50 ppm; δ(residual CHCl₃) = 7.24 ppm; ¹³C: δ (DMSO-*d*₆) = 39.52 ppm; δ(CDCl₃) = 77.0 ppm]. The spin lock for ROESY was adjusted to 400 ms. The signal multiplicity is indicated by ‘s’ for singlet, ‘d’ for doublet and ‘um’ for unresolved multiplet. IR spectra were recorded using Smart OMNI-Transmission Nicolet iS10 spectrophotometer. Samples were measured in KBr pellets.

8.1.3 Electrospray Mass Spectroscopy (ESI-MS)

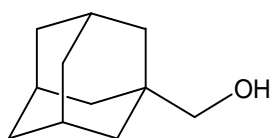
Electrospray mass spectra (ESI-MS) were recorded using an Amazon X ion-trap mass spectrophotometer (Bruker Daltonics, Bremen, Germany) equipped with an electro spray ionization source. All the experiments were conducted in the positive ion-polarity mode. Individual samples were infused into the ESI source in methanol: water (1:1 v:v) and DMSO: water (1:1 v:v) solutions using a syringe pump with a constant flow rate of 4 μl min⁻¹. The other instrumental conditions were as follows: an electrospray voltage of -4.2 kV, a capillary exit voltage of 140 V, a drying gas temperature of 220°C, a drying gas flow rate of 6.0 dm³ min⁻¹ and a nebulizer pressure of 55.16 kPa. *Host-guest complexes*: An aqueous solution of the guest molecule (6.25 μM) and the corresponding host molecule (5.0 and 2.5 eq of β-CD, 3 eq. of CB[7] for binary systems or an aqueous solution of the guest molecule (6.25 μM), CB[7] (1 eq) and β-CD (5.0 eq) for the ternary complexes was infused into the ESI source at a constant flow rate of 4 μl min⁻¹. The other instrumental conditions were as follows: an electrospray voltage of -4.0 kV, a capillary exit voltage of 140 up to -50 V, a drying gas temperature of 300°C, a drying gas flow rate of 6.0 dm³ min⁻¹ and a nebulizer pressure of 206.84 kPa. Nitrogen gas was used as both the nebulizing and drying gas for all of the experiments. Tandem mass spectra were collected using CID with He as the collision gas after the isolation of the required ions.

8.1.4 Isothermal Titration Calorimetry

Isothermal titration calorimetry measurements were carried out in water using a VP-ITC MicroCal instrument at 30 °C. The concentrations of the host in the cell and the guest in the microsyringe were approximately 0.13–0.15 and 0.46–0.50 mM respectively. The raw experimental data were analysed with the MicroCal ORIGIN software. The heats of dilution were taken into account for each guest compound. The data were fitted to a theoretical titration curve using the ‘One Set of Binding Sites’ model. 1-Methyl-3-butylimidazoliumbromide and α -phenylalanine with respective association constants of 1.17×10^7 and $6.72 \times 10^6 \text{ dm}^3 \text{ mol}^{-1}$ were used as competitors.

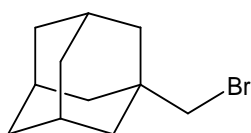
8.2 Guests with tri substituted centrepiece

8.2.1 Synthesis of 1-adamantylmethanol (1)



Procedure was slightly modified from reference.²³⁸ Et₂O (100 cm³) was taken in a three necked round bottomed flask and cooled to 0°C. LiAlH₄ (6.0000 g, 158.10 mmol) was added to it in portions for 30 minutes at 0° C. Resulting suspension was stirred at 0°C for 5 to 10 minutes and then adamantane-1-carboxylic acid (10.0000 g, 55.48 mmol) was added to the reaction mixture at the same temperature. Heat generated along with evolution of H₂ during the addition of adamantane-1-carboxylic acid. Reaction mixture was allowed to cool for few minutes and then refluxed for 40 h. Reaction progress was monitored by GC-MS. Reaction was quenched by 7.5 cm³ of water, 7.5 cm³ of 15% NaOH and finally with 22.5 cm³ of water. The solid formed in the round bottomed flask was filtered and washed with Et₂O (100 cm³). Et₂O layer was taken in separating funnel and washed with 1.16 M aqueous solution of K₂CO₃ (3×100 cm³). Organic layer was dried over anhydrous Na₂SO₄ and evaporated in vacuo. Crude product was recrystallized from hexane to obtain (7.2400 g, 78 % yield, with respect to adamantane-1-carboxylic acid) colourless solid. The product was confirmed by comparing GC-MS and NMR spectra from the reference with isolated product.²³⁹ Reaction was successfully scaled up in later stage to get 29.06 g of compound **1**.

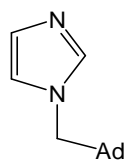
8.2.2 Synthesis of 1-(bromomethyl)adamantane (2)



Compound **1** (29.0000 g, 174.43 mmol) was taken in 1000 cm³ round bottomed flask followed by the addition of 48% HBr solution (56.56 cm³, 499.96 mmol) and zinc dibromide (98.0600 g, 435.40 mmol). Reaction mixture was refluxed at 100°C for 12 hours. Reaction progress was monitored by GC-MS. Upon completion, reaction mixture was cooled to room temperature, water was added to the reaction mixture and extracted with Et₂O (3×500 cm³). Organic layer was dried over anhydrous Na₂SO₄ and evaporated in vacuo. Product was recrystallized from hexane-acetone mixture (48:2 v:v) to obtain **2** (39.1804 g, 98% yield with

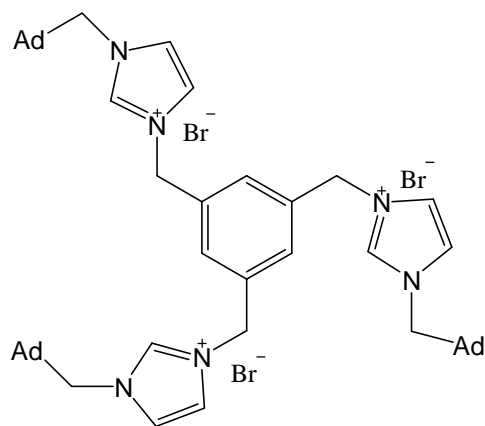
respect to **1**) as a light brown solid. Product was confirmed by comparing with NMR and mass spectra from the reference.²⁴⁰

8.2.3 Synthesis of 1-(1-adamantylmethyl)-1H-imidazole (**3**)



Imidazole (2.0000 g, 29.8 mmol) was dissolved in DMF (20 cm³) and stirred at room temperature for 5 minutes. NaH (60% suspension in mineral oil, 1.2300 g, 30.84 mmol) was added to this suspension in portions at room temperature under nitrogen atmosphere. Solution was stirred at room temperature for 30 min. Then compound **2** (6.6900 g, 29.19 mmol) was added at once. Reaction was heated to 100°C for 26 h. Reaction progress was monitored by TLC as well as GC-MS. Reaction mixture was cooled to room temperature and quenched with cold H₂O (5 cm³) to destroy excess of NaH. Then H₂O (50 cm³) was added to the reaction mixture and extracted with EtOAc (3×100 cm³). Organic layer was dried over anhydrous Na₂SO₄ and evaporated in vacuo. Crude material was purified by recrystallization using hexane-acetone mixture (48:2 v:v) to obtain light yellow coloured crystals (4.8004 g, 76 % yield with respect to **2**) of **3**. Product was confirmed by comparing with NMR and mass spectra available in the literature.²⁴¹ This reaction was scaled up successfully to obtain total 10 g of compound **3** using the same procedure.

8.2.4 Synthesis of α,α',α'' -tris(3-(1-(1-adamantylmethyl)imidazolium))mesitylene tribromide (**4**)



Commercially available 1,3,5-tris(bromomethyl)benzene (TBMB) (0.1000 g, 0.28 mmol) and compound **3** (0.1815 g, 0.84 mmol) were taken in dry toluene (10 cm³) and reaction mixture was heated to 100 °C for 56 h. Reaction progress was monitored by ESI-MS. The compound **3** was added time to time as mass reports showed formation of mono and double quaternarized compound. After 50 h of heating, reaction showed the formation of colourless solid. Upon completion of reaction confirmed by ESI-MS, reaction was allowed to cool to room temperature. Dry THF (30 cm³) was added to reaction mixture. The solid was collected by centrifugation, washed by dry THF (30 cm³) to remove all soluble impurities. Dried in vacuo to get **4** as a colourless solid (0.3020 g, 78 % yield with respect to TBMB).

Melting point: 204–206 °C

Elemental Analysis: C, 57.12%; H, 7.19%; N, 7.53% (calculated for tetrahydrate).

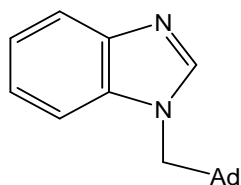
^1H NMR (DMSO- d_6): δ = 1.45 (um, 18H), 1.55 (um, 9H), 1.67 (um, 9H), 1.96 (um, 9H), 3.98 (s, 6H), 5.52 (s, 6H), 7.62 (s, 3H), 7.71 (um, 3H), 7.90 (um, 3H), 9.50 (um, 3H) ppm.

^{13}C NMR (DMSO- d_6): δ = 27.4, 33.2, 36.0, 38.9, 51.3, 59.9, 122.0, 124.3, 128.8, 136.2, 136.9 ppm.

IR (KBr disc): 651 (m), 750 (m), 876 (w), 1105 (m), 1134 (m), 1157 (s), 1176 (m), 1449 (s), 1559 (s), 2846 (s), 2902 (s), 3065 (m), 3127 (m), 3415 (bs) cm^{-1} .

ESI-MS: m/z 149.3, 255.3, 308.3, 382.4, 422.3.

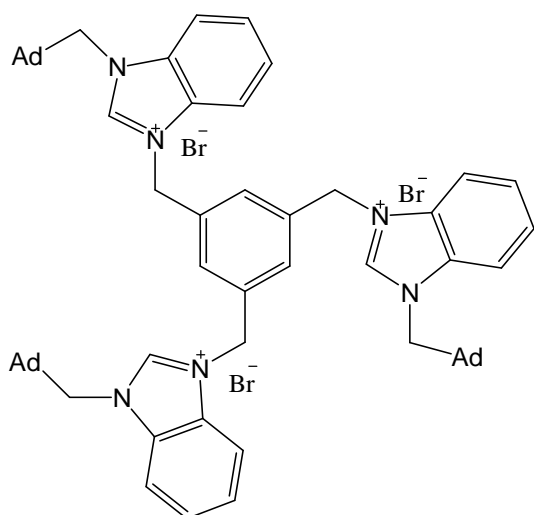
8.2.5 Synthesis of 1-(1-adamantylmethyl)-1H-benzo[d]imidazole (5)



Benzimidazole (2.0000 g, 16.92 mmol) was taken in DMF (20 cm^3) under nitrogen atmosphere and stirred at room temperature. NaH (60% suspension in mineral oil, 0.7110 g, 17.77 mmol) was added to this solution in portions. Solution was stirred at room temperature for 30 min. followed by the addition of **2** (3.8600 g, 16.84 mmol) at once. Reaction mixture was heated to 100 $^\circ\text{C}$ for 26 h. Reaction progress was monitored by TLC as well as GC-MS. Reaction mixture was cooled to room temperature and quenched with cold H_2O (5 cm^3) to destroy excess of NaH. Then H_2O (50 cm^3) was added to the reaction mixture and product was extracted with EtOAc (3 \times 100 cm^3). Organic layer was dried over anhydrous Na_2SO_4 and evaporated in vacuo. Crude material was purified by recrystallization using hexane-acetone mixture (49:2 v:v) to yield **5** as a cream coloured solid (3.5300 g, 79 % yield with respect to **2**). Product formation was confirmed by comparing NMR and mass spectra from the literature.²⁴¹ This reaction was scaled up successfully to get 10 g of the compound **5** using the same procedure.

8.2.6 Synthesis of α,α',α'' -tris(3-(1-(1-adamantylmethyl)benzo[d]imidazolium))mesitylene tribromide (pentahydrate) (6)

Commercially available TBMB (0.1000 g, 0.28 mmol) and **5** (0.2390 g, 0.90 mmol) were taken in 15 cm^3 of toluene in a 100 cm^3 round bottomed flask under nitrogen atmosphere and reaction mixture was heated to 100 $^\circ\text{C}$ for 56 h. Reaction progress was monitored by ESI-MS. **5** was added time to time as mass reports showed formation of mono and doubly quaternarized compounds. After 50 h, reaction showed the formation of colourless solid. Upon completion of reaction (confirmed by ESI-MS), reaction was allowed to cool to room temperature. Dry THF (30 cm^3) was added to reaction mixture. The solid was collected by centrifugation, washed with dry THF (30 cm^3) to remove all soluble impurities. Organic layer was evaporated in rotary evaporator to get **6** as a pentahydrate and colourless solid (0.2400 g, 69 % yield).



Melting point: 273–275 °C

Elemental analysis: C, 60.64%; H, 6.64%; N, 6.53% (calculated for pentahydrate).

^1H NMR (DMSO- d_6): δ = 1.55-1.57 (um, 27 H), 1.65 (um, 9H), 1.95 (um, 9H), 4.34 (s, 6H), 5.81 (s, 6H), 7.47 (dd, J = 7.9 Hz, 3H), 7.64 (dd, J = 8 Hz, 3H), 7.82 (d, J = 8.4 Hz, 3H), 7.88 (s, 3H), 8.14 (d, J = 8.5 Hz, 3H), 10.20 (s, 3H) ppm.

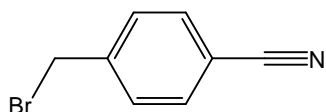
^{13}C NMR (DMSO- d_6): δ = 27.4, 34.3, 35.9, 39.1, 49.3, 57.3, 113.5, 114.4, 126.2, 126.5, 128.7, 130.2, 132.6, 135.6, 143.2 ppm.

IR (KBr disc): 1177 (m), 1200 (m), 1344 (m), 1366 (m), 1426 (m), 1448 (m), 1559 (s), 2846 (s), 2901 (s), 3405 (bs) cm^{-1} .

ESI-MS: m/z 149.1, 305.2, 383.3, 497.3.

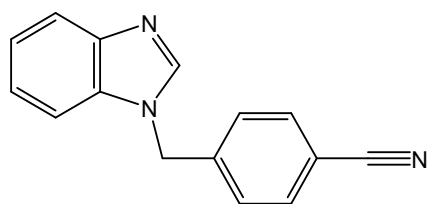
8.3 Guests with disubstituted centrepiece

8.3.1 Synthesis of 4-(bromomethyl)benzonitrile (**7**)



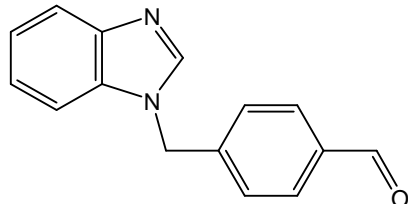
This compound was prepared via slightly modified procedure from the literature.²⁴² 4-Tolunitrile (5.0000 g, 42.68 mmol), NBS (7.5900 g, 42.65 mmol) and catalytic amount of dibenzoyl peroxide were taken in CCl_4 (40 cm^3) under nitrogen atmosphere. Reaction was refluxed at 80°C under the influence of (W-lamp, 60 W) light for 4 h. Reaction progress was monitored by GC-MS. Upon completion of reaction, reaction mixture was cooled to room temperature, filtered to remove succinimide. H_2O (100 cm^3) was added to the CCl_4 layer to remove any traces of succinimide and product was extracted with chloroform (3×200 cm^3). Organic layer was dried over anhydrous Na_2SO_4 and evaporated on rotary evaporator. Crude material was recrystallized from hexane-acetone mixture (49:2 v:v) to obtain light yellow crystals of **7** (4.700 g, 57 % yield). The product was confirmed by comparing NMR and mass spectra available in literature.²⁴²

8.3.2 Synthesis of 4-((1*H*-benzo[*d*]imidazol-1-yl)methyl)benzonitrile (**8**)



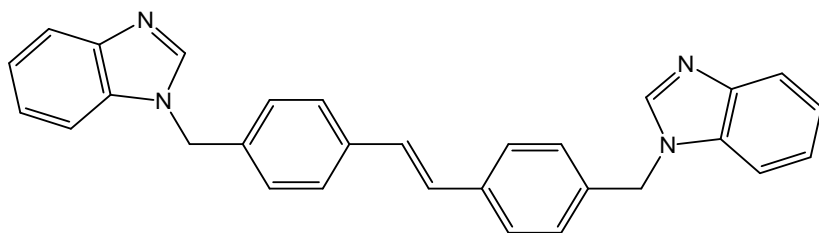
The synthetic procedure was adopted from the literature.²⁴³ Benzimidazole (1.2000 g, 10.16 mmol) was dissolved in DMF (20 cm³) under inert atmosphere. NaH (60% suspension in mineral oil, 0.4280 g, 10.71 mmol) was added to it in portions at room temperature. Reaction mixture was allowed to stir at room temperature for 30 min. To this mixture, 4-(bromomethyl) benzo nitrile (2.0000 g, 10.20 mmol) was added. Reaction mixture was heated to 100 °C for 5 h. Reaction progress was monitored by GC–MS. After all the starting material was consumed, reaction was cooled to room temperature and excess of NaH was quenched by ice cold H₂O (5 cm³). Ice cold H₂O (70 cm³) was added to the reaction mixture and product was extracted with EtOAc (3×100 cm³). Organic layer was dried over anhydrous Na₂SO₄ and evaporated in rotary evaporator. Crude material was purified by column chromatography on silica gel column eluted in MeOH:CHCl₃ (2:98 v:v) system. Upon evaporation light yellow coloured compound **8** (1.700 g, 72 % yield with respect to benzimidazole) was obtained. The product was confirmed by comparing NMR and mass spectrometric data from literature.²⁴³

8.3.3 Synthesis of 4-((1*H*-benzo[*d*]imidazol-1-yl)methyl)benzaldehyde (**9**)



Compound **8** (0.2000 g, 0.86 mmol) was taken in benzene (10 cm³) under nitrogen atmosphere and DIBAL-H (1.2 M in toluene, 1.78 cm³, 2.144 mmol) was added to the reaction mixture dropwise at room temperature over the period of 5 min. Reaction mixture was heated to 45 °C for 30 min under inert atmosphere. Reaction progress was monitored by GC–MS. Upon completion, reaction mixture was cooled to room temperature and poured into 5 cm³ 20% ice cold sulphuric acid solution and cooled to 0 °C. Above mixture was basified with 20% NaOH solution. Extraction was carried out using EtOAc (3×30 cm³). Organic layer was dried over anhydrous Na₂SO₄, evaporated in rotary evaporator. Crude material was purified over silica gel column eluted in MeOH:CHCl₃ (2:98 v:v) system to get **9** as (0.1000 g, 49 % yield with respect to **8**) off-white solid material. This compound was confirmed by comparing NMR and mass spectrometric data with standard literature.⁶ Synthetic procedure from literature was used to synthesize this compound with change in temperature.²⁴⁴ Same compound was scaled up for more 0.2 g.

8.3.4 Synthesis of (*E*)-(4,4'-bis((1*H*-benzo[*d*]imidazol-1-yl)methyl)stilbene (10)



McMurry coupling was carried out using slightly modified procedure from the literature.²⁴⁵ Zn powder (0.5930 g, 9.07 mmol) was taken in dry THF (5 cm³) under argon atmosphere and was cooled to -5 °C. TiCl₄ (0.5 cm³, 4.56 mmol) was added dropwise so that the inner temperature does not exceed 10 °C. This suspension was warmed to room temperature and stirred for 30 min followed by reflux for 2.5 h. Reaction mixture was cooled to -5 °C and charged with pyridine (0.183 cm³, 2.26 mmol) and stirred for 10 min at -5 °C. Compound **9** (0.2140 g, 0.9067 mmol) was dissolved in dry THF (5 cm³) and added to above mentioned reaction mixture dropwise. Reaction mixture was refluxed at 70 °C for 4 h. Completion of reaction was observed by TLC. Reaction mixture was cooled to 0 °C and saturated solution of NaHCO₃ was added dropwise till the evolution of CO₂ stops. Reaction mixture was filtered and the residue was washed with EtOAc till all the product is transferred to filtrate. This mixture was extracted with EtOAc (3×30 cm³). Organic layer was dried over anhydrous Na₂SO₄, evaporated in rotary evaporator. Crude material was purified on silica gel column eluted in MeOH:CHCl₃ (2:98 v:v) system to get **10** (0.0032 g, 0.8% yield with respect to **9**) as off white solid.

Melting Point: 238–241 °C

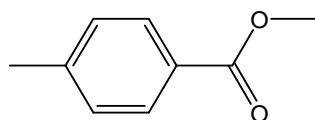
ESI-MS: m/z 441.2

¹H NMR (DMSO-*d*₆): δ = 5.49 (s, 4H), 7.18-7.20 (m, 6H), 7.29-7.31 (d, 4H), 7.50-7.54 (m, 6H), 7.65-7.66 (d, 2H), 8.40 (s, 2H) ppm.

¹³C NMR (DMSO-*d*₆): δ = 47.5, 110.8, 119.6, 121.6, 122.4, 126.8, 127.9, 128.2, 133.7, 136.4, 136.6, 143.7, 144.3 ppm.

IR (KBr disc) : 422 (m), 526 (m), 611 (w), 634 (w), 738 (s), 814 (m), 845 (w), 887 (w), 928 (w), 972 (m), 1099 (m), 1199 (m), 1261 (s), 1280 (w), 1334 (m), 1367 (m), 1440 (m), 1458 (m), 1493 (s), 1612 (w), 1720(m), 2850 (w), 2920 (m), 3026 (w), 3448 (bs) cm⁻¹

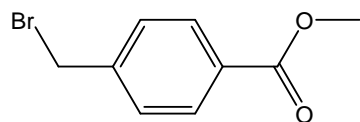
8.3.5 Synthesis of methyl 4-methylbenzoate (11)



CH₃OH (21.0000 cm³, 518.46 mmol) was taken in a 500 cm³ sized round bottomed flask and dry pyridine (39.76 cm³, 491.60 mmol) was added. 4-Methylbenzoyl chloride (20.00 g, 129.37 mmol) was added to above mentioned reaction mixture dropwise at room temperature under nitrogen atmosphere. Reaction was stirred at room temperature for 5 h. Reaction was monitored by GC-MS. Upon completion, reaction mixture was poured over crushed ice. After 2 minutes, solid formation takes place. The solid was filtered and washed with plenty of

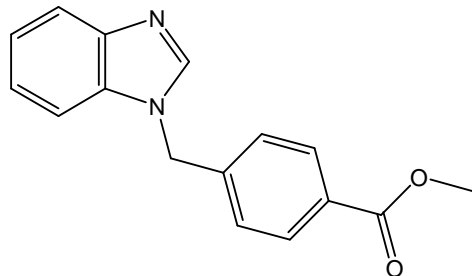
water till the smell of pyridine disappeared. Vacuum drying yielded **11** (16.00 g, 82 % yield with respect to 4-methylbenzoyl chloride) as a white solid. The product was confirmed by comparing NMR and mass spectra with the data available in literature.²⁴⁶ The reaction was scaled up as per the need.

8.3.6 Synthesis of methyl 4-(bromomethyl)benzoate (**12**)



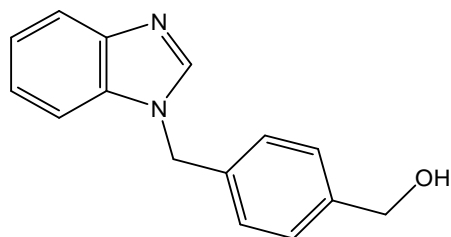
Compound **11** (5.0000 g, 33.29 mmol), NBS (5.9200 g, 33.30 mmol), and catalytic amount of dibenzoyl peroxide were taken in dry DCM (50 cm³) and refluxed under the influence of light (W-lamp, 60 W) for 5 h under nitrogen atmosphere. Reaction progress was monitored by TLC and GC-MS. Upon completion, reaction was cooled to room temperature and H₂O (150 cm³) was added. Extraction was carried out with DCM (3×75 cm³). Organic layer was washed with plenty of H₂O to remove the traces of succinimide. Organic layer was dried over anhydrous Na₂SO₄ and evaporated in rotary evaporator. Crude material was recrystallized from hexane to obtain **12** (4.300 g, 56 % yield with respect to **11**) as a light yellow solid. Product was confirmed by comparing the mass and NMR spectra with the data available in the literature.²⁴⁷ This reaction was scaled up as per the requirement.

8.3.7 Synthesis of methyl 4-((1*H*-benzo[*d*]imidazol-1-yl)methyl)benzoate (**13**)



Benzimidazole (7.1100 g, 60.24 mmol) was dissolved in DMF (100 cm³) under nitrogen atmosphere. NaH (60% suspension in oil, 2.9100 g, 72.79 mmol) was added to above solution in portions over a period of 10 min. The reaction mixture was stirred at room temperature for 30 min. **12** (11.5000 g, 50.2 mmol) was added to the reaction mixture at once. The colourless mixture became dark red. Reaction mixture was heated to 100 °C for 4 h. Reaction progress was monitored by TLC and GC-MS. Reaction mixture turned yellow in colour and appeared dense. Upon completion, reaction mixture was cooled to room temperature and poured over crushed ice to quench excess of NaH. After the ice was dissolved, product was extracted with EtOAc (4×500 cm³). Organic layer was washed with ice cold H₂O (3×200 cm³) to remove DMF. Organic layer was dried over anhydrous Na₂SO₄, evaporated in rotary evaporator. Crude material was purified in silica gel column eluted with MeOH:CHCl₃ (2:98 v:v) system to get light yellow coloured **13** (9.0606 g, 68% yield with respect to **12**). Product was confirmed by comparing the NMR and mass spectra with the standard spectra from literature.²⁴⁸ Reaction was scaled up as per the requirement.

8.3.8 Synthesis of 4-((1*H*-benzo[*d*]imidazol-1-yl)methyl)phenyl)methanol (**14**)



Procedure was adopted from the literature.²⁴⁹ LiAlH₄ (1.7800 g, 46.89 mmol) was added in dry THF (30 cm³) in portions over a period of 15 min at 0 °C. Reaction mixture was stirred at 0 °C for 10 min. **13** (2.500 g, 9.39 mmol) was dissolved in 15 cm³ of dry THF and this solution was added to the suspension of LiAlH₄ in THF at 0°C over a period of 15 minutes. Reaction was brought to room temperature and stirred for 3 h under nitrogen atmosphere. Reaction progress was monitored by GC–MS. Upon completion, reaction mixture was quenched by EtOAc (8 cm³). Reaction mixture was stirred at 0 °C till the formation of solid which was filtered by using Büchner funnel. This solid was washed with plenty of EtOAc till all the product comes out of it. Collected portions of EtOAc were washed with H₂O (50 cm³), dried over anhydrous Na₂SO₄ and evaporated in rotary evaporator. Crude product was purified from silica gel column eluted in MeOH:CHCl₃ (2:98 v:v) system to obtain **14** as cream coloured product (2.2300 g, 100 % yield with respect to **13**).

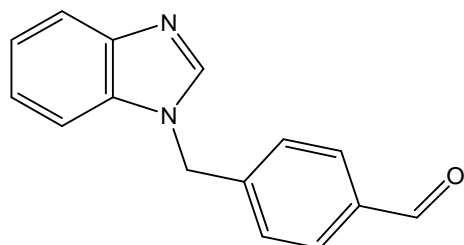
Melting point: 137–139 °C

¹H NMR (DMSO-*d*₆): δ = 4.47 (s, 2H), 5.69 (s, 2H), 7.32-7.33 (m, 2H), 7.41-7.42 (m, 2H), 7.49-7.51 (m, 2H), 7.79–7.84 (m, 2H), 9.48 (s, 1H) ppm. (Signal for —OH proton is lost in DMSO-*d*₆ peak)

¹³C NMR (DMSO-*d*₆): δ = 48.9, 62.3, 78.5, 78.8, 79.0, 112.6, 116.0, 125.0, 125.1, 126.7, 127.6, 132.9, 142.7 ppm.

IR (KBr disc) : 424 (w), 505 (w), 569 (w), 719 (w), 740 (s), 779(m), 829 (w), 893 (w), 958 (w), 979 (w), 1016 (m), 1173 (w), 1190 (m), 1261 (m), 1284 (m), 1346 (w), 1381 (w), 1421 (w), 1458 (m), 1496 (s), 1614 (w), 2341 (w), 2360 (m), 2862 (w), 2935 (w), 3259 (bs) cm⁻¹

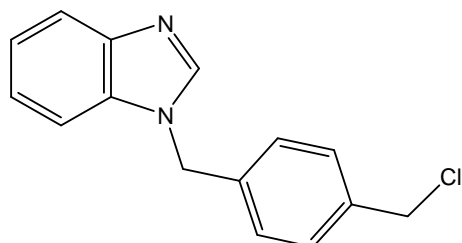
8.3.9 Synthesis of 4-((1*H*-benzo[*d*]imidazol-1-yl)methyl)benzaldehyde (**9**)



H₅IO₆ (3.4700 g, 15.22 mmol) was allowed to dissolve in dry CH₃CN (30 cm³) under inert atmosphere. After dissolution of H₅IO₆, Cr(III) acetylacetonate (0.2660 g, 7.61 mmol) was added. Then **14** (1.8100 g, 7.60 mmol) was added at once under nitrogen atmosphere. Reaction mixture was stirred at room temperature for 7 h. Reaction progress was monitored by GC–MS and TLC. After completion, saturated solution of Na₂SO₃ (100 cm³) was added. Extraction was carried out by using EtOAc (3×400 cm³). Organic layer was dried over

anhydrous Na_2SO_4 and evaporated in rotary evaporator. Crude material was purified with silica gel column eluted in $\text{MeOH}:\text{CHCl}_3$ (2:98 v:v) to get off white coloured **9** (1.52 g, 85% yield with respect to **14**). This compound was confirmed by comparing NMR and mass spectrometric data with standard literature.²⁴³

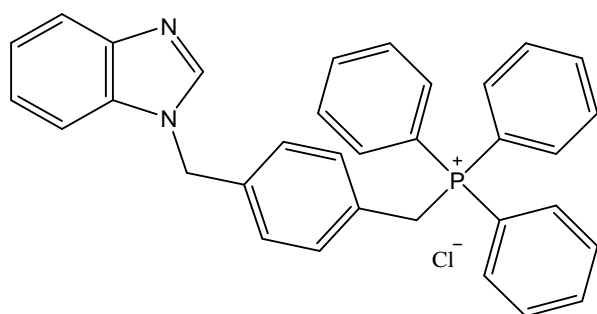
8.3.10 Synthesis of 1-(4-(chloromethyl) benzyl)-1H-benzo[d]imidazole (**15**)



Compound **15** was prepared by slightly modified procedure from PhPCl_4 to SOCl_2 and time of reflux was reduced to 30 min²⁵⁰. **14** (0.6770 g, 2.84 mmol) was taken in SOCl_2 (8 cm^3 , 0.1102 mol) and refluxed for 30 min. Reaction progress was monitored by GC-MS. After completion, reaction mixture was cooled to room temperature and excess of SOCl_2 was evaporated in rotary evaporator to get highly viscous material. To this material was added saturated solution of Na_2CO_3 till pH turned basic (till 8). Then extraction was carried out using EtOAc ($3 \times 100 \text{ cm}^3$). Organic layer was dried over anhydrous Na_2SO_4 and evaporated in rotary evaporator. Evaporation was stopped immediately after slightly gummy material appeared. Chloroform (20 cm^3) was added to this material and used for ylide formation immediately. The GC-MS report taken during reaction monitoring confirmed the formation of **15**. No NMR and other analyses except GC-MS were taken as product was highly unstable and could not be stored for long time.

GC-MS Analysis: m/z 256

8.3.11 Synthesis of 4-((1H benzo[d]imidazolyl-1-yl)methylbenzyl)triphenylphosphonium chloride (**16**)



This compound was prepared by using the slightly modified procedure from literature with change in solvent from toluene to CHCl_3 .²⁵¹ **15** (0.6770 g, 2.64 mmol) was taken in CHCl_3 (20 cm^3) and PPh_3 (1.0400 g, 3.97 mmol) was added. Reaction was heated to 60°C for a period of 72 h. CHCl_3 was added time to time to the reaction mixture as the quantity of chloroform kept on reducing. Reaction progress was monitored by TLC. Reaction was never completed as traces of alkyl chloride were still present after 72 h. Dry Et_2O (30 cm^3) was added to reaction mixture to solidify the product which was isolated by centrifugation process. Product was washed with dry Et_2O (40 cm^3) for 3 times to remove all the traces of

starting material. Product was dried in rotary evaporator to get fine colourless powder of **16** (1.2000 g, 88% yield with respect to **15**).

Melting point: 280–283°C

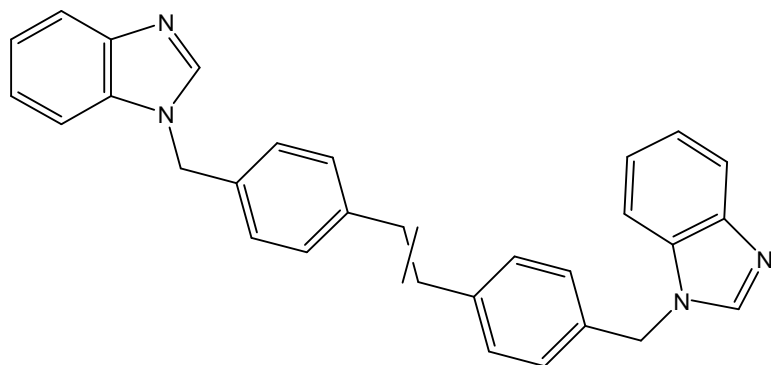
ESI-MS: m/z 483.2

^1H NMR (CD_3OD): $\delta = 4.87\text{--}4.90$ (d, 2H, signal splitting of 2H attached to PPh_3 group due to heteronuclear coupling, $^2J(\text{H,P}) = 14.8$ Hz), 5.48 (s, 2H), 6.95–6.96 (d, 2H), 7.14–7.15 (d, 2H), 7.56–7.65 (m, 15H), 7.83–7.87 (m, 4H), 8.32 (s, 1H) ppm.

^{13}C NMR (CD_3OD): $\delta = 20.8, 102.4, 109.1, 109.8, 110.6, 114.4, 114.9, 119.3, 119.7, 121.8, 123.1, 125.1, 125.7, 126.9, 129.0, 134.4, 135.3$ ppm.

IR (KBr disc): 428 (w), 482 (s), 555 (m), 636 (w), 690 (s), 719 (s), 746 (s), 850 (w), 995 (w), 1111 (s), 1190 (w), 1261 (w), 1284 (w), 1325 (w), 1363 (w), 1383 (w), 1437 (s), 1491 (m), 1514 (w), 1612 (w), 2785 (w), 2856 (w), 2987 (w), 3055 (w), 3423 (bs) cm^{-1}

8.3.12 Synthesis of (*E*)/(*Z*)-(4,4'-bis((1*H*-benzo[*d*]imidazol-1-yl)methyl)stilbene (**17**)



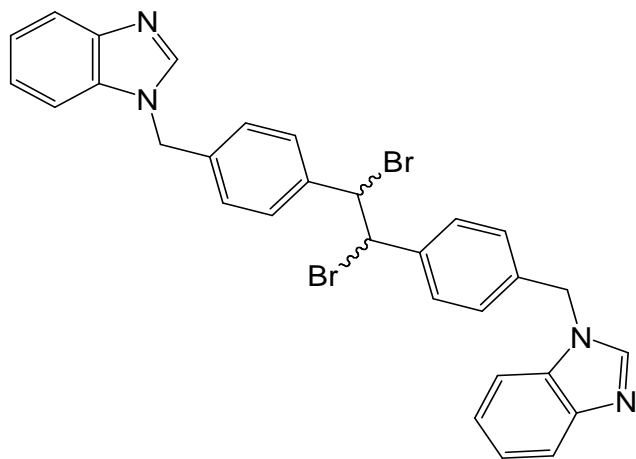
Compound **9** (0.9000 g, 3.813 mmol) was dissolved in 25 cm^3 of DCM. **16** (1.9800 g, 3.82 mmol) was added. 25 cm^3 of 0.1 M NaOH solution was added to the reaction mixture and stirred for 6 h at room temperature under nitrogen atmosphere. Completion of reaction was confirmed by TLC. H_2O (50 cm^3) was added to the reaction mixture and product was extracted with CHCl_3 (3 \times 100 cm^3). CHCl_3 layer was dried over anhydrous Na_2SO_4 and evaporated in rotary evaporator. Crude material was purified by silica gel column eluted with MeOH: CHCl_3 (2:98 v:v) system as a mixture of (*E*) and (*Z*) isomers. NMR spectrum confirmed 40:60 mixture of (*E*) and (*Z*) isomers. Mixture appeared light yellow solid in appearance (1.2600 g, 75 % yield with respect to **9**). Numerous attempts to separate the mixture were performed but none of them was of any use.

ESI-MS: m/z 441.2, 301.1, 221.1

^1H NMR (DMSO-d_6): $\delta = 5.44$ (s), 5.49 (s), 6.56 (s), 7.11–7.18 (m), 7.29–7.30 (m), 7.48–7.55 (m), 7.65–7.67 (m), 8.38–8.41 (m) ppm.

8.3.13 Bromination of 17 (18)

Bromination was carried out by using the procedure mentioned in the literature.²⁵² **17** (0.6000 g, 1.363 mmol) was dissolved in dry CHCl_3 (15 cm^3) under inert atmosphere. Br_2 (0.077 cm^3 , 1.50 mmol) was added dropwise to the reaction mixture. Reaction was heated to 60°C for 4 h. Reaction progress was monitored by TLC. As time passed, product **18** started to appear in the reaction mixture as a solid and after 3 h, product **18** subsided at the bottom of round bottomed flask leaving CHCl_3 layer clear. Reaction was cooled to room temperature and CH_3OH (30 cm^3) was added to the reaction mixture to dissolve all the solid material. Solid $\text{Na}_2\text{S}_2\text{O}_3$ was added to above mixture directly to quench the excess of bromine. Anhydrous Na_2SO_4 was added to this mixture to remove the traces of water and organic layer was evaporated in rotary evaporator. The solid material was analysed on ESI-MS and NMR which confirmed the formation of isomeric mixture. Both the compounds were impossible to separate on column as the solubility of the mixture was very poor. Hence, crude product was taken for next step without separation and purification.

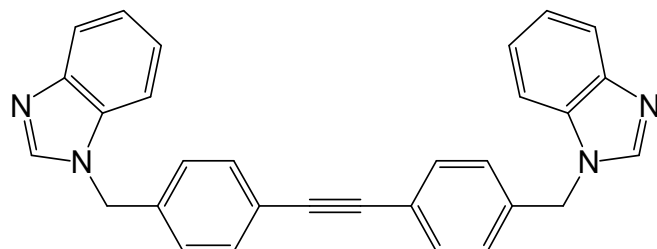


The reaction produced **18** (0.8630 g, 53% yield with respect to **17**) light brown coloured solid. Being mixture, it was not possible to measure melting points and IR spectra.

ESI-MS: m/z 601.1, 441.2, 212.9

^1H NMR (DMSO-d_6): δ = 5.57 (s), 5.72 (s), 6.11 (s), 7.24–7.25 (m), 7.42–7.49 (m), 7.59–7.63 (m), 7.80–7.84 (m), 9.41 (s), 9.53 (s) ppm.

8.3.14 Synthesis of (1,2-bis((1H-benzo[d]imidazol-1-yl)methyl)phenyl)ethyne (19)



The procedure with slight modifications was adopted from the literature.²⁵³ Mixture (**18**) (1.9400 g, 3.23 mmol) was taken in $t\text{-BuOH}$ (30 cm^3), $t\text{-BuOK}$ (1.8100 g, 16.13 mmol) was added and reaction mixture was heated to 80°C for 6 h under nitrogen atmosphere. Reaction progress was monitored by TLC. After completion, mixture was cooled to room temperature

and H₂O (100 cm³) was added. Extraction was carried out using CHCl₃ (3×100 cm³). CHCl₃ layer was dried over anhydrous Na₂SO₄ and evaporated in rotary evaporator to get **19** (1.4100 g, 73% yield with respect to **18**) as yellow solid. Because of poor solubility, no further purification was done.

Melting point: 217–219 °C

ESI-MS: m/z 439.2, 321.1

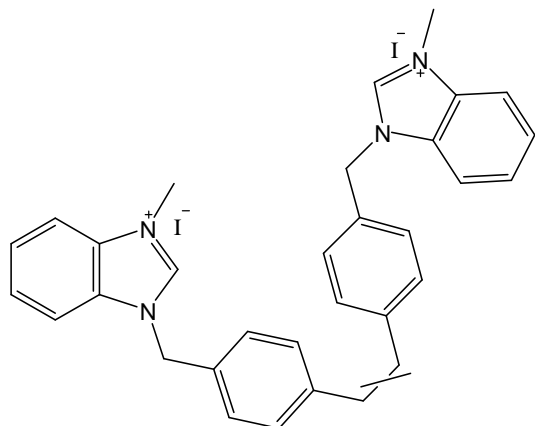
¹H NMR (DMSO-d₆): δ = 5.54 (s, 4H), 7.17–7.20 (m, 4H), 7.30–7.32 (m, 4H), 7.49–7.50 (m, 6H), 7.66–7.67 (d, 2H), 8.40 (s, 2H) ppm.

¹³C NMR (DMSO-d₆): δ = 47.2, 89.1, 110.5, 119.4, 121.4, 121.5, 122.4, 126.6, 127.6, 127.7, 131.6, 137.6 ppm.

IR (KBr disc): 424 (w), 509 (w), 611 (w), 739 (s), 760 (w), 779 (w), 812 (m), 854 (w), 887 (w), 974 (w), 1117 (w), 1190 (m), 1263 (m), 1282 (w), 1334 (w), 1367 (m), 1415 (w), 1438 (m), 1458(m), 1493 (s), 1518 (w), 1614 (w), 1693 (w), 2341 (w), 2360 (w), 2850 (w), 2922 (m), 3444 (bs) cm⁻¹

8.4 Synthesis of quaternary ammonium salts

8.4.1 Synthesis of (*E*)/(*Z*)-(3-methyl-1-((4-(-2-(4-((3-methyl-1*H*-benzo[*d*]imidazol-1-yl)methyl)phenyl)vinyl)phenyl)methyl)-1*H*-benzo[*d*]imidazolium diiodide (**20**)



(*E*)/(*Z*) mixture **17** (0.3500 g, 0.79 mmol) was dissolved in dry DMF (10 cm³) and CH₃I (0.123 cm³, 1.98 mmol) was added through micropipette. Reaction was heated under nitrogen atmosphere for 24 h 35 °C. Reaction progress was monitored by TLC. Et₂O (25 cm³) was added to reaction mixture to precipitate out the product. Solid was collected via centrifugation process. NMR confirmed the formation of (*E*)/(*Z*) mixture. Crude product was treated with MeOH:CHCl₃ (1:50 v/v) system to precipitate out yellow coloured (*E*) isomer (0.1800 g, 31% yield with respect to **17**). Mother liquor containing mostly (*Z*) isomer along with the traces of (*E*) isomer was evaporated and (*Z*) isomer was purified via neutral alumina column chromatography eluted with MeOH:CHCl₃ (8:92 v/v) system to get isomerically pure colourless (*Z*) isomer (0.3500 g, 61% yield with respect to **17**).

Physical and analytical data for (*Z*) isomer

Melting point: 142–144 °C

ESI-MS: m/z 235.0, 455.2, 597.1

^1H NMR (DMSO- d_6): δ = 4.10 (s, 6H), 5.74 (s, 6H), 6.64 (s, 2H), 7.23–7.24 (m, 4H), 7.37–7.38 (m, 4H), 7.64–7.72 (m, 4H), 7.89–7.90 (d, 2H), 8.04–8.05 (d, 2H), 9.81 (s, 2H) ppm.

^{13}C NMR (DMSO- d_6): δ = 33.3, 49.4, 113.5, 113.7, 126.60, 126.61, 128.2, 128.9, 129.9, 130.6, 132.0, 132.9, 137.0, 142.9 ppm.

IR (KBr disc): 426 (w), 462 (w), 600 (w), 669 (m), 694 (w), 764 (m), 887 (w), 1016 (w), 1089(w), 1203 (w), 1271 (w), 1296 (w), 1342(w), 1384 (w), 1457 (w), 1488 (w), 1564 (m), 1619 (m), 2341 (s), 2360 (s), 2852 (w), 2923 (w), 2962 (w), 3020 (w), 3427 (s) cm^{-1}

Physical and analytical data for (*E*) isomer

Melting point: 270°C–272 °C

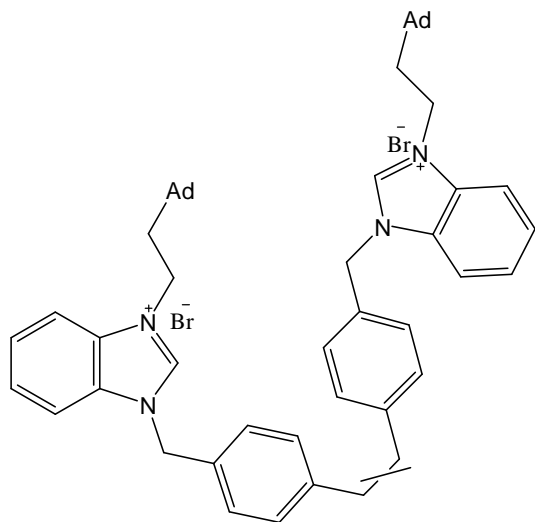
ESI-MS: m/z 235.0, 455.2, 597.1

^1H NMR (DMSO- d_6): δ = 4.11 (s, 6H), 5.77 (s, 4H), 7.29 (s, 2H), 7.51–7.53 (d, 4H), 7.63–7.69 (m, 8H), 7.94–7.95 (d, 2H), 8.03–8.05 (d, 2H), 9.82 (s, 2H) ppm.

^{13}C NMR (DMSO- d_6): δ = 33.5, 49.7, 113.7, 113.8, 126.70, 126.73, 127.1, 128.6, 128.9, 130.8, 132.2, 133.4, 137.4, 143.0 ppm.

IR (KBr disc): 422 (w), 526 (w), 569 (w), 603 (w), 659 (m), 752 (s), 787 (m), 839 (w), 860 (w), 958 (w), 979 (m), 1016 (w), 1091 (w), 1128 (w), 1162 (w), 1190 (w), 1215 (m), 1278 (w), 1342 (m), 1365 (w), 1421 (w), 1448 (m), 1459 (w), 1490 (w), 1517 (w), 1564 (s), 1610 (w), 3043 (m), 3060 (w), 3129 (w), 3396 (bs), 3496 (bs) cm^{-1}

8.4.2 Synthesis of (*E*)/(*Z*)-3-admantylethyl-1-((4-(-2-(4-((3-methyl-1*H* benzo[*d*]imidazol-1-*io*)methyl)phenyl)vinyl)phenyl)ethyl)-1*H*-benzo[*d*]imidazolium dibromide (21)



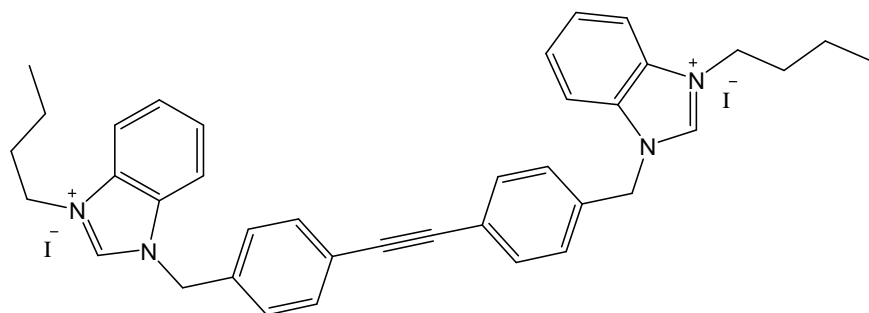
(*E*)/(*Z*) mixture **17** (0.0500 g, 0.1135 mmol) was dissolved in dry DMF (5 cm^3) and 1-(1-adamantyl)-2-bromoethane (0.082 g, 0.3407 mmol) was added at once. Reaction was heated under nitrogen atmosphere for 144 h 120 °C. Reaction progress was monitored by TLC and ESI-MS. Reaction was never completed. Little amount of mono quaternarized was still present. Et_2O (25 cm^3) was added to reaction mixture to precipitate out the product. Solid was collected via centrifugation process. Crude material was purified by silica gel

chromatography eluted with MeOH:CHCl₃ (10:90 v/v) system to get cream coloured **21** (0.055 g, 52% yield with respect to **17**). NMR confirmed the formation of (*E*)/(*Z*) mixture.

ESI-MS: *m/z* 383.2

¹H NMR (DMSO-*d*₆): δ = 1.61–1.97 (m, 68 H, (*E*)/(*Z*) isomers), 4.49–4.53 (m, 8H, (*E*)/(*Z*) isomers), 5.73–5.76(m, 8H, (*E*)/(*Z*) isomers), 6.64 (s, 3H, (*Z*) isomer), 7.22–7.30 (m, 7H, (*E*)/(*Z*) isomers), 7.38–7.40 (d, 6H, (*E*)/(*Z*) isomers), 7.52–7.53 (m, 2H, (*E*) isomer), 7.62–7.70 (m, 10 H, (*E*)/(*Z*) isomers), 7.89–7.91 (d, 3H, (*E*)/(*Z*) isomers), 7.95–7.97 (d, 1H, (*E*) isomer), 8.06–8.08 (m, 4H, (*E*)/(*Z*) isomers), 10.02–10.04 (m, 4H, (*E*)/(*Z*) isomers) ppm.

8.4.3 Synthesis of 3-butyl-1-((4-(2-(4-((3-butyl-1*H*-benzo[*d*]imidazol-1-*io*)methyl)phenyl)ethynyl)phenyl)methyl)-1*H*-benzo[*d*]imidazolium diiodide (**22**)



Compound **19** (0.2000 g, 0.46 mmol) was taken in a neat 1-iodobutane (7 cm³) and heated to 100°C for 32 h under nitrogen atmosphere. Reaction progress was monitored by TLC. Upon completion, reaction was cooled to room temperature and dry Et₂O (20 cm³) was added to the reaction mixture and the solid was collected by centrifugation. This solid was washed with 100 cm³ of dry Et₂O to remove all the traces of 1-iodobutane. Solid was purified using silica gel column eluted with MeOH:CHCl₃ (5:95 v/v) system to get yellow coloured solid **22** (0.3200 g, 87% yield with respect to **19**).

Melting point: 135–137°C

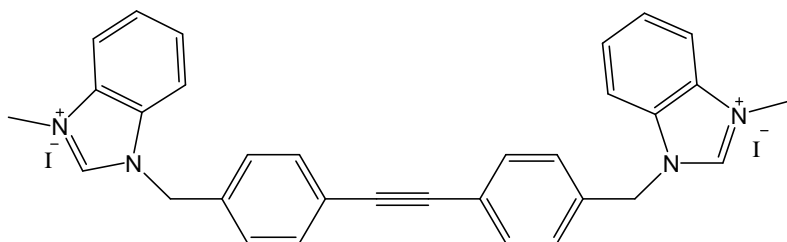
ESI-MS: *m/z* 276, 316 [mass with one bromine atom added across the double bond, less than 10% by ESI-MS].

¹H NMR (DMSO-*d*₆): δ = 0.93–0.96 (t, 6H), 1.35–1.40 (sextet, 4H), 1.91–1.95 (quintet, 4H), 4.51–4.53 (t, 4H), 5.80 (s, 4H), 7.53–7.59 (m, 8H), 7.62–7.70 (m, 4H), 7.91–7.92 (d, 2H), 8.11–8.13 (d, 2H), 9.92 (s, 2H) ppm.

¹³C NMR (DMSO-*d*₆): δ = 13.6, 19.3, 30.7, 46.9, 49.8, 89.6, 114.0, 114.2, 122.6, 126.9, 127.0, 128.8, 131.1, 131.6, 132.2, 134.9, 142.8 ppm.

IR (KBr disc): 422 (w), 542 (w), 660 (w), 748 (s), 781 (w), 848 (w), 1016 (w), 1113 (w), 1132 (w), 1192 (m), 1340 (w), 1375 (w), 1413 (m), 1442 (m), 1518 (w), 1560 (s), 1608 (w), 1685 (w), 2341 (m), 2360 (m), 2869 (w), 2929 (s), 2956 (s), 3020 (w), 3122 (w), 3442 (bs) cm⁻¹

8.4.4 Synthesis of 3-methyl-1-((4-(2-(4-((3-methyl-1*H*-benzo[*d*]imidazol-1-yl)methyl)phenyl)ethynyl)phenyl)methyl)-1*H*-benzo[*d*]imidazolium diiodide (**23**)



Compound **19** (0.0500 g, 0.11 mmol) was stirred in neat CH₃I (5 cm³) under nitrogen atmosphere at 10 °C for 72 h. Reaction progress was monitored by TLC which showed the completion of the reaction. Solid was precipitated by adding 15 cm³ of dry Et₂O. The solid was washed further with another 30 cm³ of Et₂O. The crude material was purified over alumina column eluted with MeOH:CHCl₃ (8:92 v/v) system to get **23** as a cream coloured solid (0.082 g, 100 % yield with respect to **19**).

Melting point: 222–224°C

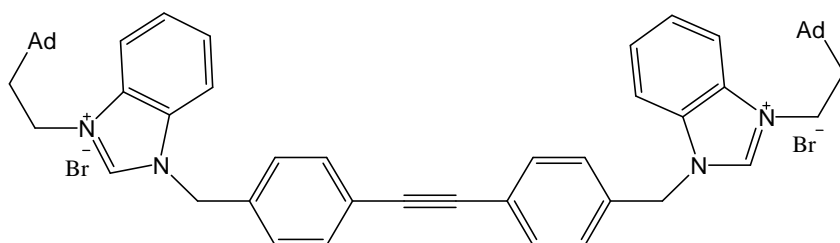
ESI-MS: m/z 234

¹H NMR (DMSO-*d*₆): δ = 4.11 (s, 6H), 5.83 (s, 4H), 7.54–7.59 (m, 8H), 7.62–7.71 (m, 4H), 7.90–7.92 (d, 2H), 8.04–8.05 (d, 2H), 9.88 (s, 2H) ppm.

¹³C NMR (DMSO-*d*₆): δ = 32.8, 48.8, 88.8, 113.0, 113.2, 121.7, 126.0, 126.1, 128.0, 130.1, 131.3, 131.5, 134.2, 142.6 ppm.

IR (KBr disc): 424 (w), 498 (w), 567 (w), 603 (w), 656 (m), 758 (s), 781 (m), 852 (m), 1016 (m), 1093 (w), 1141 (w), 1163 (w), 1192 (w), 1217 (w), 1275 (w), 1342 (m), 1363 (w), 1410 (w), 1452 (m), 1489 (w), 1518 (w), 1566 (s), 1610 (w), 2976 (w), 3024 (w), 3135 (w), 3448 (bs)cm⁻¹

8.4.5 Synthesis of 3-(2-(1-adamantyl)ethyl)-1-((4-(2-(4-((3-(2-(1-adamantyl)ethyl)-1*H*-benzo[*d*]imidazol-1-yl)methyl)phenyl)ethynyl)phenyl)ethyl)-1*H*-benzo[*d*]imidazolium dibromide (**24**)



Compound **19** (0.1500 g, 0.34 mmol) was dissolved in dry DMF (5 cm³) and 1-(1-adamantyl)-2-bromoethane (0.2500 g, 1.03 mmol) was added. Reaction was heated to 120 °C for 56 h under nitrogen atmosphere. Reaction progress was monitored by TLC and ESI-MS. Reaction never completed. Some mono monoadmantylated compound was always present. Reaction was cooled to room temperature and dry Et₂O (20 cm³) was added to precipitate out the product. The solid was separated by centrifugation and washed with 60 cm³ of dry Et₂O. This crude material was purified by silica column eluted with MeOH:CHCl₃ (5:95 v/v) system to obtain cream coloured **24** (0.1380 g, 44% yield with respect to **19**).

Melting point: 188 °C–190 °C

ESI-MS: m/z 382.2

¹H NMR (DMSO-d₆): δ = 1.62 (s, 12H), 1.64–1.79 (m, 16H), 1.99 (s, 6H), 4.50–4.53 (m, 4H), 8.81 (s, 4H), 7.54 (s, 8H), 7.59–7.68 (m, 4H), 7.91–7.92 (d, 2H), 8.01–8.03 (d, 2H), 10.06 (s, 2H) ppm.

¹³C NMR (DMSO-d₆): δ = 27.4, 31.3, 35.9, 41.0, 41.7, 42.0, 49.1, 88.9, 113.2, 113.3, 122.1, 126.1, 126.2, 128.1, 130.4, 130.7, 131.3, 133.9, 141.9 ppm.

IR (KBr disc): 426 (w), 565 (w), 748 (s), 817 (w), 850 (w), 972 (w), 1105 (w), 1130 (w), 1178 (w), 1197 (w), 1217 (w), 1253 (w), 1282 (w), 1346 (w), 1382 (m), 1448 (s), 1481 (w), 1517 (w), 1558 (s), 1614 (w), 2844 (w), 2898 (s), 3022 (w), 3120 (w), 3407 (bs) cm⁻¹

Results and Discussion

9 Tetratopic guests

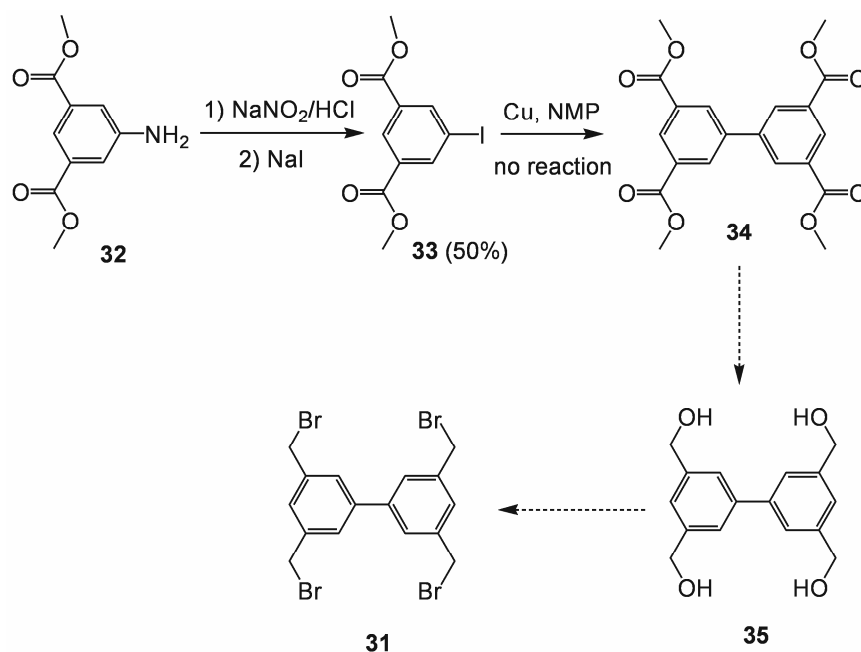
9.1 Synthesis of tetratopic guests

Synthesis of tetra substituted imidazolium and benzimidazolium quaternary ammonium salts was planned to check the effect of centerpiece on the binding with hosts cyclodextrins and cucurbiturils. Multitopic guests are of general interest in supramolecular chemistry due to their ability to exhibit interesting binding properties in complex mixtures. Another approach was to synthesize the *N*-heterocyclic carbene compounds with potential anti-tumor and anti-microbial activity. A tetrasubstituted biphenyl spacer was selected to provide final guest molecules with well-defined rigid geometries. In order to make these compounds, it was necessary to prepare a key intermediate **31** for tetratopic spacer as shown in the Scheme 1.

9.1.1 Attempted synthesis by Ullmann or Suzuki coupling

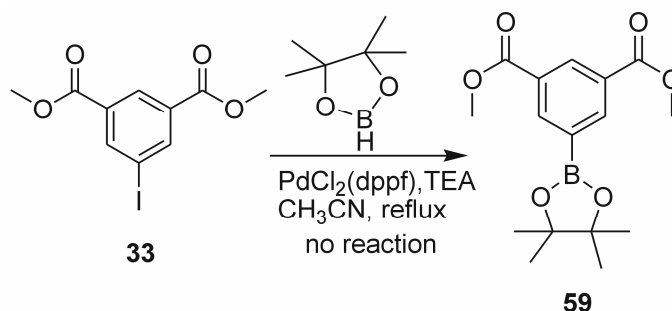
The first approach towards biphenyle **31** is depicted in Scheme 1. The synthesis started with commercially available dimethyl 5-aminoisophthalate which yielded dimethyl 5-iodoisophthalate (**33**) upon diazotization with sodium nitrite and sodium iodide.²⁵⁴ Whereas the first step, i.e., the diazotization/iodination reaction proceeded smoothly with satisfactory yield of 50 %, the following coupling step was accompanied with serious difficulties. Ullmann coupling was tried to make the biphenyl system.²⁵⁵ The aryl halide **33** was heated in autoclave at 220°C in *N*-methylpyrrolidone (NMP) with powdered metallic copper as a catalyst. Unfortunately, this experiment led to the deiodinated compound **38**. Few other solvents such as xylene and dioxane were used to carry out to prepare **35** but they ended up in the formation deiodinated compound **38**. Reaction conditions were varied time to time. Ullmann coupling was carried out at different temperatures in both autoclave and sealed tube but the final product was **38** as usual. Thus, this route was not taken into consideration.

Scheme 1: Proposed route towards compound **31**



The next approach was Suzuki coupling. In this approach, it was planned to prepare the borate ester **59** from **33**. The borate ester **59** was supposed to undergo Suzuki coupling with **33** in presence of Na_2CO_3 and $\text{PdCl}_2(\text{dppf})$. Borate ester synthesis was carried out using $\text{PdCl}_2(\text{dppf})$ using triethyl amine as a base and CH_3CN as a solvent as shown in Scheme 2.²⁵⁶ But, the expected reaction did not proceed as deiodinated compound **38** was isolated. As this borate synthesis did not work, the Suzuki coupling with **33** was not carried out.

Scheme 2: Preparation of borate ester **59**

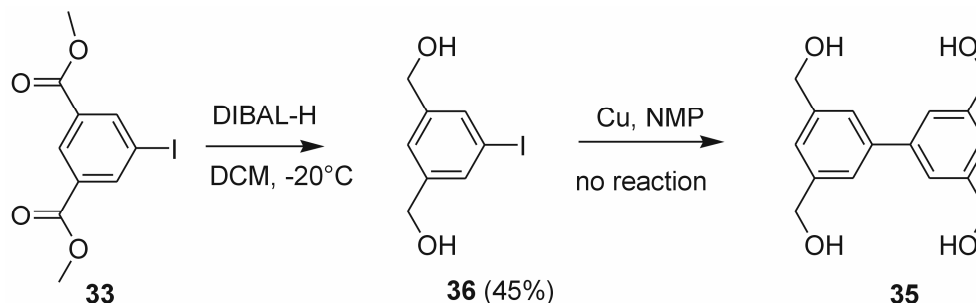


9.1.2 Reduction first approach

Considering that electron withdrawing methoxycarbonyl groups could cause undesired reactivity in coupling reactions, it was decided to transform mentioned functional groups to electron donating hydroxymethyl groups prior to the coupling step. In this route, reduction of diester **33** to corresponding alcohol **36** was carried out and then Ullmann reaction was attempted to couple the aromatic rings to form biphenyl system. This approach is shown in scheme 3. But, this approach did not work and the new strategy was employed in order to achieve the centerpiece **31**.

At first, diester **33** was reduced to corresponding alcohol **36** using DIBAL-H at -20°C in DCM²⁵⁷. Yield was 45%. But, the next step, i.e. Ullmann coupling was failed as compound with deiodinated product was obtained. Thus, this approach was abandoned.²⁵⁵

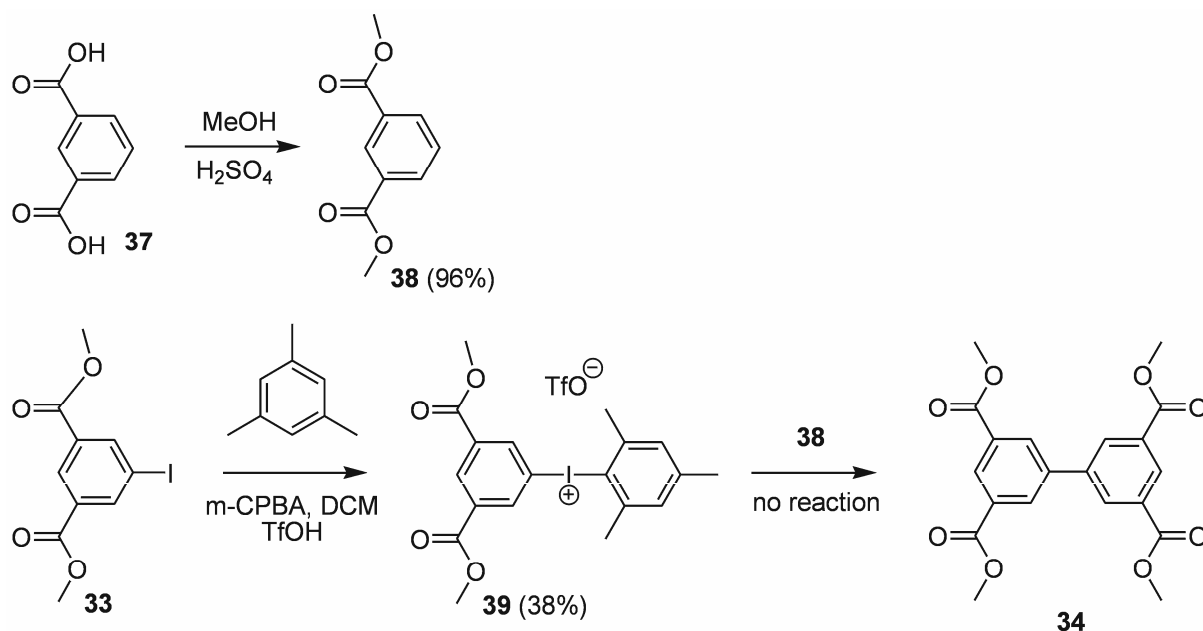
Scheme 3: Attempted Ullmann coupling



9.1.3 Coupling via iodonium salt

In order to construct biphenyl system the approach involving iodonium salt was employed as shown in Scheme 4. This procedure is based on electrophilic substitution reaction between a carbocation generated from iodonium salt and appropriate aromatic system. In the case of symmetric **34** preparation, iododiester **33** and corresponding non-iodinated compound **38** were needed. Therefore, diester **38** was prepared by esterification of isophthalic acid and iodonium salt **39** was prepared by using mesitylene, **33**, m-chloroperbenzoic acid (m-CPBA) and trifluoromethane sulfonic acid according to the previously published procedure.²⁵⁸ Then, attempt to prepare **34** by palladium cross coupling in 1,2-DCE as solvent at reflux temperature was failed as 100% deiodinated product **38** was formed which was useless for further reactions.²⁵⁹ Then conditions were varied for further attempts. Solvent was changed to dioxane but with no positive effect on result of the reaction. Further, the reaction was carried out in autoclave using the the conditions mentioned in the literature²⁵⁹ except temperature which was varied from 220°C to 250°C, Nevertheless, in all cases, **38** was the only isolated product and no desired **34** was detected.

Scheme 4: Attempted synthesis of biphenyl system

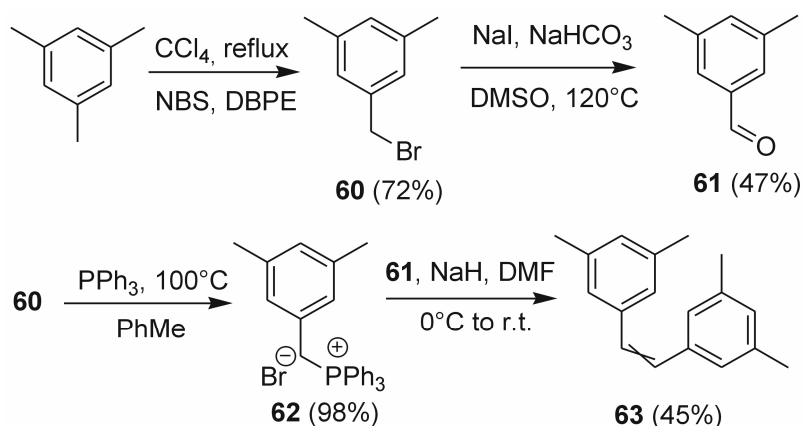


9.1.4 Synthesis of tetratopic spacers **65** and **69**

Because of unsuccessful attempts to prepare the biphenyl centerpiece for tetratopic guests, the attention was focused onto synthesis of another tetrasubstituted intermediated based on stilbene and diphenylacetylene skeletons. The synthesis of spacers **65** and **69** started with mesitylene. Mesitylene was converted to stilbene **63** (actually mixture of **64** and **66**) using procedure depicted in Scheme 5. Briefly, mesitylene underwent radical bromination with one equivalent of brominating agent NBS to get **60** in satisfactory yield.²⁶⁰ Subsequently, **60** was converted to **61** by Swern oxidation in moderate yield of about 50 %.

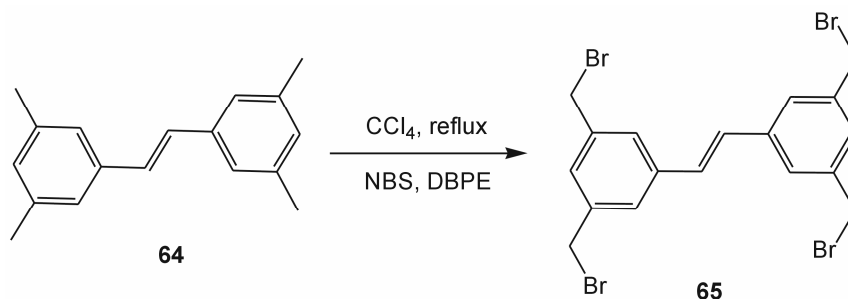
Finally, the phosphorous ylide **62** prepared from **60** in excellent yield²⁵¹ was coupled under Wittig conditions with **61** to yield mixture of diastereomers **63** as shown in Scheme 27.

Scheme 5: Synthesis of (*E/Z*)-1,2-bis(3,5-dimethylphenyl)ethane



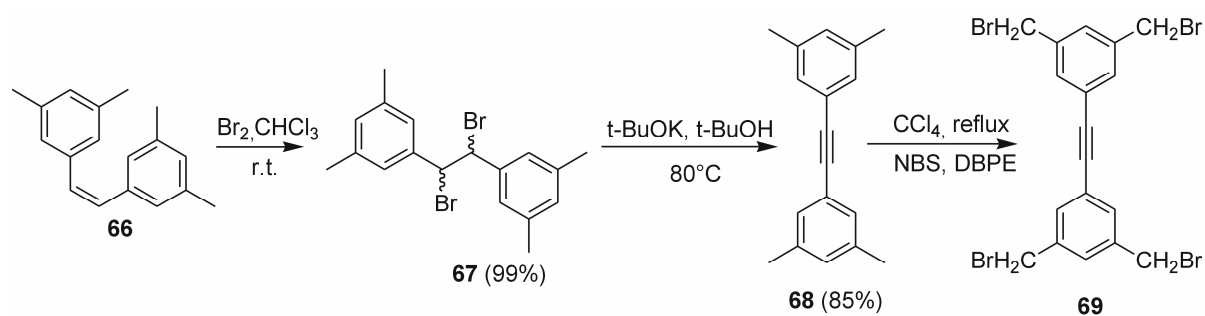
The mixture of (*Z*) and (*E*) stilbenes **63** was purified in neutral alumina column using pure hexane as a mobile phase to separate pure isomers **64** and **66**. *Z* isomer was obtained as a colorless liquid while *E* isomer was solid in nature. Subsequently the (*E*) isomer was used for terminal bromination to synthesize spacer **65** (Scheme 6). Reaction was monitored by GC-MS that showed formation of compounds with multiple brominations including addition of bromine across the double bond and multiple bromination at methyl ends of the compound **64**. In the complex mixture, the desired material **65** was detected employing analyses of the fragments in MS spectrum. Unfortunately, the amount was very low according to GC-MS and, thus, the isolation was obstructed.

Scheme 6: Synthesis of (*E*)-1,2-bis(3,5-bis(bromomethyl)phenyl)ethene (**65**)



As synthesis of **65** failed, the attention was turned towards another spacer 1,2-bis(3,5-bis(bromomethyl)phenyl)ethyne (**69**). Complete synthetic approach is shown in Scheme 7.

Scheme 7: Synthesis of acetylene **69**



The (*E*) isomer **66** was used for preparation of **69**. Bromination of **66** across the double bond provided **67** (actually a mixture of enantiomers) in excellent yield²⁵² and subsequent dehydrohalogenation²⁵³ led to acetylene **68**. However, attempt to carry out the terminal bromination of **68** failed. Reaction was carried out in CCl_4 using NBS as a brominating agent and dibenzoyl peroxide as a radical initiator. The result of this Bromination remained essentially the same as that of compound **65**. Reaction was monitored by GC–MS and products of bromination across the triple bond as well as compounds with multiple brominations at methyl ends were detected. Desired product **69** was formed in little amount that it was impossible to isolate from the complex mixture. Thus, this route was abandoned. After this failure, working in tetratopic guests was stopped and attention was turned to the tritopic guests.

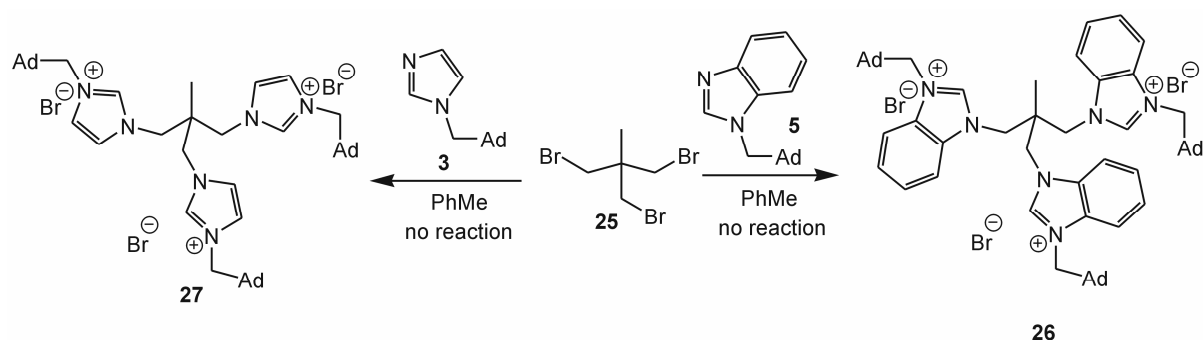
10 Tritopic guests

10.1 Synthesis of tritopic guests

10.1.1 Failed synthesis of quaternary ammonium salts from **25**

For homo-tritopic guests, two basic skeletons were chosen. The first, aliphatic, was based on 2,2-dimethylpropane and the second, aromatic, was based on mesitylene. Initially the attention was focused on the aliphatic centerpiece. As a starting precursor, 2-methyl-2-bromomethyl-1,3-dibromopropane (**25**) was prepared by using the procedure available in the literature²⁶¹. The initial proposed plan was to prepare two benzimidazolyl and imidazolyl quaternary ammonium salts from compound **25** by reaction with corresponding 1-alkylated(benz)imidazole. Quaternization reactions with **25** were carried out in different solvents such as DMSO, toluene and DMF. Result of all the reactions was the same. Reaction was monitored by ESI-MS spectrometry. Few drops of the reaction mixture were taken in eppendorf vial and diluted with 1 cm³ of CHCl₃. Analysis showed formation of mono quaternized species along with the unreacted starting compound **25**. Thus it became necessary to use another strategy. The possible reason behind the failure in this case could be high steric hindrance in the expected products.

Scheme 8: Attempted synthesis of quaternary salts **26** and **27**

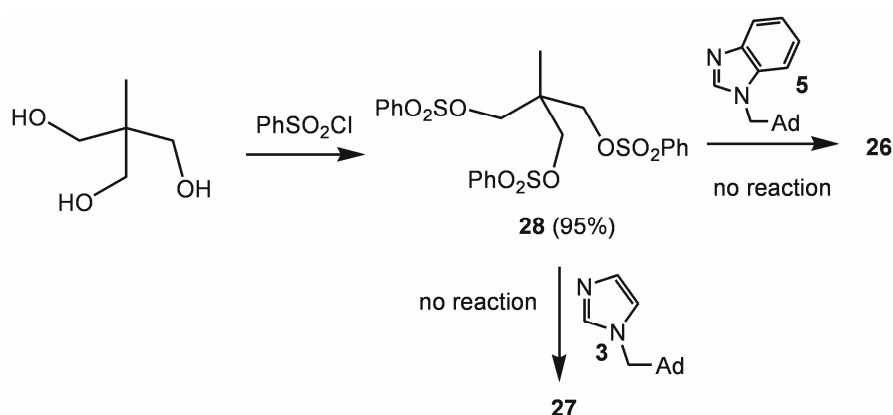


10.1.2 Alternate strategy with different leaving groups

As a modification of the first unsuccessful procedure, it was decided to replace bromine atoms in the compound **25** with some better leaving groups. Accordingly, the ester **28** was prepared from corresponding triol,²⁶² as depicted in Scheme 9. Subsequent quaternization reaction was carried out with **28** to get desired molecules **26** and **27** as shown in scheme 9. Toluene was used as solvent in this case too. But, reaction was a partial success as starting material was observed with traces of monoquaternized product using the same analytical approach as described above. The possible reason behind the failure can be attributed to the steric hindrance in the expected products.

Because of failure of this strategy, another approach was opted to obtain the compounds **26** and **27**.

Scheme 9: Failed quaternization using compound **28**



10.1.3 Alternate strategy with quaternization in last step

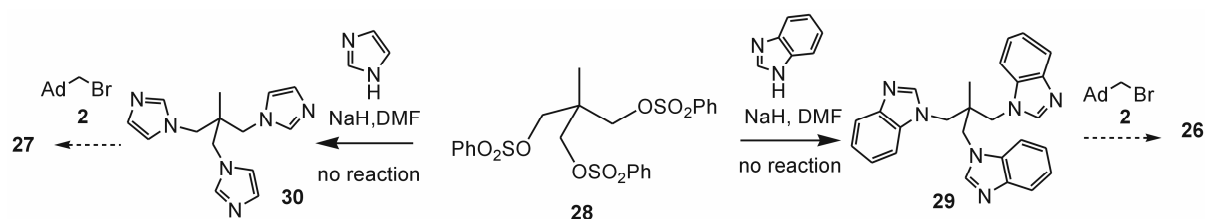
This strategy reverse the N1 alkylation and quaternization step (see Scheme 10). The ratio for this modification was that highly nucleophilic amides are applied in the first step in which the sterically hindered product is formed. The subsequent quaternization takes place rather far from centre of the molecule and should be less affected by steric hindrance.

In the first step, anion was generated on imidazole/benzimidazole moieties using sodium hydride under inert atmosphere followed by the addition of compound **28**. The expected reaction was supposed to give compounds **29** and **30** as can be seen in Scheme 3. Unfortunately, this reaction did not work and the starting compound was recovered as such. Traces of mono substituted compounds were formed during the coupling of imidazole and benzimidazole with **28** as it was detected by ESI-MS. As this step did not work, there was no possibility of quaternization of these compounds. Possible reason behind this failure could be again the same as mentioned in the previous cases, the steric hindrance in the expected product.

It was third consecutive failure in making the tripod compounds **26** and **27**. Finally, the tribromide **25** was tested in the reverse approach. Anions were generated on benzimidazole and imidazole moieties and compound **28** was added to it. Unfortunately, these reactions ended up with only starting compound.

Thus, it was decided to stop working on this aliphatic centerpiece as synthesis of **26** and **27** was proved to be wastage of time and chemicals.

Scheme 10: Another unsuccessful approach towards the tripods



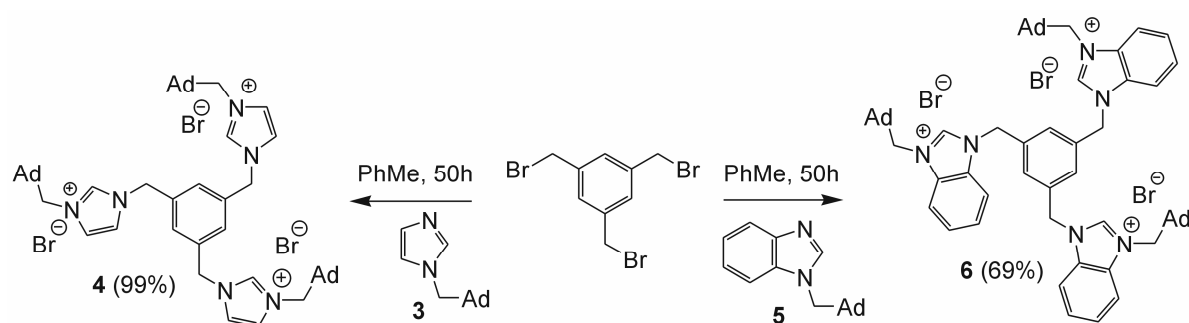
10.1.4 Synthesis of tritopic guests with 1,3,5-tris(bromomethyl)benzene (TBMB) centerpiece

The detailed synthesis of these guests is described in the experimental section. The synthetic strategy and the most important conditions are shown in Scheme 11.

Guests **6** and **4** were prepared by quaternization of centerpiece 1,3,5-tris(bromomethyl)benzene in toluene as a solvent. Reaction took 50 h to complete. During the course of reaction, monitoring was carried out using ESI-MS spectrometry. Presence of mono and di quaternized entities was observed in the initial stages of the reaction. In order to complete the reactions, some portions (approximately 0.5 equivalents) of compounds **3** and **5** were added after detection of uncompleted reaction. In this way, this addition was carried out for 3 times in both the reactions to achieve complete quaternization of the centerpiece TBMB.

As the guests **6** and **4** precipitated from reaction mixture were sufficiently pure to be considered for supramolecular studies, no column chromatography purification was carried out.

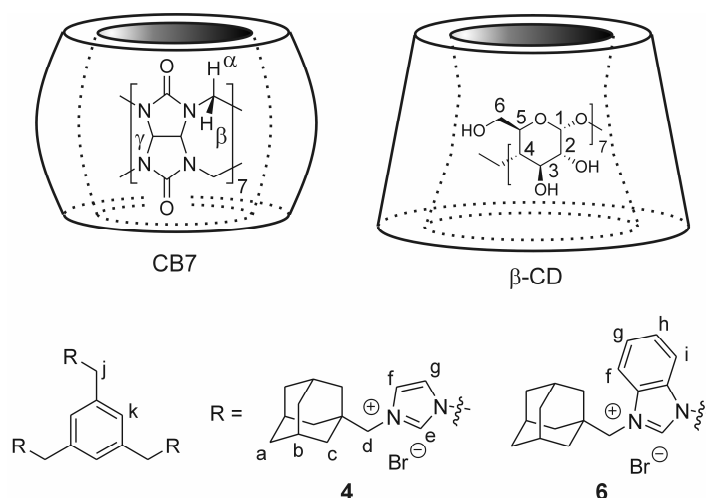
Scheme 11: Synthesis of guests **6** and **4**



10.2 Supramolecular studies of tripod guests **4** and **6**

Mass spectrometric studies, NMR studies and calorimetric titrations were performed to prepare and prove the formation of inclusion complexes with hosts such as β -CD and CB[7]. In following text, the results of these supramolecular studies are commented. The structures of guests and hosts are shown in Figure 21.

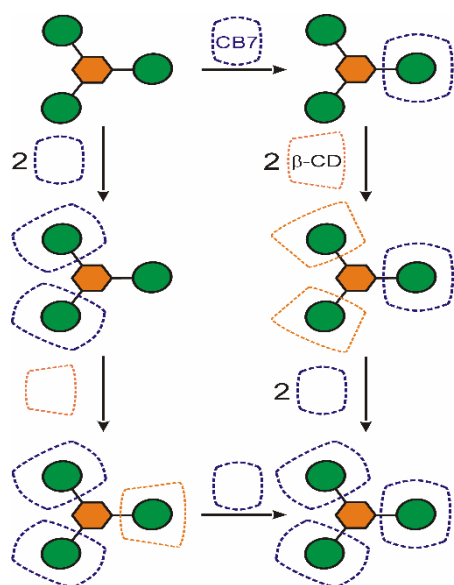
Figure 21: Structures of the trisimidazolium guests and hosts molecules



Schematic diagram displaying considered inclusion complexes and their transformations is drawn in Figure 22.

10.2.1 Binary systems

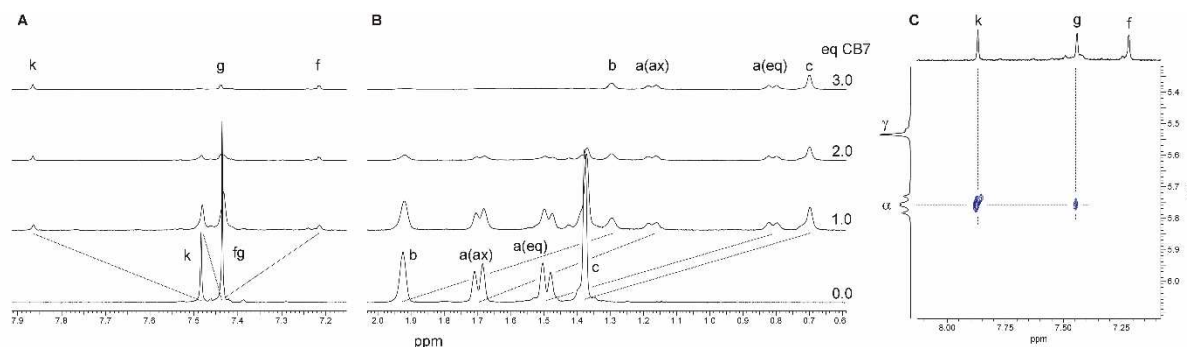
At first, we tried to find out the binding of imidazolium guest **4** with CB[7]. Therefore, compound **4** was dissolved in D_2O and portions of CB[7] solution were added. In consecutively recorded 1H NMR spectra showed two sets of signals when some CB[7] had been added. One set of signals can be assigned to complexed guest and the second for free guest.



One set of signals can be assigned to complexed guest and the second for free guest. H_k signal for the proton on centerpiece was shifted downfield (Figure 23A, for signal assignment, see Figure 21) whereas all adamantane protons showed upfield shift (Figure 23B). This indicate that adamantane cage was successfully included in CB[7] cavity. Independent support for this hypothesis was obtained from ROSEY spectrum recorded for a solution of **4** in D_2O with 3 equivalents of CB[7] (Figure 23C). In this spectrum, cross-peaks related to the intermolecular interactions between H_α of CB[7] and H_k , and H_g protons from the centerpiece can be clearly observed. With the addition of 3 equivalents of CB[7], all the signals for the free guests were vanished due to complexation which suggests the formation of $\mathbf{4}@CB[7]_3$.

Figure 22: General scheme for inclusion complex formation

Figure 23: Stacking plot of a portion of the ^1H NMR spectra for **4** and CB[7] (A, B). A portion of the ROESY spectrum of a 1:3 mixture of **4** and CB7 (C). For signal assignment, refer Figure 20.



We further studied the interactions between **4** and CB[7] by isothermal titration calorimetry (ITC). One slope binding isotherm fitted to the one set of site model supported the independent behavior of each binding site. CB[7]/competitor was titrated against solution of guest, the parameter n showed the value of 0.33 which clearly supported the formation of 1:3 inclusion complex. The association constant for single adamantane binding site was found to be $4.8 \times 10^{10} \text{ dm}^3 \cdot \text{mol}^{-1}$. Similar studies were carried out for guest **6** and the association constant obtained was $6.52 \times 10^8 \text{ dm}^3 \cdot \text{mol}^{-1}$. Similarly to the guest **4**, the value of parameter n from ITC titration was approximately equal to 0.33 supporting the formation of 1:3 inclusion complex. The only significant difference between compound **4** and **6** was that the binding strength of **6** was 74 times less than that for guest **4**, likely because of high steric hindrance of benzimidazole cation in CB[7] cavity.

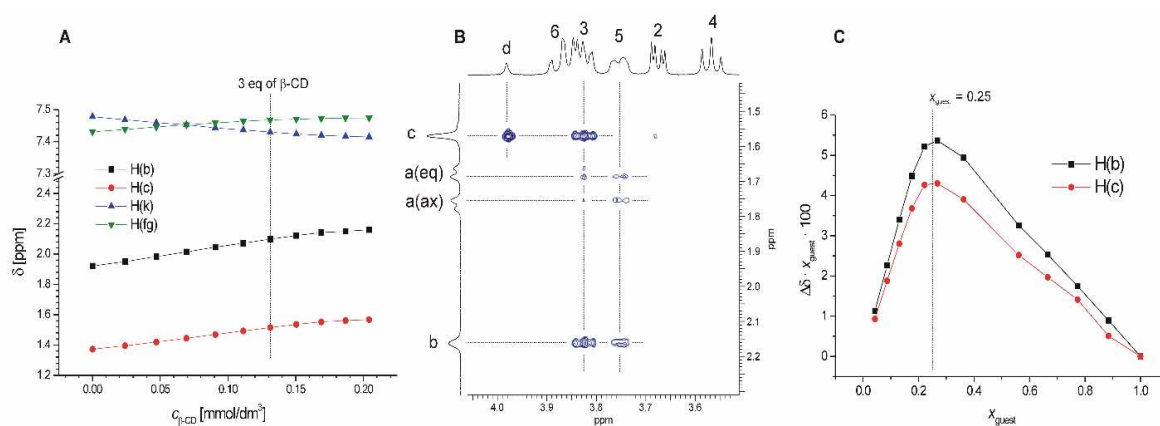
Next part in this study was to make the binary systems with another host compound β -CD. The imidazolium salt **4** was used firstly for this experiment. Guest **4** showed fast exchange with β -CD on NMR time scale giving just one set of ^1H NMR signals during titration experiments. Therefore, continuous variations method was used to determine the stoichiometry of the complex. The Job plot of **4** with β -CD is shown in Figure 24C. Curve maximum was observed to be at $x_{\text{guest}}=0.25$ which supports the formation of 1:3 (G:H) complex. The change in the chemical shifts of selected hydrogen atoms of the guest during the titration with β -CD in D_2O is shown in Figure 24A. It is well-known that the hydrogen atoms of the guest included in the β -CD cavity are shifted downfield. This can be clearly seen for adamantane H-atoms. The ROESY spectrum of guest **4** and β -CD (Figure 24B) in 1:5 (G:H) molar ratio was recorded to observe the intermolecular interactions between adamantane hydrogen atoms H_a , H_b , and H_c and inner β -CD hydrogen atoms H_3 and H_5 . The data obtained from ROESY and NMR titration experiments indicate that adamantane cage was successfully incorporated into the β -CD cavity forming $5@ \beta\text{-CD}_3$ inclusion complex. Calorimetric titrations further supported the formation of 1:3 (G:H) inclusion complex with single-site association constant $1.02 \times 10^5 \text{ dm}^3 \cdot \text{mol}^{-1}$. These experiments were conducted for guest **6** which showed similar results. For the guest **6**, calorimetric titrations gave the value of association constant $1.21 \times 10^5 \text{ dm}^3 \cdot \text{mol}^{-1}$. Thermodynamic parameters obtained from ITC experiments with the hosts β -CD and CB[7] and the guests **4** and **6** are summarized in table 3.

Table 3 Thermodynamic parameters for interactions between guests **4** and **6** and hosts CB[7] and β -CD.

Guest	Host	$K[\text{dm}^3 \cdot \text{mol}^{-1}]^a$	$-\Delta H [\text{kJ} \cdot \text{mol}^{-1}]$	$-\Delta S [\text{J} \cdot \text{mol}^{-1} \cdot \text{K}^{-1}]$	n
4	β -CD	$1.02 \times 10^5 \pm 1.29 \times 10^3$	85.7 ± 5.4	186.7	$0.367 \pm 1 \times 10^{-3}$
6	β -CD	$1.21 \times 10^5 \pm 1.19 \times 10^3$	98.8 ± 0.3	228.6	$0.312 \pm 1 \times 10^{-3}$
4	CB[7] ^b	$4.84 \times 10^{10} \pm 5.60 \times 10^6$	173.8 ± 1.0	369.0	$0.391 \pm 1 \times 10^{-3}$
6	CB[7] ^c	$6.52 \times 10^8 \pm 1.23 \times 10^6$	187.2 ± 1.7	450.8	$0.373 \pm 2 \times 10^{-3}$

^a The K values are reported for one binding site, uncertainties are obtained from single dataset fitting; ^b L-Phenylalanine or ^c 1-butyl-3-methylimidazolium bromide was used as a competitor.

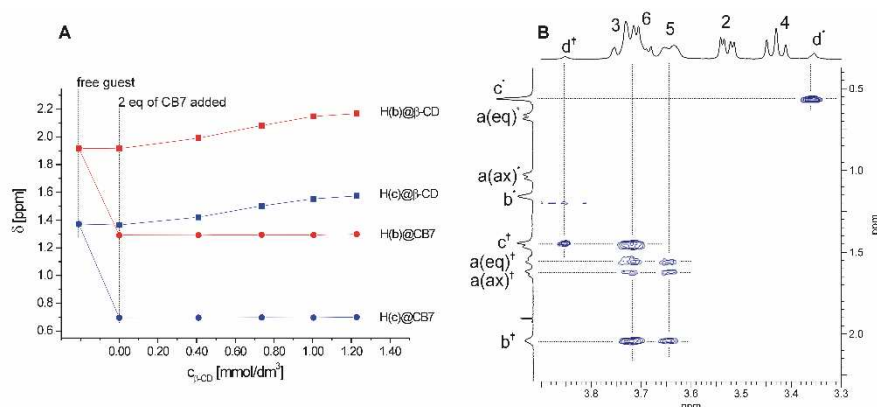
Figure 24: a) A plot of ¹H NMR complexation induced shifts of selected H-atoms of **4** against concentration of β -CD b) A portion of the ROESY spectrum of a 1:3 mixture of **4** and β -CD c) Job plot for **4** and β -CD based on ¹H NMR data. For signal assignment, refer Figure 20.



10.2.2 Ternary systems

Although the formation of 1:3 complexes was sufficiently evidenced in previous chapter, some doubt remains whether all mutual combinations of hosts molecules can be present in one complex with guests **4** and **6**. Therefore, further experiments were performed to describe formation of such ternary systems. At first, preparation of the complex **4**@(β -CD, CB[7]₂) was attempted in D₂O. It had been proved that occupancy of adamantyl site with CB[7] is easy to follow by NMR titrations. So, titration of the solution of **4** with CB[7] was carried out till the ratio of normalized integral intensity of the signal of the complexed and free guest reached to the value of 2.0. Here, two out of three binding sites of the guest **4** were occupied by two CB[7] molecules and **4**@CB₂ was predominant (with minor portions of free **4**, **4**@CB[7], and **4**@CB[7]₃). Unfortunately, NMR doesn't allow distinguishing these species. Now, the solution of β -CD was added and occupancy of free adamantyl site by β -CD was detected by means of ¹H NMR. During the titration with β -CD, signals of free adamantane moiety showed downfield shift on NMR scale as shown in the Figure 25A. This proves the inclusion of adamantane cage into β -CD cavity. The ROESY spectrum (Figure 25B) obtained for 1:2:2 mixture of **4**, β -CD and CB[7] supported the formation of **5**@(β -CD, CB[7]₂) system by showing cross-peaks related to the intermolecular interactions of adamantane cage with β -CD.

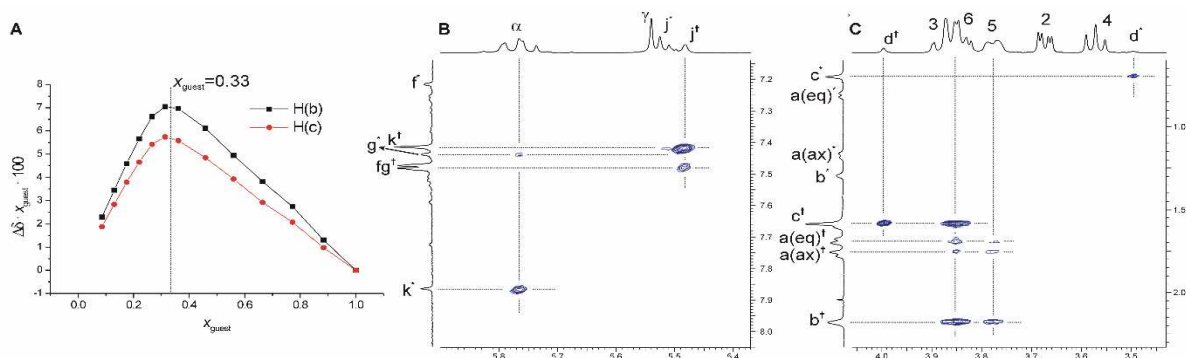
Figure 25 a) A plot of ^1H NMR complexation induced shifts of selected H-atoms of **1** against concentration of $\beta\text{-CD}$ b) A portion of the ROESY spectrum of a 1:2:2 mixture of **1**, CB[7], and $\beta\text{-CD}$. For signal assignment, check figure 20.



Similar observations were obtained for guest **6** and the formation of $\mathbf{6} @ (\beta\text{-CD}, \text{CB}[7])_2$ was also confirmed.

In further experiment, preparation of the second ternary aggregate $\mathbf{4} @ (\beta\text{-CD}_2, \text{CB}[7])$ was carried out. At first, **4** was titrated with CB[7] in such a way that only one adamantane site formed inclusion complex with CB[7] to form $\mathbf{4} @ \text{CB}[7]$ complex predominantly. Addition of $\beta\text{-CD}$ to this solution showed deshielding of H-atoms of the free adamantane cages to support the formation of $\mathbf{4} @ (\beta\text{-CD}_2, \text{CB}[7])$ complex. Separately, the ROESY spectrum was recorded for the mixture of **4** containing 1:3:1 ratio of **4**, $\beta\text{-CD}$, and CB[7]. It clearly showed the interactions between inner $\beta\text{-CD}$ protons and adamantane protons (Figure 26B and 26C). Contrary to the previously described formation of $\mathbf{4} @ (\text{CB}[7]_2, \beta\text{-CD})$, it was not completely clear whether both free adamantane sites are occupied with $\beta\text{-CD}$. In order to clarify this, Job plot was constructed. One component of the mixture was **4** and CB[7] (1:1) and the second was $\beta\text{-CD}$. As shown in Figure 26A, maximum of the curve was observed at $x_{\text{guest}} = 0.33$ which indicate that both free binding sites were occupied by $\beta\text{-CD}$ to confirm the formation of $\mathbf{4} @ (\beta\text{-CD}_2, \text{CB}[7])$ complex. Similar results were obtained for guest **6**.

Figure 26: Job plot for $\mathbf{1} @ \text{CB}[7]$ as a “guest” and $\beta\text{-CD}$ based on ^1H NMR data (A). A portion of the ROESY spectrum of a 1:3:1 mixture of **1**, $\beta\text{-CD}$, and CB[7] (B, C). For signal assignment, see Figure 20.



Finally, all the ternary complexes were converted to $\mathbf{4} @ \text{CB}[7]_3$ and $\mathbf{6} @ \text{CB}[7]_3$ by adding sufficient amount of CB[7] to the solution which contains inclusion complexes with $\beta\text{-CD}$ (at

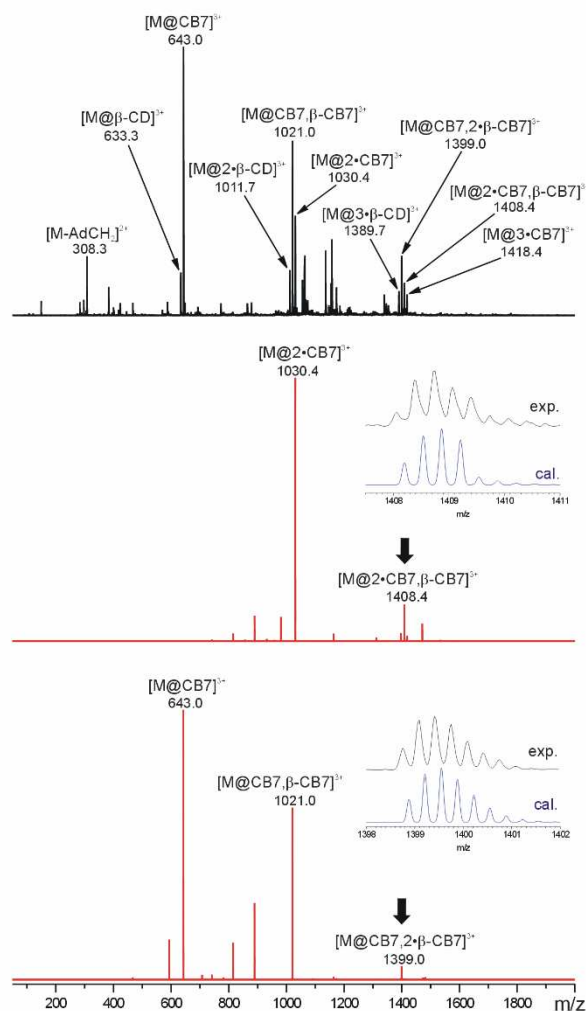
least at one binding site). Selectivity of **4** and **6** towards β -CD/CB[7] ($K_{\beta\text{-CD}} \times K_{\text{CB7}}^{-1}$) is 2.1×10^{-6} and 1.9×10^{-4} . Thus, it was not surprising that β -CD was easily replaced by CB[7]. This process was observed on NMR time scale and was very fast. Isothermal calorimetric titrations were also carried out for such systems. Solution of CB[7] ($0.54 \text{ mmol dm}^{-3}$) was placed into the cell and mixture consisting of **4** ($1.60 \text{ mmol dm}^{-3}$) and β -CD ($15.4 \text{ mmol dm}^{-3}$) was added in portions. As per Rekharsky approach²⁶³, single site binding constant for **4**@CB[7]₃ system was calculated to be $2.95 \times 10^{10} \text{ dm}^3 \text{ mol}^{-1}$. This value is in agreement with that obtained by competitive titration as shown in Table 2. Stoichiometric parameter n showed the value of 0.37 suggesting the replacement of all β -CD units by CB[7].

10.2.3 Mass spectrometry

Along with NMR and ITC experiments, mass spectrometric analysis of above prepared aggregates in aqueous solution was carried out using electrospray ionization mass spectrometry to confirm the presence of the expected supramolecular complexes. Analysis of the 1:3 mixture of guests and CB[7] showed minor signals related to $[\text{G}^{3+} \cdot 3\text{CB}[7]]^{3+}$ but the base peak was $[\text{G}^{3+} \cdot 3\text{CB}[7] \cdot \text{H}^+]^{4+}$. Mass peak $[\text{G}^{3+} \cdot 3\text{CB}[7] \cdot 2\text{H}^+]^{5+}$ was observed for guest **6**. Analysis of **4** and **6** with 5 eq of β -CD gave the peaks corresponding to $[\text{G}^{3+} \cdot \beta\text{-CD}]^{3+}$, $[\text{G}^{3+} \cdot 2\beta\text{-CD}]^{3+}$ and $[\text{G}^{3+} \cdot 3\beta\text{-CD}]^{3+}$. All above mentioned peaks were related to releasing of a neutral β -CD unit occurred upon collision induced dissociation treatment (CID).

Final MS study was carried out with aqueous mixtures containing guests **4** and **6**, CB[7] and β -CD. The ternary aggregates $\text{G}^{3+} \cdot \text{CB}[7]_n \cdot \beta\text{-CD}_{3-n}$ ($n=1,2$) were detected when mixture of guest with 1 eq of CB[7] and 5 eq of β -CD in water was tested. An example of ESI-MS result is shown in Figure 27A. Three signals pointing towards signals of guest **4** with one, two or three host molecules can be seen along with the signals of free guest and hosts. Under CID treatment, the aggregates **4**·CB7·2 β -CD and 5·2CB7· β -CD released neutral β -CD unit to form 5·CB[7] and 5·2CB[7], respectively (see, Figures 27B and 27C). Upon further CID treatment, either guest or host molecule was decomposed.

Figure 27: ESI-MS spectra of the mixture of **4**, CB7, and β -CD in 1:1:5 molar ratio in water. (A) MS in positive ion mode, ESI-MS/MS spectrum of ions at m/z 1408 (B) and 1399 (C). Precursor ions are marked with a bold downward arrow. Inserted boxes display experimental and calculated isotope pattern of the corresponding precursor ions.



11 Ditopic guests

11.1 Attempted synthesis of 1,2-diphenylethene and 1,2-diphenylethyne centerpieces

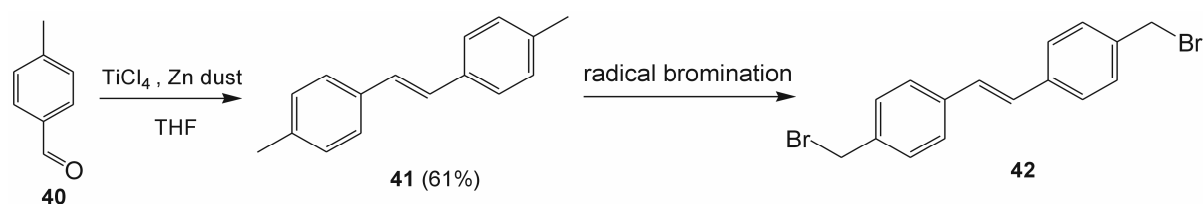
Simultaneously to the synthesis and binding studies of tritopic guests, the synthesis of ditopic guests with rigid, well-defined length of central linker, was examined. Because of ligands with a biphenyl centerpiece were described previously¹¹¹, we decided to prepare guests with longer spacers based on stilbene and diphenylacetylene skeletons. We used three strategies for their synthesis. First strategy included synthesis of the halogenated centerpieces first and quaternarization with corresponding imidazole deriviate as final step while other two strategies involved the synthesis of centerpiece including benz(imidazole) rings as a part of intermediates from the beginning.

11.1.1 Synthesis of 4,4'-dibromomethylstilbene **42**

Compound **41** was synthesized by McMurry coupling of aldehyde **40** using the procedure mentioned in the literature.⁸ The structure of product was confirmed by comparison of the NMR spectrum of the compound with the standard NMR spectrum published in literature.²⁶⁴ The main objective was to brominate **41** and to make the desired centerpiece **42**. In contrast to the successful McMurry coupling, the terminal bromination remained a permanent problem. None of the bromination strategy worked and final mixture contained several multiple brominated compounds and the separation of desired compound from the mixture was not possible as it was formed in very low quantity which was confirmed by GC-MS.

Some unsuccessful attempts to brominate methyl groups of (E)-1,2-di-*p*-tolylethyl were carried out as mentioned below.

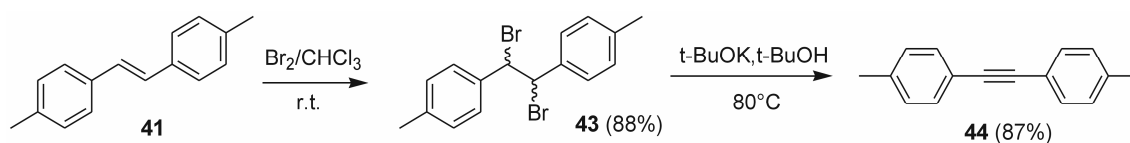
Scheme 12: Synthesis of **42**



Compound **41** was brominated with *N*-bromosuccinimide using dibenzoyl peroxide (DBPE) as radical initiator. GC-MS analyses showed formation of several compounds with multiple bromination on the methyl ends as well as compound with bromine added across the double bond of **42**.²⁶⁵ Thus it was decided to change the radical initiator. Thus, dibenzoyl peroxide was replaced by AIBN and other reaction conditions were the same as mentioned in the literature.²⁶⁵ NBS, AIBN and **41** were taken in CCl_4 and reaction mixture was refluxed for 5 h and reaction progress was monitored by GC-MS. Unfortunately, the result remained the same as in previous case. Reaction mixture showed formation of the compounds with multiple bromination on methyl ends as well as compound with bromination across the double bond. Thus, this attempt was also a failure. In next attempt, the solvent was changed from CCl_4 to benzene. Procedure remained the same as mentioned in the literature.²⁶⁵ **41**, dibenzoyl peroxide and NBS were taken in benzene and reaction mixture was refluxed for 5 h. Reaction progress was monitored by GC-MS. The result was similar as that of in the previous cases. After these consecutive failures, it was decided to stop working on the synthesis of **42** and attention was given on the synthesis of centerpiece with diphenylacetylene **45**.

11.1.2 Synthesis of bis(methylphenyl)acetylene **44**

Scheme 13: Synthesis of **44**

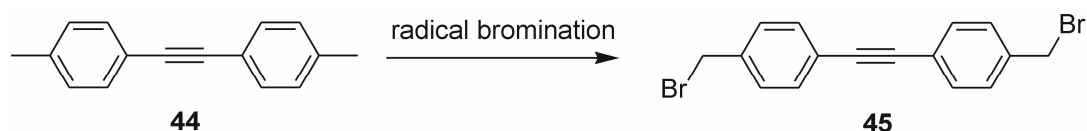


The compound **44** should be easily available by the sequence of halogenation-dehydrohalogenation from stilbene **41**. Therefore, bromine was added across the triple bond of compound **41** by using the condition mentioned in the literature.²⁵² The reaction yielded intermediate **43** which was dehydrohalogenated using *t*-BuOK to yield desired compound **44**.²⁵³ Subsequent, radical bromination of the compound **44** was the key step in order to synthesize the required spacer **45**.

11.1.3 Synthesis of 1,2-bis(4-(bromomethyl)phenyl)ethyne (**45**)

Several attempts were made to carry out the free radical bromination at the methyl ends of **44** to get our desired spacer compound but all the attempts ended up with failure. They are mentioned below.

Scheme 14: Free radical bromination of **45**



Initially, the compound **44** was brominated under conventional conditions; i.e., using *N*-bromosuccinimide as brominating agent in CCl_4 and DBPE as radical initiator at room temperature as mentioned in the literature.²⁶⁶ Reaction progress was monitored by GC-MS. Report showed formation of compounds with multiple bromination on the methyl ends and compound with addition of bromine across the triple bond of the **44**. As no formation of desired product was observed, it was decided to change the radical initiator from NBS to AIBN. Thus, the compound **44** was brominated using *N*-bromosuccinimide and AIBN as a radical initiator in CCl_4 at room temperature.²⁶⁷ Reaction progress was monitored by TLC and GC-MS. Unfortunately, the result was similar as in the previous case with inseparable mixture of multiple brominated compounds on the methyl terminals and compound with bromination across the triple bond. Now, it was decided to change the temperature instead of radical initiator. Radical bromination was carried out at reflux temperature. Compound **44**, NBS, and AIBN were taken in CCl_4 and reaction was refluxed for 5 h. GC-MS showed formation of inseparable mixture of compounds with multiple bromination on methyl terminals and compound with addition of bromine across the triple bond. In another attempt to crack this synthesis, radical bromination of **44** was carried out in aqueous medium. **44**, NBS and dibenzoyl peroxide were taken in water and heated to 90°C for 5 h. Reaction progress was monitored by GC-MS. Unfortunately, no reaction was taken place. Only starting compound **44** was observed. In next attempt, β -CD was used as a catalyst. The purpose of using β -CD was to form the inclusion complex with the compound **44** to avoid bromination across the double bond. **44**, NBS, dibenzoyl peroxide and β -CD were taken in CCl_4 and reaction was stirred at room temperature under the influence of light for 4 h. Reaction progress was monitored by GC-MS. Report showed no formation of desired product. Only unreacted starting material was observed.

Now, instead of using conventional radical brominating agent such as NBS, 1,3-dibromo-5,5-dimethylhydantoin was used. Thus, the compound **44**, 1,3-Dibromo-5,5-dimethylhydantoin, and DBPE were taken in CCl_4 and reaction was refluxed for 5 h. GC-

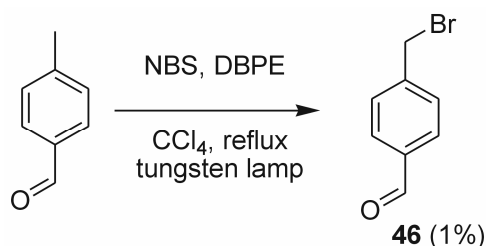
MS monitoring showed formation of compounds with multiple bromination on methyl terminals of **44**. Thus, reaction was discarded. Finally, radical chlorination of **44** was attempted. In this reaction, *N*-chlorosuccinimide (NCS) was used as a chlorinating agent. The compound **44**, NCS and dibenzoyl peroxide were taken in CCl₄ and reaction mixture was refluxed for 5 h. GC–MS report showed formation of compounds with multiple chlorination on the methyl ends of **44**.

After so many failures, working on the radical halogenation of **44** was stopped and new synthetic strategy was designed to reach the targets.

11.2 Alternate strategy towards benzimidazolium-derived centerpiece

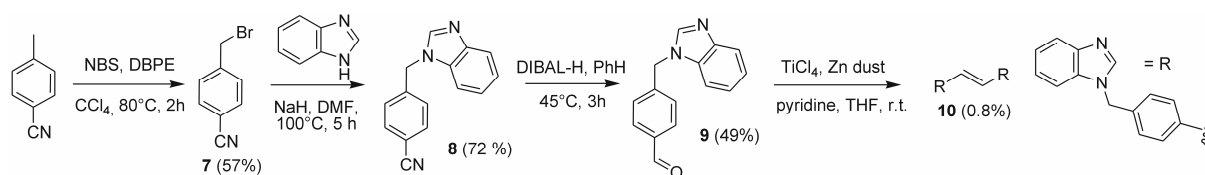
This strategy was based on the stepwise synthesis of benzimidazole precursors and final cross-coupling step to form a double bond. Initially, the procedure started from 4-methylbenzaldehyde towards aldehyde **8** as a suitable starting material for McMurry coupling was tested. Thus, 4-methylbenzaldehyde was brominated first.²⁶⁸ (Scheme 15). Unfortunately, the yield of this first step was poor (up to 2% with respect to 4-methylbenzaldehyde). Therefore, we decided to modify this synthetic strategy by using 4-methylbenzonitrile as a starting material (Scheme 16).

Scheme 15: Bromination of 4-methyl benzaldehyde



This approach started with free-radical bromination of 4-tolynitrile using *N*-bromosuccinimide to yield **7**²⁴² which was reacted²⁴³ with sodium salt of benzoimidazole to produce compound **8**. This compound **8** was subsequently converted to aldehyde **9** using DIBAL-H.²⁴⁴ The yields up to this stage proceeded smoothly with acceptable overall yield of aldehyde **9** of 20%. In contrast, the last step; i.e., McMurry coupling,²⁴⁵ yielded very low amount of **10** (0.8%). Thus, this approach was not good to move ahead and we decided to modify this approach to allow a Wittig reaction as a final cross-coupling step. Because of the synthesis of symmetrical alkene, the aldehyde **9** and corresponding haloderivate were needed. Although the required haloderivate could be prepared from **9** by sequence of reduction and nucleophilic substitution, we were afraid of low yield of desired halocompound and therefore we used corresponding methyl 4-methylbenzoate (**11**) as a starting material (Scheme 17).

Scheme 16: Synthesis of **10** by McMurry coupling



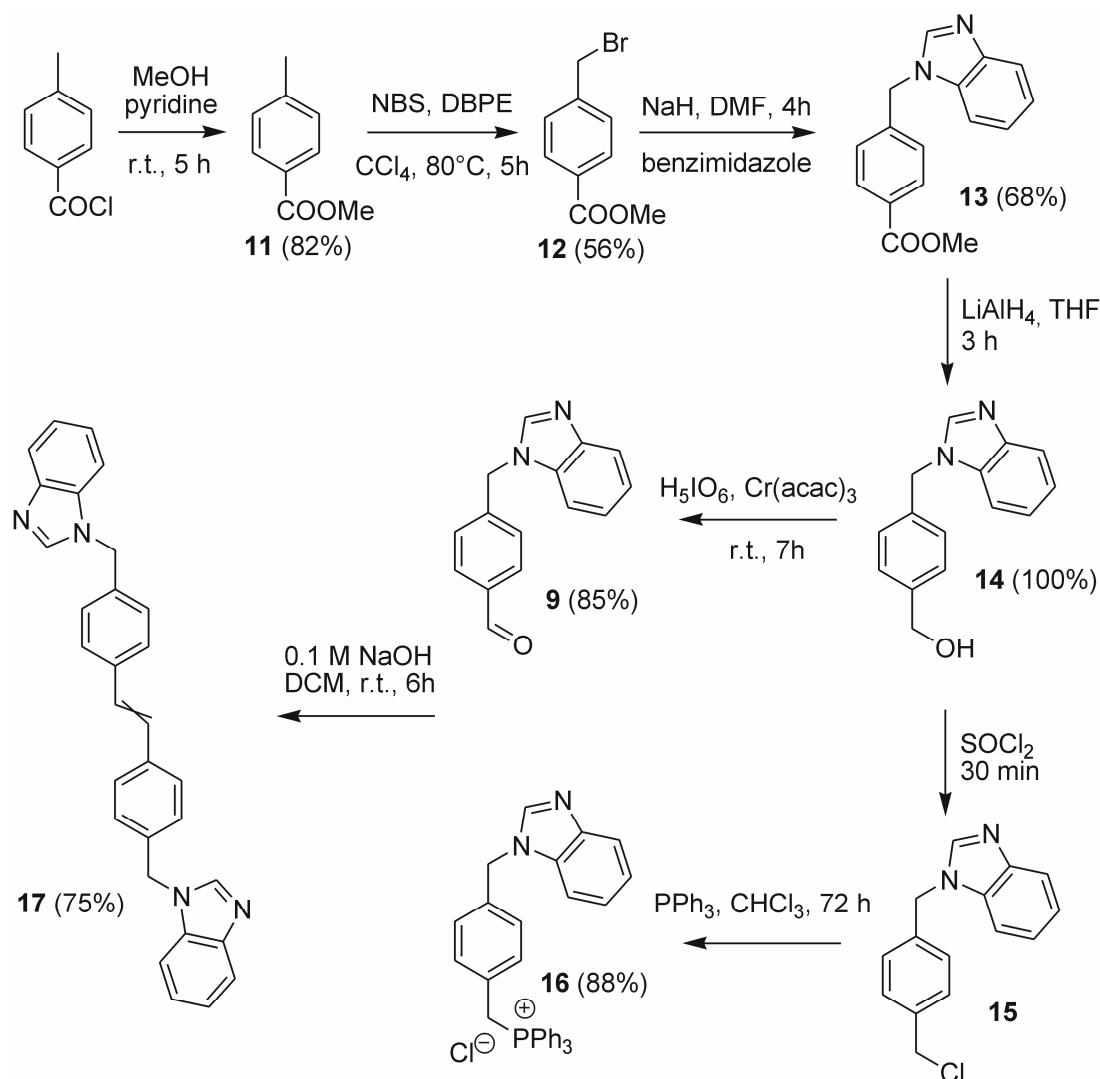
The synthesis started with 4-methylbenzoyl chloride. Methylation²⁴⁶ of 4-methyl benzoyl chloride produced **11** which was subsequently converted to **12** using radical bromination²⁴⁷

with *N*-bromosuccinimide. Upon coupling with benzimidazole²⁴⁸, compound **12** produced **13** which was subsequently reduced to **14** using LiAlH₄²⁴⁹. In this stage, the chemistry was split into two pathways as can be seen in Scheme 13. The compound **14** was used to prepare the corresponding aldehyde **9** and simultaneously to synthesize phosphorous ylide **16**. It should be noted that the intermediate **15** was highly reactive and therefore it was not isolated in pure form. Initially, intermediate **15** was worked up by extracting with ethyl acetate. Upon complete evaporation of the solvent in rotary evaporator, the solid obtained was confirmed as a polymeric material formed by intermolecular reaction between the molecules of **15**. Thus, in scale ups, complete evaporation of the solvent was not carried out and the material was taken to next step without characterization by means of NMR. Nevertheless, the compound **15** was confirmed by GC-MS.

Subsequently, the compound **15** was converted to **16** using triphenyl phosphine in chloroform as a solvent.²⁵¹ This reaction was carried out using three different solvents such as toluene, DMF and CHCl₃. In all the three solvents, reaction was successful but CHCl₃ was taken as solvent in the further scale ups because the respective yield was 70 %, 92 %, and 99 %. Despite the best yield which was achieved in DMF, the chloroform was selected as the best choice due to serious difficulties with removing of the DMF from the crude product. The required Wittig salt was conveniently obtained in solid form from CHCl₃ by addition of dry Et₂O.

In the next step, Wittig reaction was carried out between **9** and **16** in dry DCM using 0.1 M NaOH solution as a base. It was expected to form **10** preferably as the (*E*) isomer but surprisingly, mixture of (*E*) and (*Z*) isomers (**17**) in the ratio of 4:6 was obtained. The Wittig reaction was carried out by using some other bases such as *t*-BuOK and NaH to improve the (*E*):(*Z*) ratio. Unfortunately, none of these reactions produced required alkene(s). Thus, it was necessary to separate the isomers. Isomer separation was tried using column chromatography but it was unsuccessful. It should be noted, that separation of these isomers was needed only for stilbene guests preparation. In further steps towards diphenylacetylenes, the stereo-information is lost as the triple bond is formed. Therefore, the mixture of (*E*) and (*Z*) isomers was taken in the next steps as such to make the quaternary ammonium salts with stilbene as a centerpiece and diphenylacetylene unit **19**.

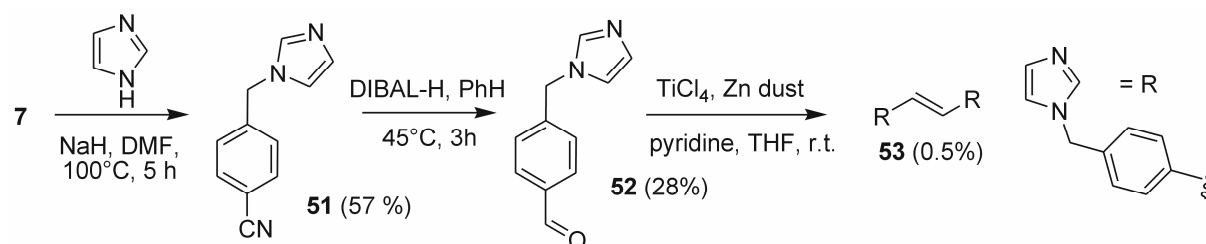
Scheme 17: Synthesis of **17** using Wittig reaction



11.3 Synthesis of imidazolium compounds

Imidazolium analogues of compounds described above were the subject of the next part of this project. Synthetic strategy used for preparation of compound **53** was similar to corresponding benzimidazole derivative which is described above. Briefly, 4-tolunitrile was converted to **7** by radical bromination.²⁴² Compound **7** was coupled with imidazole to yield **51**²⁴³ which was subsequently reduced to **52** using DIBAL-H.²⁴⁴ The aldehyde **52** underwent McMurry coupling²⁴⁵ to form isomerically pure (*Z*)-**53**. (See Scheme 18) However, the problem with low yield of final step appeared also in this series as the yield of McMurry coupling was lower than 1%. With such a poor yield, it was not reasonable to upscale this reaction. Poor yield in this synthetic strategy led to think of a new strategy with better yield. The new strategy involved synthesis of double bond by Wittig reaction.

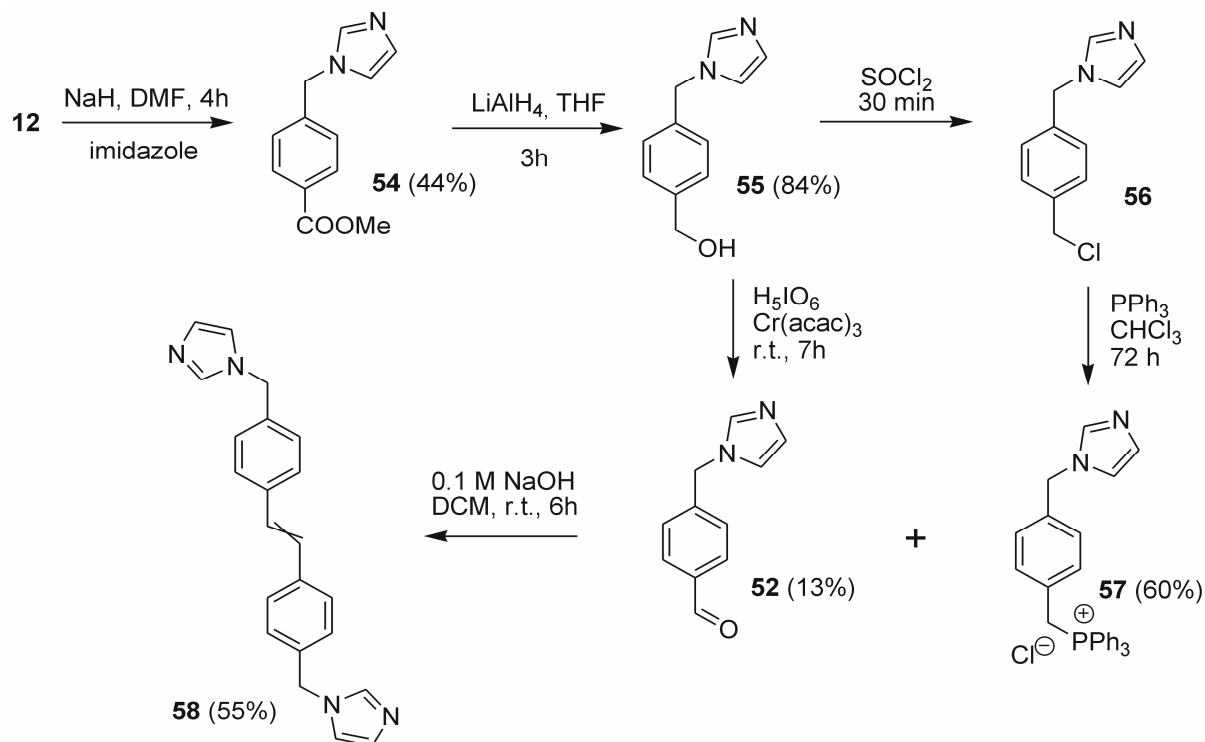
Scheme 18: Strategy involving McMurry coupling approach



Synthetic strategy used for yield improvement of the isomeric mixture **58** was similar to its benzimidazole analogue **17**. The synthetic strategy is shown in Scheme 19.

Compound **12** was prepared by using the procedures which are mentioned in details in the experimental section. The bromoester **12** was coupled with imidazole²⁴⁸ to get **54** which was reduced to corresponding alcohol **55** using LiAlH₄.^{2, 249} Yield of this reaction was much less than its benzimidazole counterpart (50 % with respect to **54**). Subsequently, aldehyde **52** and Wittig salt **57**²⁵¹ were prepared. Isolation problem for **56** was similar to that described for benzimidazole analogue as self-polymerization was observed in this case as well. Thus, compound **56** was confirmed by only GC-MS analysis immediately after work up. Sample was submitted to GC-MS while it was dissolved in ethyl acetate. Compound **56** was treated with PPh₃ in chloroform as solvent to get corresponding salt **57**. The problem with this salt was its purity. It was not possible to purify it on silica gel column and NMR of this compound was not at all completely clear. The NMR spectrum showed presence of many unknown impurities. However, salt **57** was used as such without any purification for the Wittig reaction. Reaction conditions used for Wittig reaction were similar to that of its benzimidazole analogue to get the isomeric mixture **58**. The common problem for all these reactions was low yield compared to their benzimidazole counterparts. The possible reason behind the low yields can be the more solubility of imidazole derivatives in water. So, during the work up, when water was added to the reaction mixture, some compound remained miscible with water and they did not transfer to the organic phase giving low yields in every step. Attempts to separate (*E*) and (*Z*) isomers from mixture **58** were carried out but none of them worked. Since the column chromatography was the main separation method, the separation of the (*E*)/(*Z*) mixture was initially tested on TLC plates (silica gel or neutral alumina) but the mixture did not separate. Attempt to separate both the isomers using the differences in the solubilities of both the isomers was tested but no separation was observed. Further chemistry, namely quaternization, was not carried out because of very low overall yield of **58** (less than 3 %) and it became more important to focus on benzimidazole chemistry as it was showing better results.

Scheme 19: Approach towards **58** via Wittig reaction

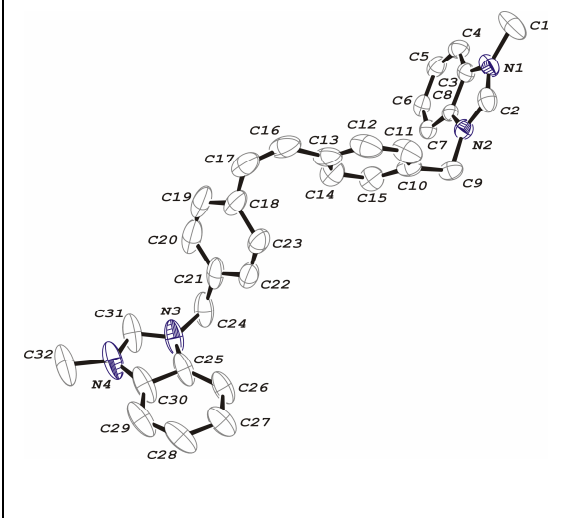


11.4 Synthesis of methyl and adamantyl salts from **17**

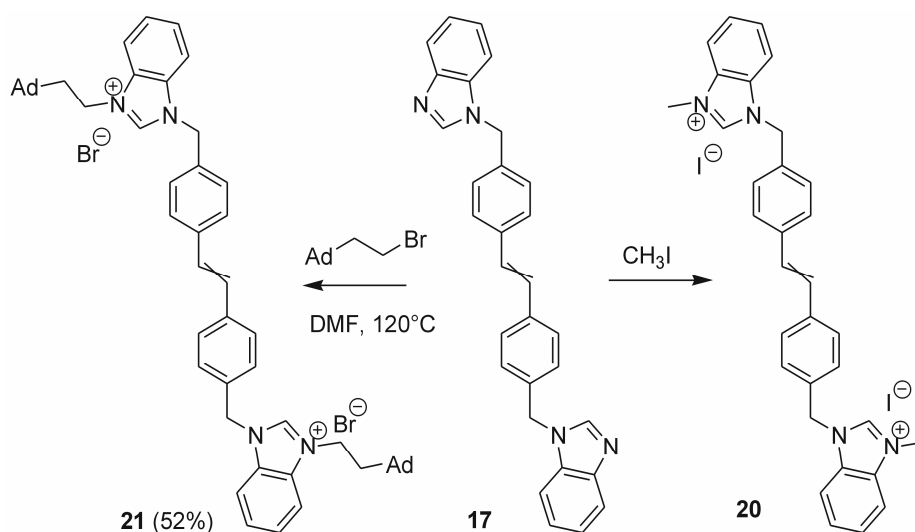
As it was mentioned above, intermediate **17** was a mixture of (*E*) and (*Z*) isomers and no reasonable method for their separation was available. Thus, the compound **17** was used as a mixture and quaternized products were believed to be easier separable. Methylation of **17** proceeded smoothly to yield **20** as a mixture of (*E*) and (*Z*) isomers. These isomers were separated due to their different solubility in many solvents. Since (*E*) isomer is very poorly soluble in MeOH:CHCl₃ (1:50 v/v), it was easily isolated and purified by trituration whereas the mother liquor contained (*Z*) isomer along with small quantity of (*E*) isomer. This almost pure *Z* isomer was finally purified by column chromatography. It should be noted that the clear distinguishing of (*E*)/(*Z*) geometry was not easy. Initially, only indirect support was available. Namely, melting points of (*E*) isomers are usually of higher value than that of (*Z*) isomers; hydrogen atoms at (*E*) double bond are usually more deshielded than those at (*Z*) double bond. Since the guest **20** is symmetrical, the value of ³J_{H,H} of double bond hydrogen atoms could not be used for clarifying of this issue. When an inclusion complex of likely (*Z*)-**20** with β-CD was prepared in water solution, it was found that the exchange mode of this complex is slow and guest molecule becomes non-symmetrical in NMR spectrum (for details, see Chapter 11.5.1). Thus, the ³J_{H,H}=12.40 Hz was obtained. Unfortunately, this value could not bring any new light because the reported values for (*Z*) and (*E*) isomers are in the range of 6–15 Hz and 11–18 Hz, respectively. However, we succeeded in growing of single crystal of (*Z*)-**20** to definitely confirm its geometry by means of X-ray diffraction analysis. The ORTEP of single molecule of (*Z*)-**20** and selected crystallographic parameters are given in figure 28. Two interesting points should be mentioned. Although the compound (*Z*)-**20** was prepared with two iodide counterions, two chlorines were observed by diffraction analysis. This

halogen exchange took place likely due to HCl which could be present in the chloroform from which the single crystals were grown. In addition, the crystallization was repeated for several times under the same conditions with no success. Because three molecules of water are present in the asymmetric unit, some moisture was needed for successful crystal development. Based on this observation, the usage of water-saturated CHCl_3 can be advised for future attempts. Separately, the compound **17** was treated with 2-(bromomethyl)adamantane to get the isomeric mixture **21**. This mixture was not possible to separate into individual isomers, however, it was used for some further studies dealing with (*E*)/(*Z*) equilibration under various conditions. The synthesis of **20** and **21** is shown in Scheme 20.

Figure 28: ORTEP diagram of the compound (*Z*)-**20** and selected crystallographic data. The H-atoms, water molecules and chlorine atoms are omitted for clarity.

	Compound	(<i>Z</i>)- 20
	Empirical formula	$\text{C}_{32}\text{H}_{36}\text{Cl}_2\text{N}_4\text{O}_3$
	Formula weight	595.55
	Color, shape	milky, block
	Crystal size (max – min, mm)	0.15–0.10
	Measured temperature (K)	120
	Crystal system	Triclinic
	Space group	P-1
	Unit cell dimensions (\AA , $^\circ$)	
	a, b, c	9.5329(2), 12.5236(4), 13.2762(4)
	α , β , γ	99.892(2), 103.089(2), 98.899(2)
	Volume (\AA^3)	1489.59(7)
	Z	2
	Absorption coefficient	0.258
	θ range for data collection ($^\circ$)	3.845–29.2530
	Reflections collected	17504
	Reflections unique	5334
Unique reflections with $I \geq 3\sigma(I)$	5061	
Number of param./restraints	372/297	
Final R indices [$I \geq 3\sigma(I)$]	$R_1=0.0934$, $wR_2=0.2289$	
R indices (all data)	$R_1=0.0962$, $wR_2=0.2305$	

Scheme 20: Synthesis of isomeric mixtures **20** and **21**



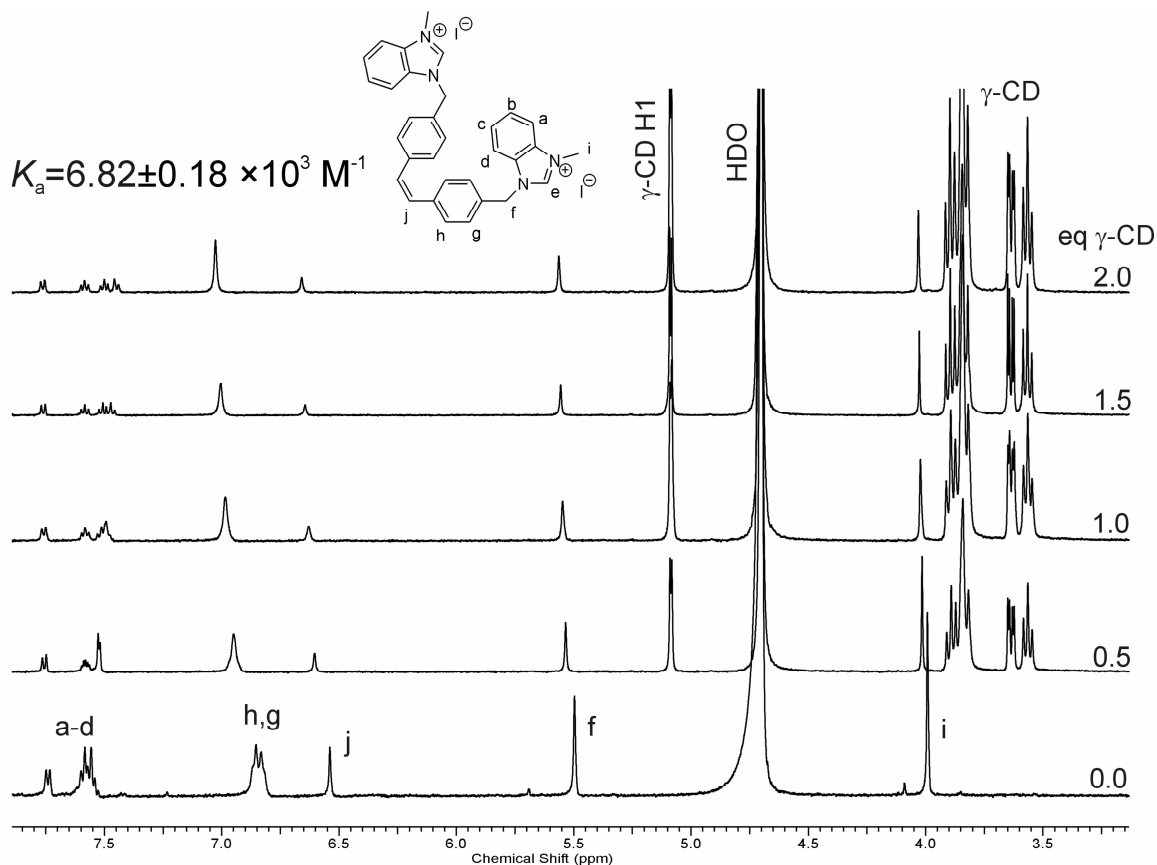
11.5 Binding studies of the guests with stilbene centerpiece

11.5.1 Binding properties of (*Z*)-**20**

As it was mentioned above, two isomers of **20** were successfully separated employing their different solubility. On the other hand, the very low solubility of (*E*)-**20** in water disabled systematic study on binding behavior. Therefore, only binding properties of (*Z*)-**20** are discussed in following text. It should be noted that ESI-MS spectra were recorded for mixtures of both isomers with CDs and CBs and no significant qualitative differences between (*Z*)-**20** and (*E*)-**20** were observed. In other words, at low concentrations which were used for MS studies, both isomers formed aggregates with β -CD, γ -CD, CB[7], and CB[8].

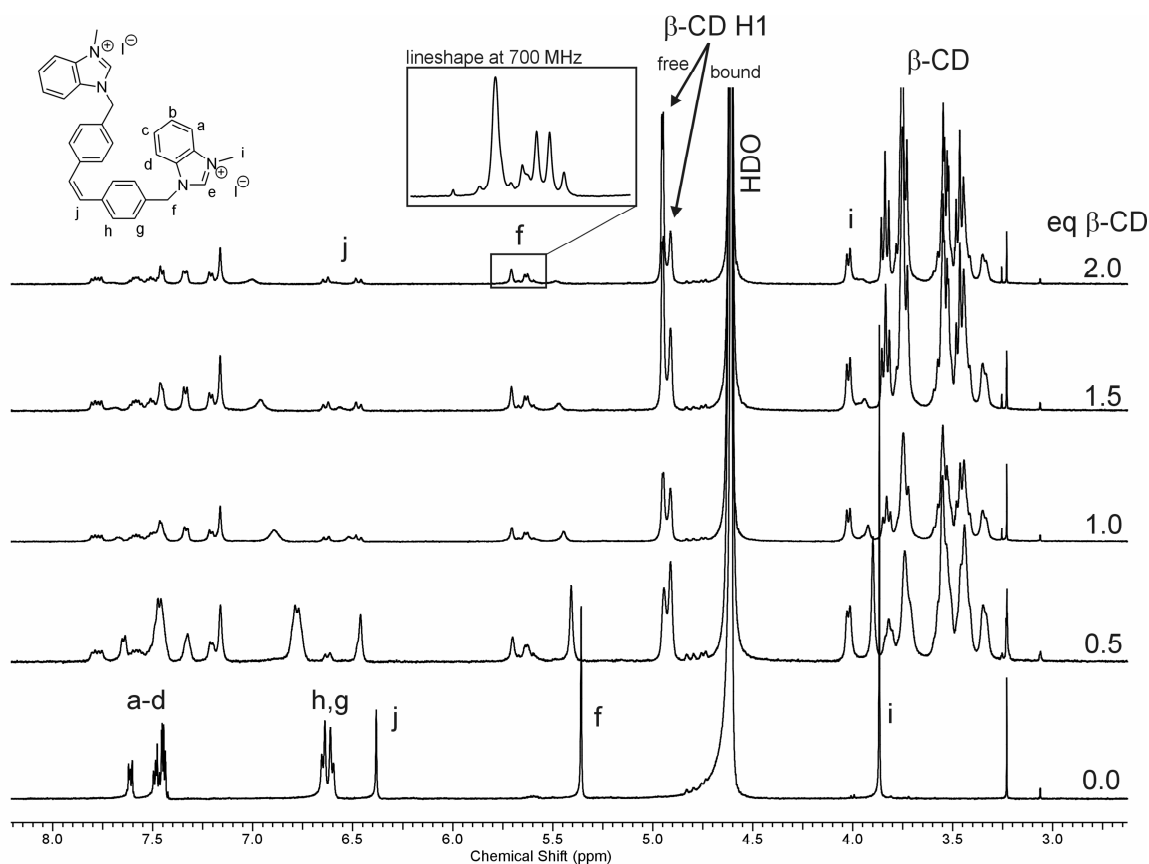
In order to study the binding ability of (*Z*)-**20**, β - and γ -cyclodextrins were selected as a appropriate hosts. Since the effective diameter of central part of the guest **20** was estimated upon X-ray diffraction data to be approximately 7Å, initial study was carried out with γ -CD as the cavity size of γ -CD is sufficiently large to form an inclusion complex with (*Z*)-**20**. Upon titration of (*Z*)-**20** with γ -CD, significant downfield shift of H_i, H_j, and H_f signals was observed as seen in figure 29. The chemical shifts observed for H_f and H_j plotted against γ -CD concentrations were fitted with rectangular hyperbola function and K_a value was calculated to be $6.82 \pm 0.18 \times 10^3 \text{ M}^{-1}$. Unfortunately, no cross-peaks related to the intermolecular interactions were observed in ROESY spectrum of the mixture of (*Z*)-**20** with γ -CD likely due to low binding strength which is combined with wide γ -CD cavity.

Figure 29: NMR titration of guest **20** with γ -cyclodextrin.



Having obtained these promising results, we were wondering if β -CD with narrower cavity can also form an inclusion complex with (Z)-**20**. This experiment gave the most interesting results as unexpected splitting of some signals was observed in ^1H NMR spectra (figure 30). It is clear for the first sight that two sets of signals appeared after addition of β -CD to indicate slow exchange mode of the (Z)-**20**@ β -CD complex. Note, that some, not completely clear, downfield shift of H_i , H_j , and H_f signals can be observed. This can be explained by formation of some non-specific, weak (and thus in fast exchange regime), aggregate which is in equilibrium with much tighter inclusion complex. The second interesting observation is that signals of guest were separated into two sets as guest molecule lost its symmetry being firmly bound in the β -CD cavity. This allowed determination of $^3J_{\text{H,H}}$ as discussed in the Chapter 11.6. The third, and most interesting observation, was that shape of two signals of the H_f atoms from two ends of the guest was not identical (see inserted box in figure 30). Whereas one signal is essentially singlet (A_2 spin system of isolated $-\text{CH}_2-$ group), shape of the second signal matches that of the AB spin system. This clearly means that one half of the guest display different dynamics then the second half. Thus chemical environment of one methylene group is averaged to produce one singlet whereas the second methylene group moves slowly to make the two H-atoms diastereotopic. Such a selective hindering of one half of the guest can be attributed to the positioning of the slowly and quickly moving parts in wider secondary rim and narrower primary rim, respectively.

Figure 30: Titration of (Z)-**20** with β -cyclodextrin in water.



In order to check the binding ability of the guest with cucurbiturils, subsequent titration experiments were carried out with CB[8] and CB[7]. As cucurbiturils can also form supramolecular inclusion complexes and guest could possibly fit into some bigger macrocycle, initial binding study was carried out with CB[8]. The results are shown in Figure 31. Clear movement of all the guest signals indicates some aggregation process. However, it can be seen for instance for H_j signal that these H-atoms were deshielded by 1 eq of CB[8] and then slightly shielded with excess of CB[8]. This observation can be attributed to the change of the binding mode with excess of CB[8] from inclusion complex (Z)-**20**@CB[8] onto likely external complex (Z)-**20**·CB[8]₂. Similar results were obtained by titration of the guest (Z)-**20** with CB[7]. For the stacking of ¹H NMR spectra which were recorded during this titration, see Figure 32. The graph which is inserted in Figure 32 displays plot of chemical shifts against number of equivalent of CB[7].

Figure 31: Binding of CB[8] with guest molecule (Z)-**20** in water.

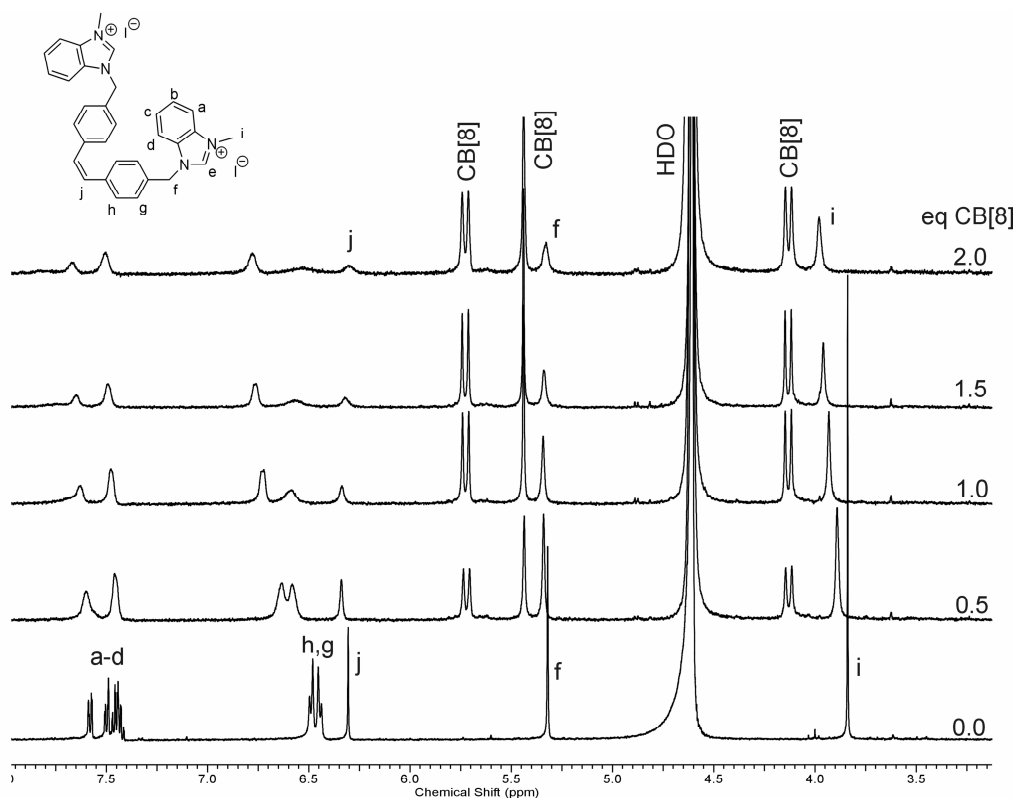
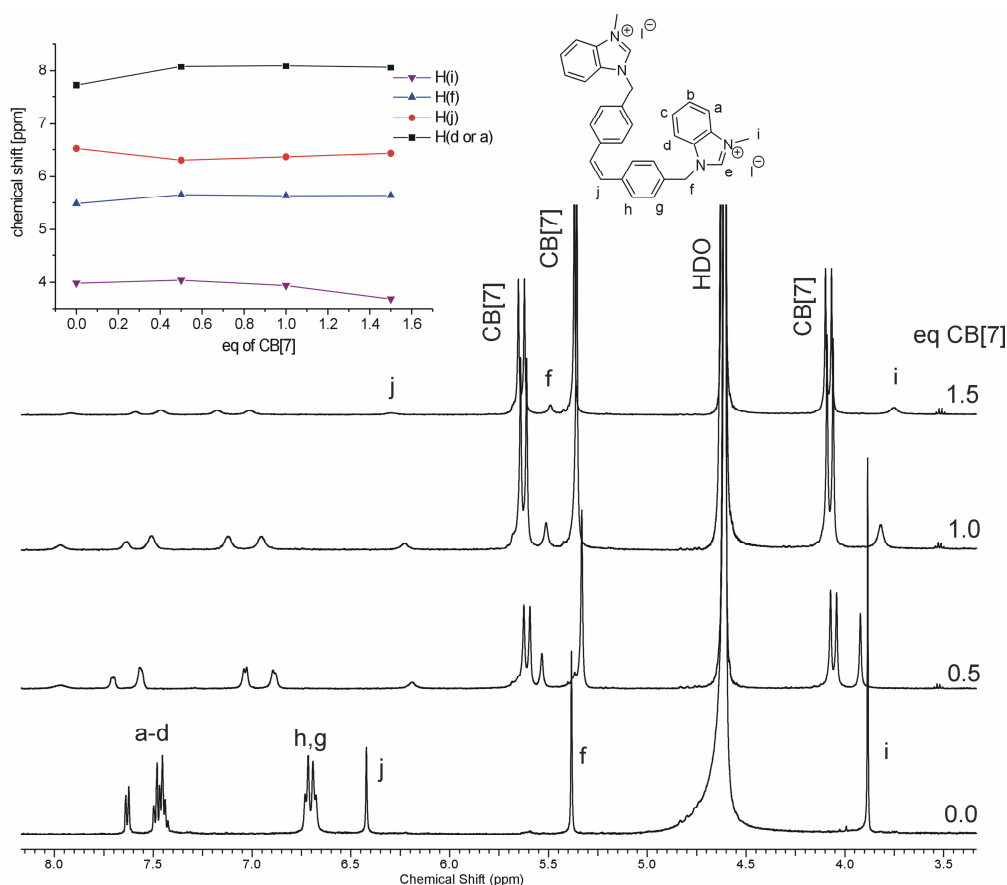


Fig. 32: Binding of CB[7] with guest (*Z*)-**20** in water.



In order to determine the thermodynamic parameters, isothermal titration calorimetry experiments were carried out. The association constants were calculated to demonstrate some interesting trends. The ITC data are summarized in Table 4. The typical result of titration experiment is shown in Figure 33.

Table 4: Thermodynamic parameters obtained by ITC for interaction of guest (*Z*)-**20** in water at 303 K.

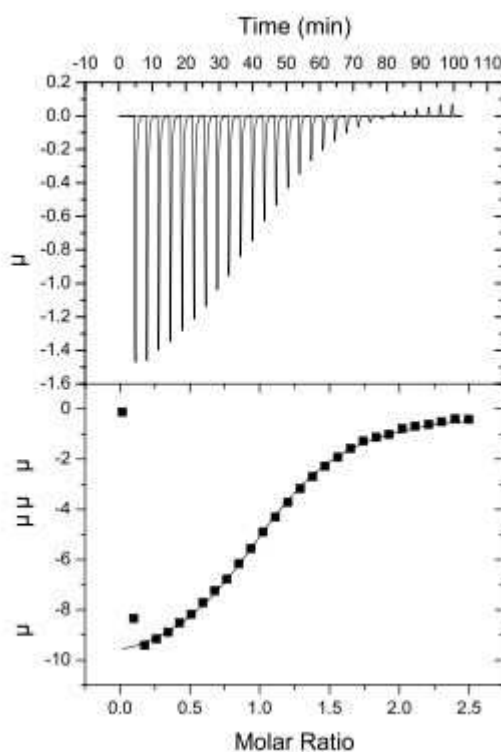
Guest	Host	n	$K[M^{-1}]$	$-\Delta H[kJ \cdot mol^{-1}]$	$\Delta S[J \cdot mol^{-1} K^{-1}]$	$-\Delta G [kJ \cdot mol^{-1}]$
<i>(Z)</i> - 20	β -CD	0.858	8.20×10^3	17.43	17.46	22.71
	γ -CD*	1	6.82×10^3	na	na	na
	CB7	0.938	1.99×10^5	43.84	-43.13	30.75
	CB8 [†]	0.825	2.24×10^7	37.10	18.42	42.66

* K_a was determined by means of 1H NMR titration, $n=1$ was an assumption. [†] Methylviologen was used as a competitor.

The association constant obtained for (*Z*)-**20**@ β -CD is comparable with that for other similar guests. The binding of (*Z*)-**20** with γ -CD was accompanied with too small thermal effects to disable any analysis of ITC data. Fortunately, the association constant was calculated from 1H NMR titration data. Interesting results were obtained for CB[7] and CB[8]. Note that binding strength of **20**@CB[7] is much lower than that of **20**@CB[8]. This can be likely attributed to the better accommodation of the guest **20** by wider CB[8] cavity. In addition, note that the enthalpy contribution in the case of **20**@CB[7] is negative to strongly decrease the overall energetic gain. We can speculate that this can be caused by freezing of

conformational movements of the guest molecule which can be expected for binding of **20** inside rather narrow CB[7] cavity.

Figure 33: ITC result recorded for guest **20** with CB7 in water at 303K. OneSetSites model was used for data analysis.



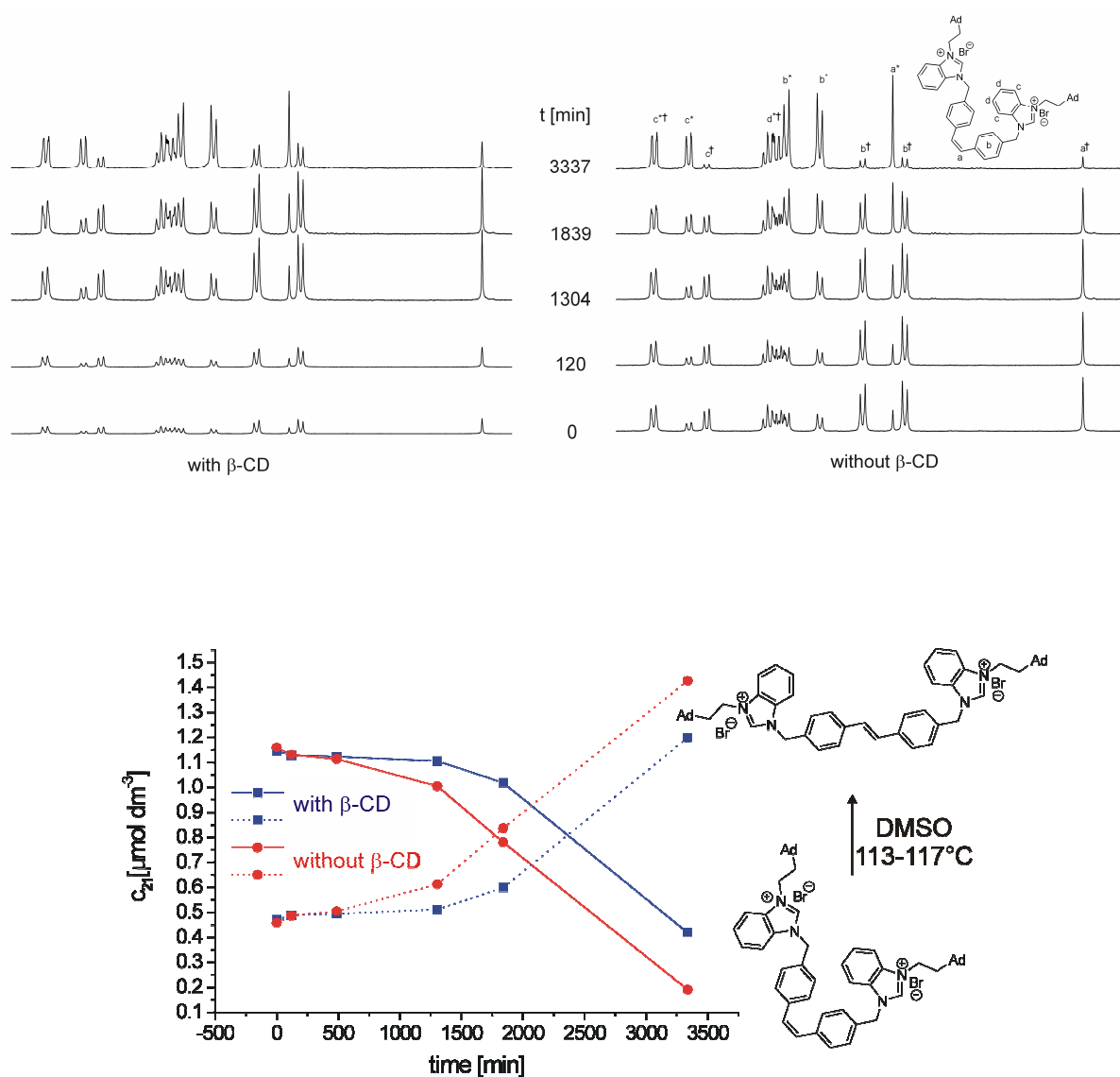
11.5.2 (*E*)/(*Z*) interconversion of guests **20** and **21** under UV irradiation and thermal treatment

It is well-known and documented in Theoretical section that [2+2] cycloadditions of stilbene substrates have been extensively studied. In supramolecular chemistry, the influence of macrocyclic hosts on the stereoselectivity was particularly concerned. In addition, stilbenes are known for their reversible (*E*) \rightarrow (*Z*) \rightarrow (*E*) conversions moderated by UV-VIS irradiation and thermal treatment, respectively. In order to examine this properties of our stilbenes, some preliminary experiments were carried out. Thermal rearrangements of **21** (mixture of isomers) and (*Z*)-**20** were conducted in DMSO at approximately 115°C. The irradiation experiments were performed at ambient temperature using a mercury medium-pressure 125W lamp and an acetone filter. Reactions were performed in borosilicate glass NMR tubes to allow monitoring of reaction progress by NMR without any further manipulations with the samples. Obtained results can be briefly summarized as follows.

The conversion of (*Z*) isomer to (*E*) isomer was observed for both **20** and **21** under both thermal and irradiation treatment. The rate of conversion was much lower for the guest **20**. In another words, the adamantylated guest **21** underwent the (*Z*) \rightarrow (*E*) conversion much more rapidly than methylated guest **20** under both conditions. Subsequently, it was found that the presence of 2.5 eq of β -CD (other molar ratios were not tested) significantly decreased the

conversion rate of thermal (*Z*)→(*E*) rearrangement of **21** whereas other tested reactions (i.e., thermal rearrangement of (*Z*)-**20**→(*E*)-**20** and UV-rearrangements of (*Z*)-**20/21**→(*E*)-**20/21**) were not influenced. The stacking plots of ¹H NMR spectra for thermal rearrangement of (*Z*)-**21**→(*E*)-**21** are shown in figure 34 (top). Formation of no side-products was observed in NMR spectra. Mixtures were treated for slightly more than 55 h at approximately 115°C. As can be clearly seen in Figure 34 (bottom) the amount of (*Z*)-**21** was decreased faster in the sample where no β-CD was added. Further experiments will be designed and performed to clarify whether there is some non-specific (protic component of reaction environment, increased viscosity,...) or specific (formation of inclusion complex) influence of β-CD.

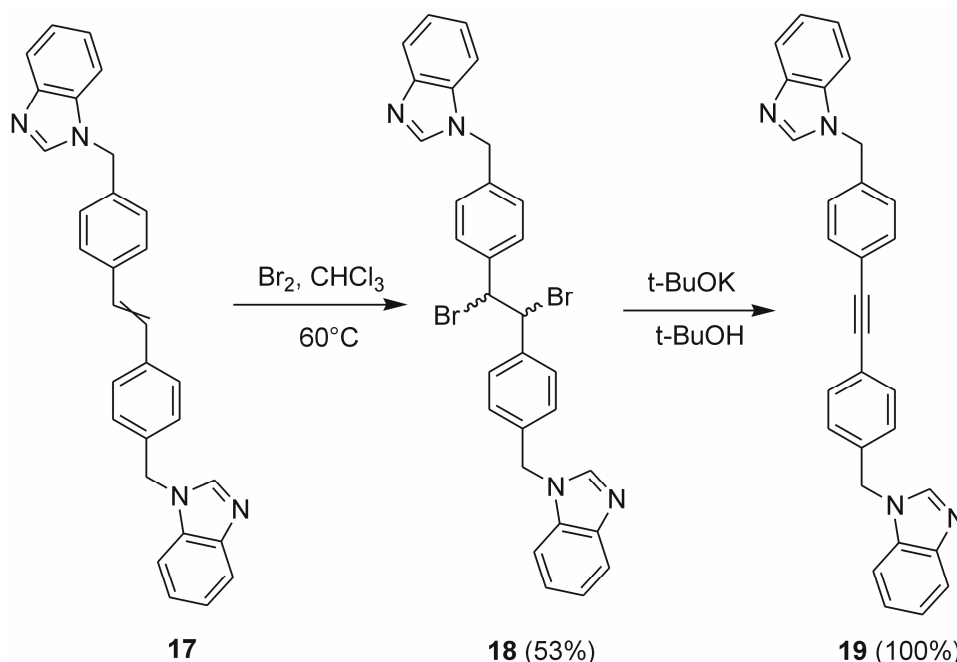
Figure 34: (*Z*)-**21**→(*E*)-**21** transformation with and without β-CD at 113–117°C. Stacking plot of ¹H NMR spectra (top) and plot of the **21** concentrations against time (bottom).



11.6 Synthesis of 1,2-diphenylacetylene spacer

The preparation of diphenylacetylene spacer represents a logical extension of previously described study on stilbene derivatives. One important reason is that diphenylacetylene spacer is rigid structure with well-defined distance between possible terminal binding sites (in agreement with initial justification of this project). The second reason is that preparation of diphenylacetylene derivatives is simple two-step extension of the stilbene synthetic procedure. Accordingly the compound **17** (actually, the *(E)/(Z)* mixture) was taken as a starting material for this diphenylacetylene chemistry.

Scheme 21: Synthesis of diphenylacetylene spacer



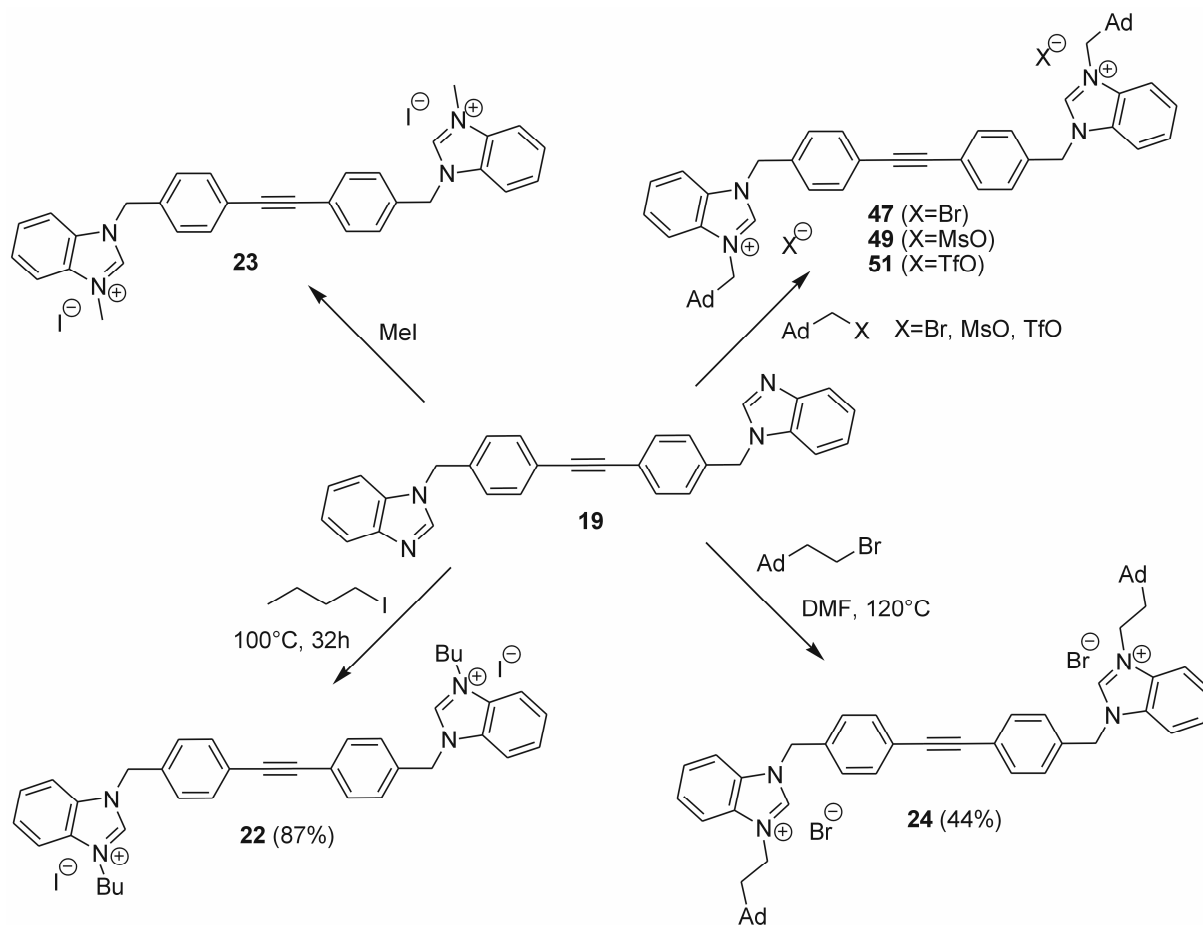
Since the quaternization was assumed as a final synthetic step, the compound **19** was required intermediate to make the quaternary ammonium salts with different alkyl halides. Thus, compound **19** was prepared as shown in Scheme 21. Starting stilbenes **17** were brominated to get the mixture of enantiomers and diastereoisomers of **18**²⁵² which was impossible to separate. This mixture was dehydrohalogenated²⁵³ using $t\text{-BuOK}$ to get the required acetylene spacer **19**. The solubility of both **18** and **19** was poor. Thus, purification was not carried out in both the cases. Still, the compound **19** was sufficiently pure to be used in the next steps.

11.7 Synthesis of quaternary benzimidazolium salts with diphenylacetylene centerpiece

Methylation of **19** was carried out using methyl iodide under many conditions. Most of the reactions yielded multiple methylated compounds. The reaction conditions and results were as follows. Initially, the compound **19** was stirred in neat CH_3I at room temperature under inert atmosphere for 24 h. Reaction progress was monitored by TLC. Diethyl ether was added to the reaction mixture to precipitate the solid which was analysed on ESI-MS. It showed formation of trimethylated product predominantly and dimethylated compound in traces. Both the products were likely quaternary salt and thus the mixture was impossible to

separate. In order to support the formation of desired dimethylated compound **23**, it was decided to use CHCl_3 as a solvent to dilute the highly reactive methyl iodide. Accordingly, the compound **19** and CH_3I were taken in chloroform. Reaction was stirred at room temperature for 24 h under inert atmosphere. Reaction progress was monitored by TLC. Diethyl ether was used to precipitate out the solid which was analyzed on ESI-MS. Unfortunately, the result was the same as described above. Solid obtained was inseparable mixture of di and tri methylated compounds and thus it became necessary to think for different reaction condition. From above experiments, it was concluded that higher temperature has caused trimethylation of **19**. In next attempt, temperature of reaction was maintained at 0°C . Compound **19** and neat CH_3I were stirred at 0°C for 72 h. Reaction mixture was directly submitted for ESI-MS analysis which showed formation of desired dimethylated compound **23** but still large amount of unreacted starting material **19** was present. Thus, it was necessary to increase the temperature slightly to speed up the reaction. In the last successful attempt, **19** and neat CH_3I were stirred under nitrogen atmosphere at 10°C for 72 h. ESI-MS analysis showed formation of desired dimethylated quaternary ammonium salt **23** without formation of any other compound. The product was precipitated out by dry DEE and purified by column chromatography as described in experimental section 7.4.4.

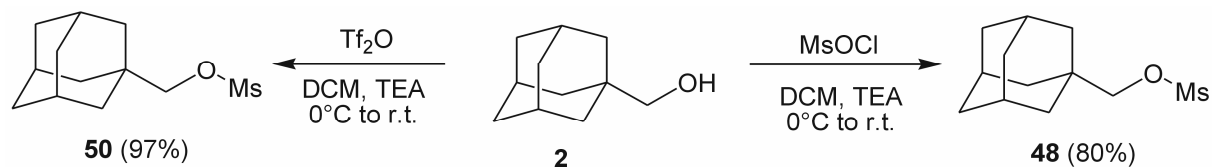
Scheme 22: Synthetic approach towards bisbenzimidazolium salts with diphenylacetylene centerpiece.



From supramolecular point of view, the guest molecule with title centerpiece and two terminal adamantane-based binding sites with high affinity towards CB[7] and β -CD is of high importance. Thus the synthesis of the compound **47** was attempted. The adamantylmethyl(benz)imidazolium site is well-known in our group and 1-adamantylmethylbromide (**2**) is usually used for the quaternization step. Unfortunately, in this case, the utilization of **2** to synthesize **47** failed as no reaction progress was observed. All the unsuccessful attempts are mentioned in following text. Initially, the compound **19** and **2** were dissolved in DMF and reaction mixture was stirred at room temperature for 48 h. Reaction progress was monitored by TLC. Since only starting compound was observed, it was decided to increase the temperature to 60°C. Unfortunately, after additional 48 h at 60°C, the result was similar as that at room temperature. Another option to achieve the required product was to increase the temperature even more. Thus, another reaction of **19** and **2** was carried out at 120°C. The result of this reaction was similar as in previous cases. Only starting material **19** was observed in TLC. To observe some progress, solvent was changed from DMF to acetonitrile. But also in this case, only starting material **19** was observed. Thus, working on the synthesis of **47** was stopped as no reaction was successful. This failure can be attributed to the possible inertness of **2** towards **19**. Thus, another strategy was implemented where bromine from **2** was replaced by better leaving groups such as mesylate and triflate.

As all three attempts with **2** were failed, use of some another strategy was necessary to prepare the guest with admantylmethyl substituent. Changing of leaving group from bromide to mesylate could have been a useful strategy. Mesylate is well-known good leaving group as compared to bromide. Synthesis of adamantylmethyl mesylate is shown in Scheme 23.

Scheme 23: Synthesis of mesylate and triflate esters



Synthesis of mesylate **48** was carried out by using a procedure from literature without difficulties.²⁶⁹

With mesylate **48** in hands, the quaternization step with **19** was tested. Compounds **19** and **48** were dissolved in DMF under inert atmosphere. Reaction mixture was stirred at room temperature for 96 h while the reaction progress was monitored by TLC. Unfortunately, starting material was found unreacted and no progress was observed. Thus, reaction was discarded and starting compound **19** was recovered. As mesylate was proved to be bad choice, implementation more labile triflate group as a leaving group was carried out. In this strategy, preparation of adamantylmethyl triflate (**50**) was planned and it was used to carry out quaternization of **19**. Scheme 23 shows formation of adamantylmethyl triflate **50** from triflic anhydride according to the procedure mentioned elsewhere.²⁷⁰

Subsequently, **19** and **50** were dissolved in CHCl_3 under inert atmosphere and heated to 50°C for 72 h. Reaction progress was monitored by TLC. Starting material was found unreacted and no formation of desired salt **51** was observed. Thus, reaction was discarded and starting compound **19** was recovered.

After so many attempts to synthesize quaternary benzimidazolium salt with adamantylmethyl substituent, it was decided to carry out the quaternization using 2-(bromoethyl)adamantane to check if changing of the reagent works or not. The reaction is shown in Scheme 16. Surprisingly, the reaction of **19** with 1-(2-bromoethyl)adamantane proceeded smoothly in DMF at 120°C and required salt **24** was isolated in acceptable yield of 44 %. The starting 1-(2-bromoethyl)adamantane was prepared in our group by somebody else using the procedure from literature.²⁷¹ Finally, bisimidazolium salt **22** with two terminal butyl binding sites (useful for CB[6] or α -CD) was prepared by reaction of compound **19** with butyliodide (Scheme 16). Reaction was hold in neat BuI at 100°C for 32 h to get **22** as yellow solid.

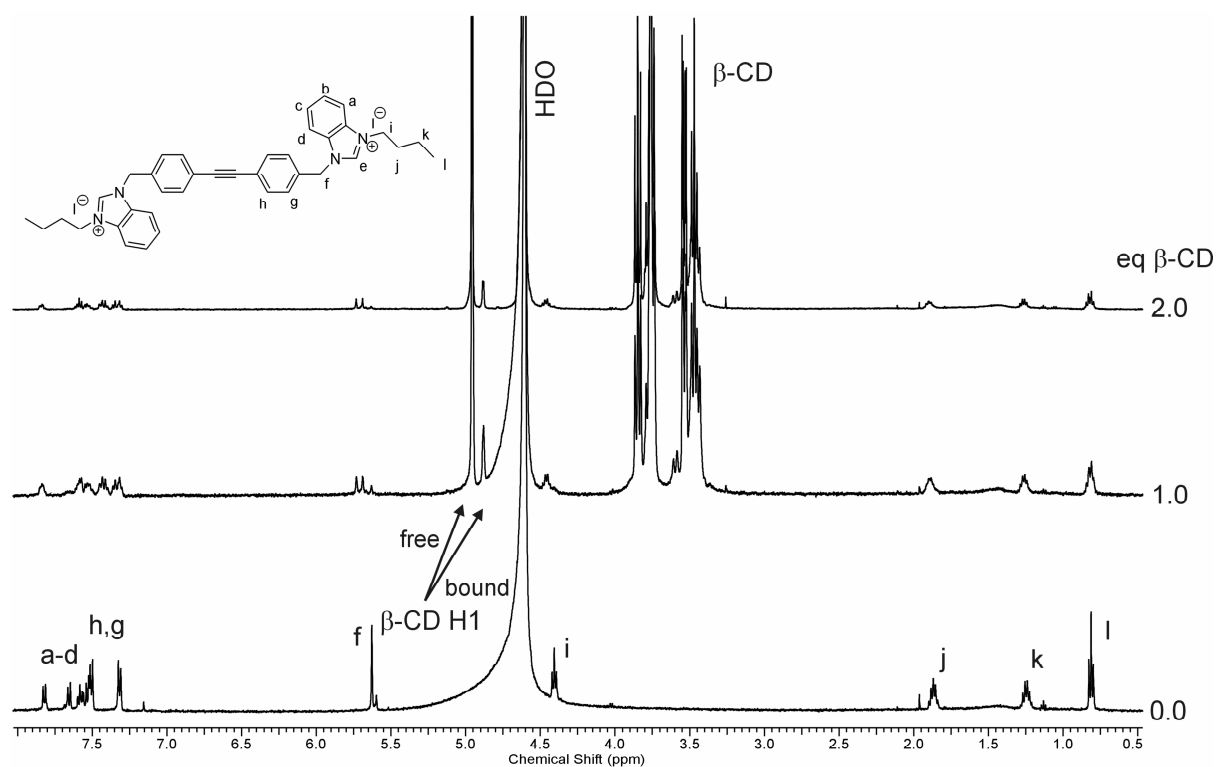
11.8 Binding studies of the guests with diphenyl acetylene centerpiece

Three compounds were prepared in this series with butyl, adamantylethyl and methyl substituents. The most serious problem for all the three derivatives was their poor solubility in any available environment. The studies of binding properties are limited by solubility of hosts. Whereas cyclodextrins are sufficiently soluble in water, methanol, and DMSO, cucurbiturils are essentially insoluble in any other solvents than water. In addition, the water environment is necessary for hydrophobic effect, which is the main driving force in the case of cyclodextrins complexes. Unfortunately, it was not possible to reach required concentrations for all the guests and, thus, only few NMR titration experiments could be performed with qualitative outputs. Therefore, results of binding studies of acetylene guests are rather indicative than fully descriptive.

11.8.1 Biding properties of guest **22**

The guest **22** was studied initially for its binding ability towards CB[7]. Unfortunately, the first addition of the CB[7] into solution of the guest **22** led to the unexpected precipitation of the complex (most likely). All signals of guest disappeared from the spectrum to disabled any analysis of data. NMR spectra recorded after addition of CB[7] showed only presence of CB[7]. So, in order to observe some interactions between ligand and host, mixed solvent D₂O:DMSO (2:1 v:v) was used. NMR titrations showed some binding of ligand **22** with both host compounds. The results obtained for CB[7] indicated that terminal butyl sites were occupied by the host molecules. Subsequently, the interactions between guest **22** and β -CD were studied in water by means of NMR. Stacked NMR spectra describing the titration of **22** with β -CD are shown in figure 35. As can be clearly seen, two sets of signal were observed during titration which indicates the slow exchange mode. In addition, the signal of H_f is splitted as the guest molecule lost its symmetry being included in non-symmetrical cavity of β -CD. Encouraged with this result, the compound **22** was now dissolved in DMSO:D₂O mixture (2:1 v:v). Unfortunately, no binding was detected in this environment as no complexation-induced shift of any guest signal was observed.

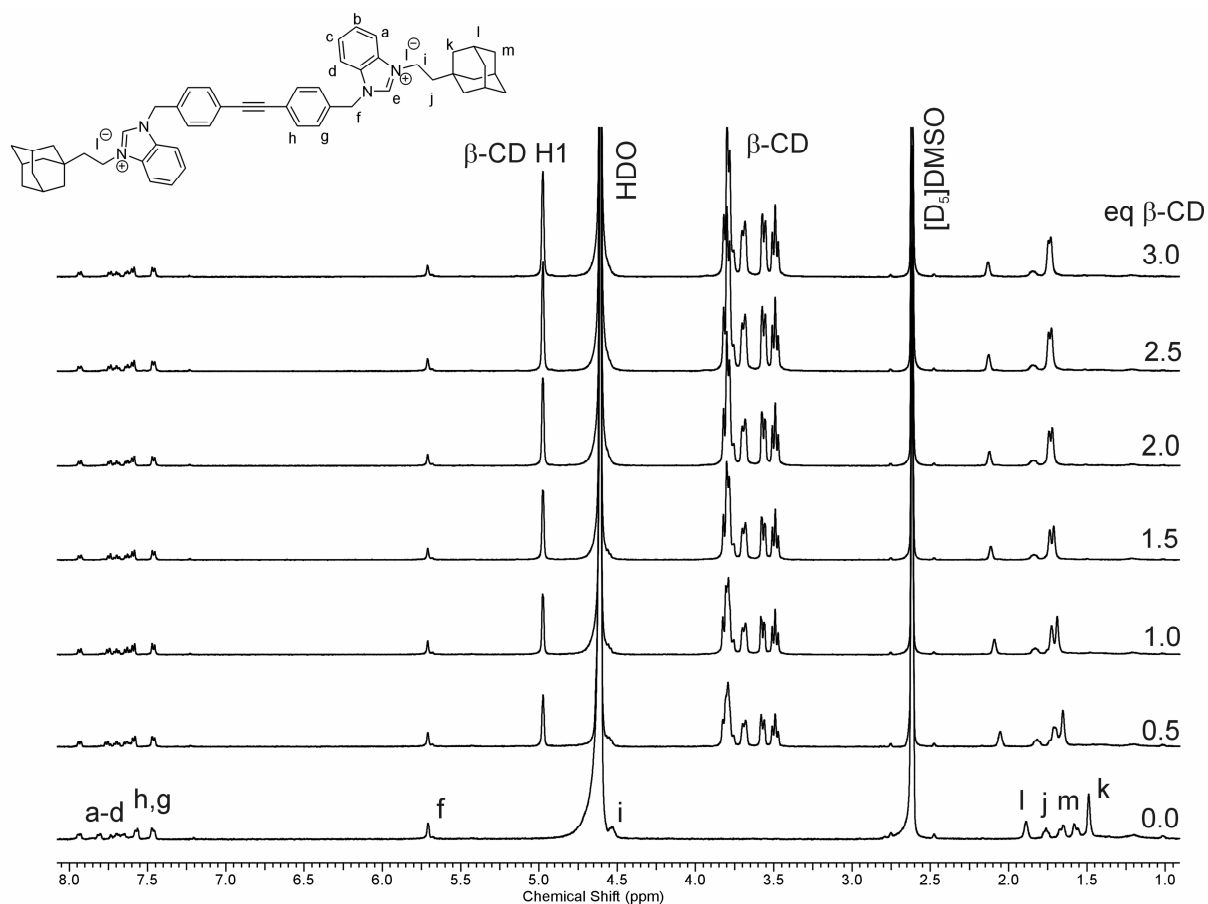
Figure 35: Binding of β -CD with **22** in water



11.8.2 Binding properties of guest **24**

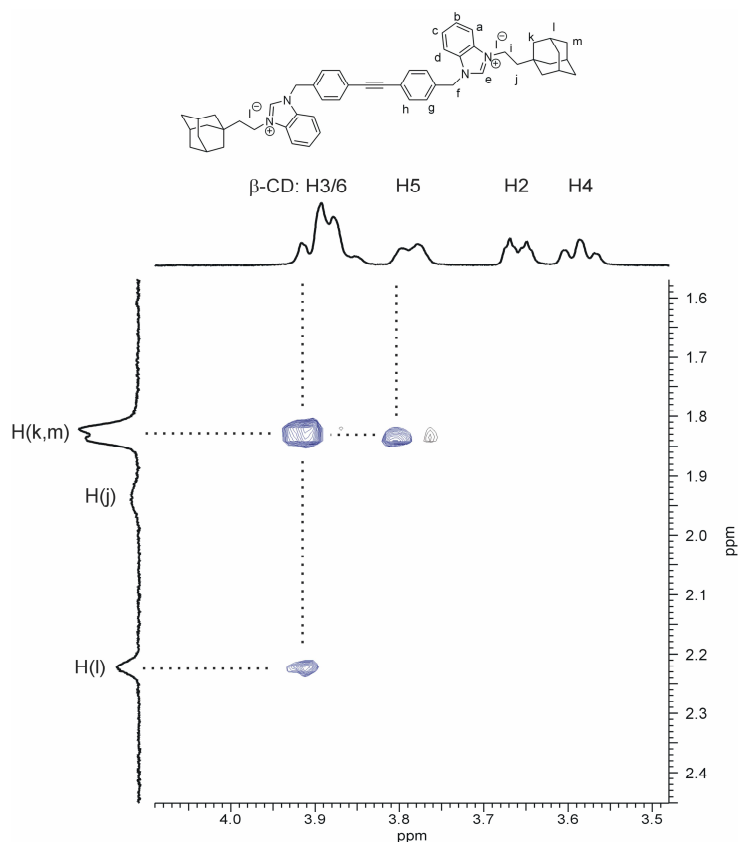
Guest **24** was initially tested for its binding ability towards β -CD. In the first experiment, **24** was attempted to dissolve in water. But, compound **24** was found to be essentially insoluble in water as no signals were observed in NMR spectrum. Nevertheless, after addition of β -CD, signals of guest protons appeared in the spectrum. This observation indicated that complex, likely in the inclusion manner, was formed with significantly higher solubility than that of free guest. Thus, further experiment was performed in $[D_6]DMSO:D_2O$ (1:2, v:v) system to dissolve the guest. The spectra recorded during this titration are shown in Figure 36. It can be clearly seen that signals of adamantane cage move downfield to indicate inclusion of adamantane cage inside the β -CD cavity. It should be noted that guest was present in the initial sample as a fine dispersion and was subsequently dissolved with increasing portion of β -CD. Therefore, any quantitative analysis of obtained data was disabled.

Figure 36: Binding of **24** with β -CD in DMSO:D₂O (1:2 v:v)



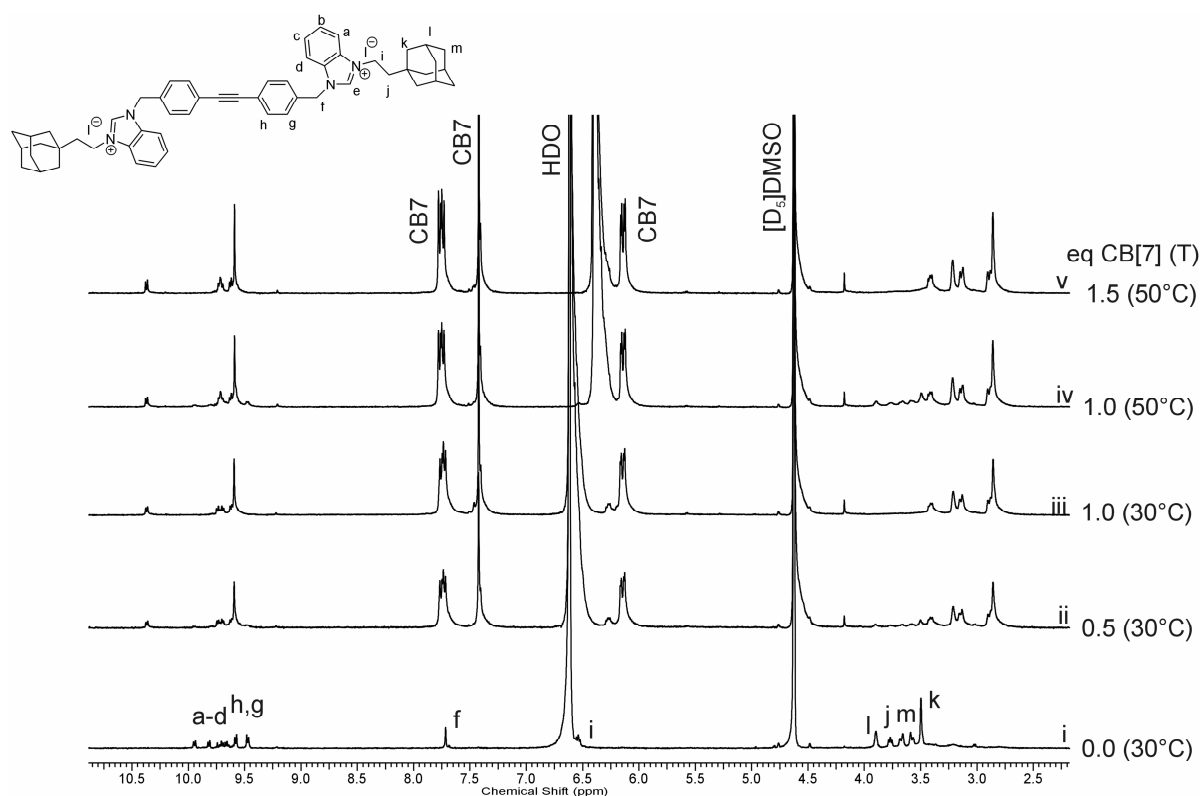
The hypotheses that the adamantane cages were included inside the β -CD cavities were supported by the ROESY spectrum shown in figure 37. This ROESY spectrum was recorded for the authentic sample after ¹H NMR titration experiment, i.e., three equivalents of β -CD were present in the solution. The observation of cross-peaks related to the intermolecular interaction between internal β -CD hydrogen atoms (H3, H5) and hydrogen atoms of adamantane cage clearly evidenced the inclusion complex. However, the information about stoichiometry of the complex remained disabled.

Figure 37: Portion of ROESY spectrum of **24**: β -CD (1:3) mixture in D_6 -DMSO: D_2O (1:2, v:v)



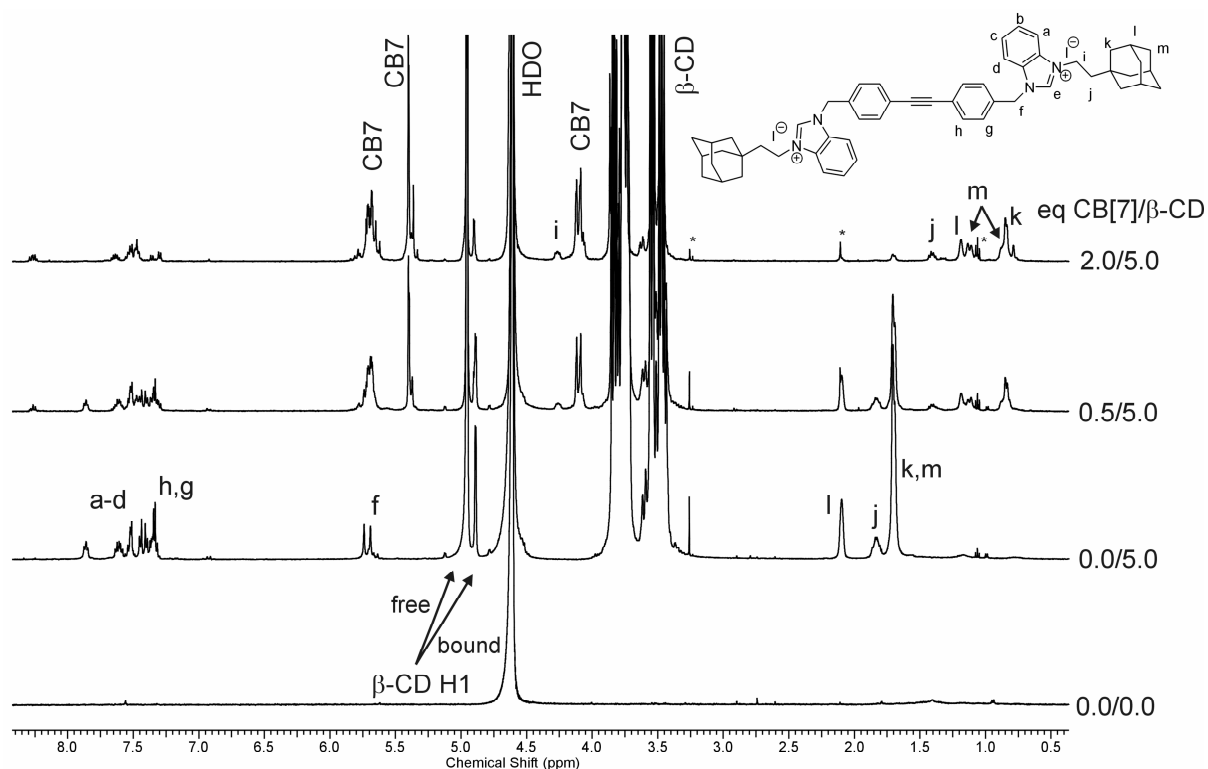
In order to check the binding of guest **24** with CB[7], the guest **24** was dissolved in DMSO: D_2O (2:1 v:v) and titrated with 250 μ l portions of CB[7] at 30°C. Because of low solubility of the guest **24**, the higher temperature was applied for the last two measurements. All details are given in Figure 38. First, it should be noted that the titration did not start with clear solution as significant portion of guest remained not dissolved. Therefore, all the adamantane signals were completely shifted upfield after addition of 1 eq of CB[7] (see Figure 38, lines i→iii). This observation indicates, that addition of CB[7] did not increase the solubility of guest too much, if any. To enhance solubility of the guest, the temperature was ramped up to 50°C. As can be seen in figure 38, line iv some signals related to the non-occupied adamantane site appeared. We can only speculate if it was caused by dissociation of the complex or, more likely, by dissolving of larger portion of guest. However, no signals of free adamantane site were observed after addition of further 0.5 eq of CB[7] (i.e., total amount of CB[7] was 1.5 eqs, see Figure 38, line v). Therefore, we can conclude that guest **24** forms a complex, likely in the inclusion manner, with CB[7] at 30–50°C. However, any quantitative information about stoichiometry is not available.

Figure 38: Binding of **24** with CB[7] in DMSO:D₂O (2:1 v:v)



Finally, the guest **24** was used for the formation of ternary aggregate with CB[7] and β -CD. This experiment can be followed in Figure 39. The guest was taken in D₂O and, as expected, no guest signals were observed in ¹H NMR spectrum. The guest signals appeared after addition of 5 eq of β -CD because the complex of **24** with β -CD is better soluble in water than **24**. Therefore, observed signals can be attributed likely to the complexed guest. Signal of the two H-atoms of —CH₂— group showed splitting from one singlet to two singlets. This can be attributed to the situation that one proton is present in the wider part of β -CD cavity and the other proton is present in the narrower part of the β -CD cavity. Two more β -CD molecules should form inclusion complex with the adamantyl group. Subsequently, two portions of CB[7] were added which led to the significant upfield shift of the adamantane signals. Note that the signal related to the H1 of firmly bound β -CD can be clearly observed in final spectrum. This can be understood as a strong support for the predominant formation of the aggregate with one β -CD unit at the central acetylene site and two CB[7] units at the terminal adamantane sites.

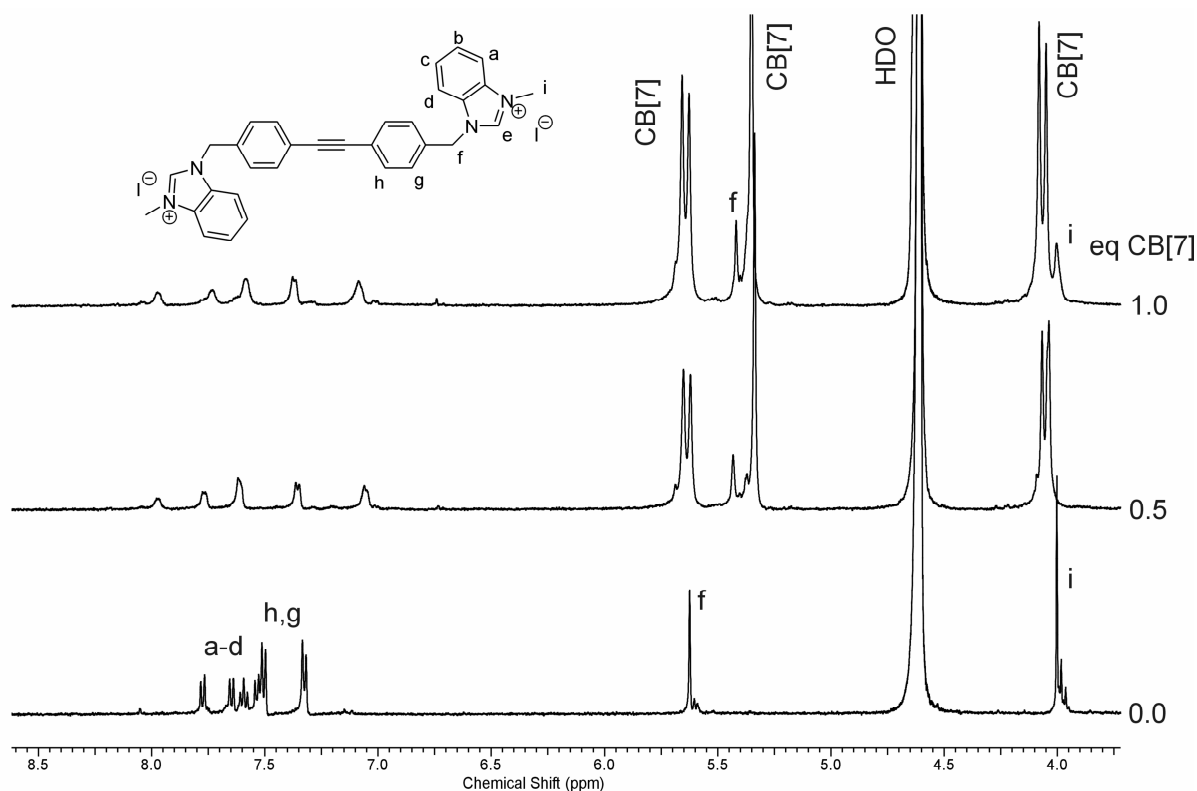
Figure 39: Titration of **24** with β -CD and CB7.



11.8.3 Binding properties of guest **23**.

The problem with solubility was present as usual in the diphenylacetylene guest's family. Fortunately, guest **23** was partially soluble in D_2O which allow some 1H NMR experiments. Initially, the guest **23** was titrated with CB7 in D_2O as solvent (Figure 40). The signals of the hydrogen atoms of benzene ring (H_g and H_h) have shown up field movement while the signals of the benzimidazole H-atoms (H_a and H_d) have shown some down field movement (this interpretation of 1H NMR spectra will be supported by assignment of signals of complexed guest in near future). More clearly, the signals of H-atoms of methyl H_i and methylene H_f showed downfield and upfield shift, respectively. This observations indicates formation of a complex in pseudorotaxane manner with the CB[7] unit positioned at the central binding site. It should be pointed out that only one set of signals was observed during titration. This indicate fast exchange mode which is usually related to the relatively weaker binding.

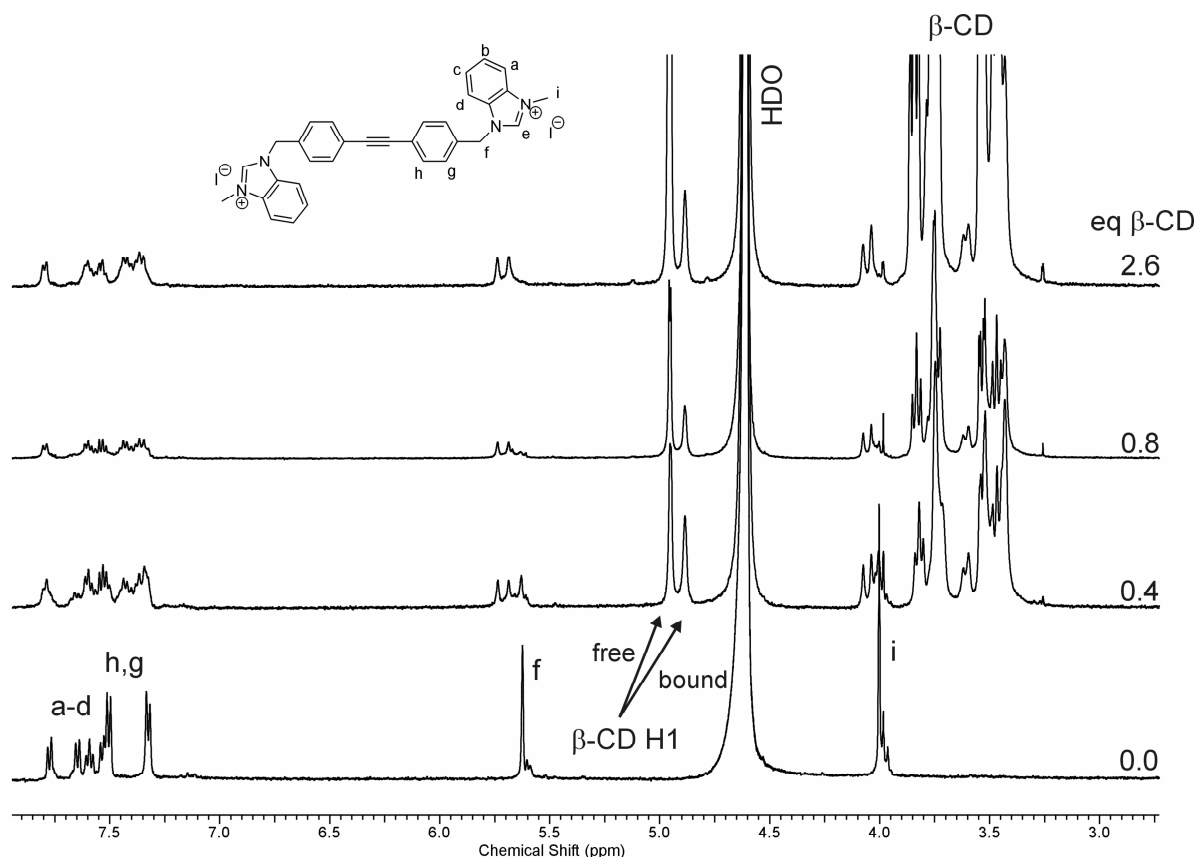
Figure 40: Binding of **23** with CB[7] in water



Subsequently, the binding properties of **23** with β -cyclodextrin were studied in water by means of ^1H NMR. In contrast to the previous experiment, two sets of signals appeared with the addition of the β -CD solution to indicate slow exchange mode. In addition the splitting of some signals of bound guest into two sets was observed. This can be attributed to the arrangement in which one H_f proton is positioned in the wider side of the CD cavity and the second H_f in the narrower CD side. Similar splitting can be unambiguously observed for the signal of the H_i whereas analysis of overlapped aromatic signals is not possible. Figure 41 shows stacked ^1H NMR spectra recorded during titration of the guest **23** with β -CD.

In subsequent experiment, CB[6] was used to check the binding ability of guest **23** towards this macrocycle with narrower cavity. The problem of solubility of the guest persisted but the solubility was expected to increase after formation of inclusion complex. The spectrum of pure guest showed very weak signals and upon addition of the host CB[6] no unambiguous shifting of any signals was observed. Therefore, we can conclude that CB[6] does not form inclusion complex with the guest **23**, and if do, the binding is too weak to be observable in NMR spectrum.

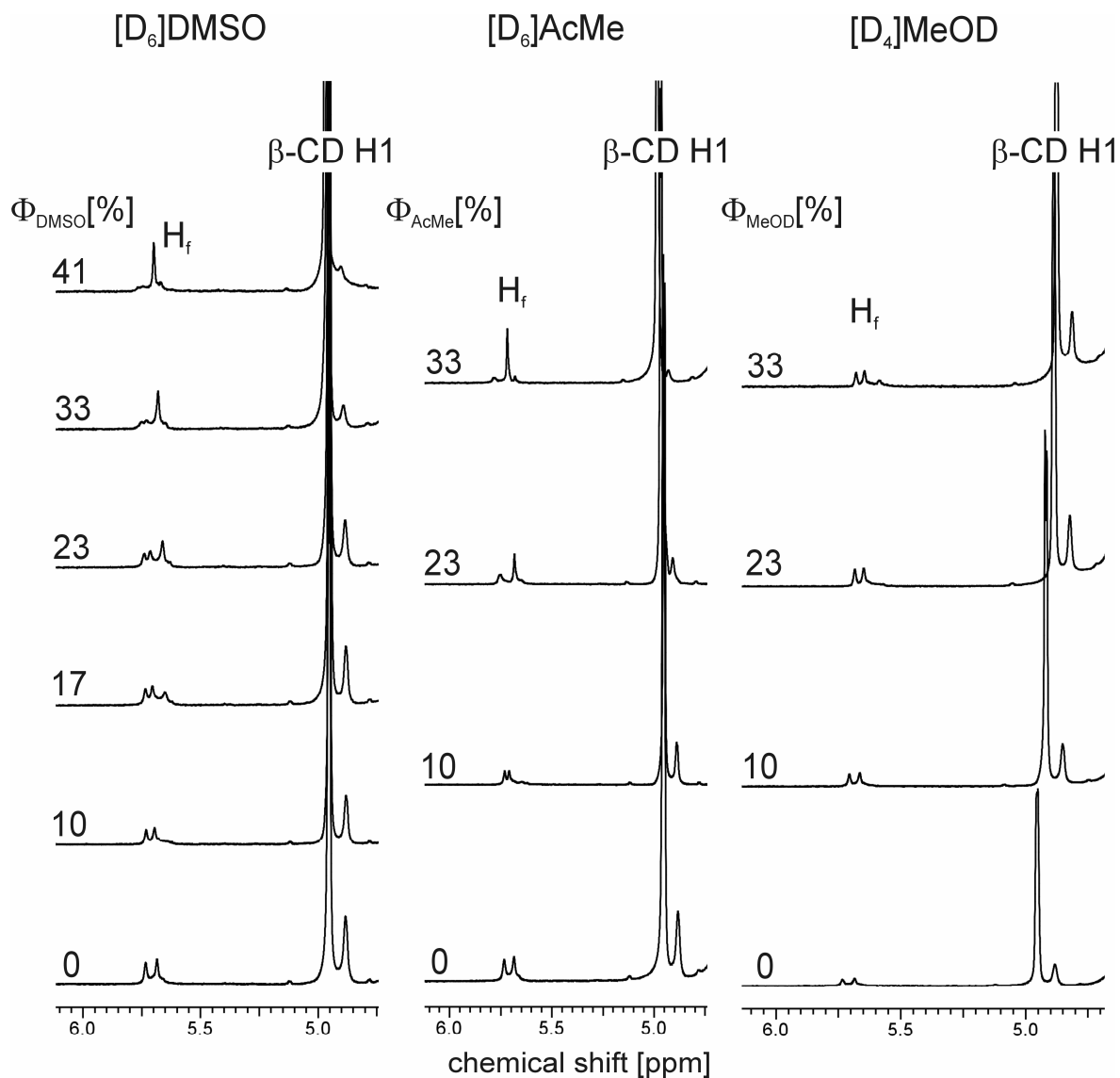
Figure 41: Binding of **23** with β -CD in water



As the solubility of the guest **23** in water is low, the new series of experiments was planned in mixed solvents. Preliminary experiments showed that the guest **23** forms an inclusion complex with β -CD in mixture of DMSO:D₂O 1:1 v:v. In contrast to the experiment in D₂O, the exchange mode was found to be fast in the NMR timescale. In order to examine the influence of the DMSO concentration on the exchange mode switching, the D₂O solution of **23** was titrated with [D₆]DMSO. As can be seen in Figure 42 (left), the two peaks at approximately 5.7 ppm assigned to the guest proton H_f are decreasing in their intensity with increasing portion of DMSO and new single peak appeared. Two explanations can be formulated. Either the inclusion complex **23**@ β -CD was dissociated upon addition of DMSO or the exchange mode was switched from slow (two peaks for H_f) to fast (only one peak for H_f). The latter hypothesis was strongly supported by independent titration experiment. The solution of guest **23** was titrated with β -CD in mixture DMSO:water 1:2 v:v. In this case, unambiguous downfield shift of adamantane signals was observed to indicate formation of an inclusion complex. Subsequently we examined influence of some other solvents, namely, acetone and methanol. The spectra related to the titration experiment with acetone can be seen in Figure 42 (middle). Result was essentially the same like in the previous case; i.e., signals assigned to the slow exchange diminished with approximately 30 %_{vol} of acetone in the mixture. In strong contrast, no significant reducing of the portion of the slow exchange was observed during titration with [D₄]methanol. This observation indicates that switching of the binding model is solvent-dependent. We can only speculate whether the

protic nature of methanol is the source of its extraordinary property. To clarify this issue, some other solvents; e.g., $[D_6]$ ethanol, CD_3CN , $[D_8]$ dioxane, will be tested in near future.

Figure 42: Changing of exchange mode during titration of water solution of **23**@ β -CD with various solvents. Φ is volume ratio.



Conclusion

Trisimidazolium and trisbenzimidazolium guests **4** and **6** containing adamantane binding sites with C_3 symmetry were prepared by synthetic procedures mentioned in the experimental section. The 1,3,5-trisubstitute benzene was used as a central structural motif. It was subsequently observed by ^1H NMR spectroscopy that the guests formed 1:3 complexes with the hosts such as CB[7] and β -CD. Their association constants with β -CD and CB[7] were found in order of 10^5 and $10^{9-10} \text{ dm}^3 \text{ mol}^{-1}$, respectively. Ternary aggregates with all the possible combinations of β -CD and CB[7] with the tris imidazolium and benzimidazolium salts were prepared; i.e., $G@(\beta\text{-CD}_2, \text{CB}[7])$ and $G@(\beta\text{-CD}, \text{CB}[7]_2)$. It was observed that β -CD units present in both the aggregates were easily replaced by CB[7]. Thermodynamic selectivity of the guests **4** and **6** towards β -CD/CB[7] was observed in the range of 2.1×10^{-6} and 1.9×10^{-4} , respectively. These results indicate that the tritopic guest **4** and **6** can be considered for using as supramolecular cross-linkers for β -CD grafted polymers. CB[7] can be used as an efficient modulator of the cross-linking process.

Bisbenzimidazolium guests **20** and **21** with stilbene spacer were prepared by Wittig reaction between corresponding aldehyde **9** and phosphonium salt **16** followed by quaternization with methyl iodide and 2-(bromomethyl) adamantane, respectively. Mixture of diastereomers of **20** was separated into *E* and *Z* isomers using trituration with MeOH:CHCl₃ (1.50 v/v) system while it was not possible to separate *E* and *Z* isomers **21**. *Z* isomer of **20** showed exceptional binding with β -CD. Separation of the NMR signals into two sets was observed for (*Z*)-**20** as stable inclusion complex with β -CD was formed in slow exchange mode. In addition, the signals of the isolated CH₂ groups from opposite ends of the guest displayed A₂ and AB spin coupling. This indicates that one part of the initially symmetrical guest became hindered in its free rotation likely by positioning in the narrower CD portal. (*Z*)-**20** showed binding with CB[7] as well. The association constants with β -CD, CB[7] and CB[8] were determined by means of isothermal titration calorimetry to be of 8.20×10^3 , 1.99×10^5 and $2.24 \times 10^7 \text{ dm}^3 \text{ mol}^{-1}$, respectively. The *Z* geometry of (*Z*)-**20** was confirmed by X-ray diffraction analyses. Mixture of diastereomers of **21** displayed slow conversion towards (*E*) under the influence of heat or UV irradiation. Interestingly, the thermal conversion in DMSO was inhibited by 2.5 equivalents of β -CD. The mechanism of β -CD influence remains unclear and will be examined in future.

Bisbenzimidazolium guests **22**, **23**, and **24** with diphenylacetylene centerpiece were prepared by quaternization of **19**. The main problem for all these guests was their poor solubility in aqueous environments. Thus, complete quantitative binding parameters for all these guests remain unavailable. However, formation of inclusion complex with one β -CD unit at central acetylene site was observed in D₂O using ^1H NMR. The formation of complex with CB[7] at terminal butyl sites was also indicated in [D₆]DMSO:D₂O mixture. In contrast, complexes of **22** with β -CD in [D₆]DMSO:D₂O mixture and **22** with CB[7] in D₂O were not detected. The guest **24** was essentially insoluble in D₂O. Nevertheless, when β -CD was added, small portion of the guest was taken into solution by formation an inclusion complex. Based on ^1H NMR spectrum, the this complex was hypothesized to be of 1:3 stoichiometry with one β -CD at the central site and two β -CD units at the terminal adamantane sites. The enhancing of the guest **24** solubility by addition of β -CD was used for preparation of ternary aggregate **24**@(CB[7]₂^T, β -CD^C) in water solution (C and T means central and terminal binding sites, respectively). Guest **23** also displayed some interesting properties. Despite low solubility in

water, inclusion complexes with CB[7] and β -CD in fast and slow exchange mode were clearly detected by means of ^1H NMR, respectively. The slow exchange mode of **23**@ β -CD in water environment was changed to fast by addition of solvent of lower polarity. Interestingly, this effect was observed in the case of DMSO and acetone whereas methanol had no significant effect on the exchange mode.

References

- 1) Xing, M.; Yanli, Z. *Chem. Rev.* **2015**, *115*, 7794–7838.
- 2) Li, M.; Zhou, C.; Quanzhu, Y.; Xiaogang, Y.; Chao, Z.; Liqiong, L. *Curr. Org. Chem.* **2014**, *18*, 1937–1947.
- 3) Wang, D.; Tong, G.; Dong, R.; Zhou, Y.; Shen, J.; Zhu, X. *Chem. Commun.* **2014**, *50*, 11994–12017.
- 4) Dong, R.; Zhou, Y.; Zhu, X. *Acc. Chem. Res.* **2014**, *47*, 2006–2016.
- 5) Hu, J.; Liu, S. *Acc. Chem. Res.* **2014**, *47*, 2084–2095.
- 6) Zhang, J.; Ma, P.X. *Adv. Drug. Deliv. Rev.* **2013**, *65*, 1215–1233
- 7) Kejik, Z.; Kaplanek, R.; Britza, T.; Kralova, J.; Martasek, P.; Kral, V. *Supramol. Chem.* **2012**, *24*, 106–116.
- 8) De Greef, T.F.A.; Smulders, M.M.J.; Wolffs, M.; Schenning, A.P.H.J.; Sijbesma, R.P.; Meijer, E.W. *Chem. Rev.* **2009**, *109*, 5687–5754.
- 9) Dong, S.; Bo, Z.; Wang, F.; Huang, F. *Acc. Chem. Res.* **2014**, *47*, 1982–1994.
- 10) Sicard, P.J.; Saniez, M.H. *Duchene, D.* (Ed). *Edition de Sante, Paris.* **1987**, 77–103.
- 11) Fromming, K.H.; Szejtli, J. *Cyclodextrins in Pharmacy*, Kluwer Academic Publishers, **1994**.
- 12) Hashimoto, H. *Edition de Sante, Paris*, **1991**, 97–156.
- 13) Vaution, C.; Hutin, M.; Glomot, F.; Duchene, D. *Edition de Sante, Paris*, **1987**, 299–350.
- 14) Riley, C.M.; Rytting, J.H.; Kral, M.A. *Takeru Higuchi, a Memorial Tribute, vol.3.* Equilibria and Thermodynamics, Allen Press, Lawrence, **1991**.
- 15) Loftsson, T.; Brewster, M.E.; *J. Pharm. Sci.* **1996**, *85*, 1017–1025.
- 16) Tomasik, P.; Schilling, C.H.; *Adv. Carbohydr. Chem. Biochem.* **1998**, *53*, 345–426.
- 17) Gabelica, V.; Galic, N.; De Pauw, E. *J. Am. Soc. Mass Spectrom.* **2002**, *13*, 946–953.
- 18) Loftsson, T.; Masson, M.; Brewster, M.E. *J. Pharm. Sci.* **2003**, *93*, 1091–1099.
- 19) Loftsson, T.; Hreinsdottir, D.; Masson, M. *Int. J. Pharm.* **2005a**, *302*, 18–28.
- 20) Faucci, M.T.; Melani, F.; Mura, P. *J. Pharm. Biomed. Anal.* **2000**, *23*, 25–31.
- 21) Loftsson, T.; Masson, M.; Brewster, M.E. *J. Pharm. Sci.* **2004b**, *93*, 1091–1099
- 22) Loftsson, T.; Ossurardottir, I. B.; Duan, M.; Zhao, N.; Thorsteinsson, T.; Masson, M. *J. Incl. Phenom. Macroc. Chem.* **2005c**, *52*, 109–117.
- 23) Duan, M.; Zhao, N.; Ossurardottir, I. B.; Thorsteinsson, T.; Loftsson, T. *Int. J. Pharm.* **2005**, *297*, 213–222.
- 24) Bonini, M.; Rossi, S.; Karlson, G.; Almgren, M.; Lo Nostro, P.; Baglioni, P. *Langmuir* **2006**, *22*, 1478–1484.
- 25) Stella, V.J.; Rajewski, R.A. *Pharm. Res.* **1997**, *14*, 556–567.
- 26) Loftsson, T.; Konradsdottir, T.K.; Masson, M. *Pharmazie* **2006**, *61*, 83–89.
- 27) Loftsson, T.; Brewster, M.E.; Masson, M. *Am. J. Drug Deliv.* **2004a**, *2*, 261–275.
- 28) Duchene, D.; Ponchel, G.; Bochet, A. *Eur. J. Pharm. Sci.* **2005**, *25S1*, S1–S2.
- 29) Trichard, L.; Duchene, D.; Bochet, A. *Cyclodextrins and Their Complexes: Chemistry, Analytical Methods, Applications* **2006**, 423–449.
- 30) Anderson, G.H.; Robbins, F. M.; Domingues, F.J.; Moores, R.G.; Long, C.L. *Toxicol. Appl. Pharmacol.* **1963**, *5*, 257–266.
- 31) Szejtli, J.; Sabestyen, G. *Starch/Stärke.* **1979**, *31*, 385–389.
- 32) Lipinski, C.A.; Lombardo, F.; Dominy, B.W.; Feeney, P.J. *Adv. Drug Deliv. Rev.* **2001**, *46*, 3–26.
- 33) Loftsson, T.; Jarho, P.; Masson, M.; Jarvinen, T. *Expert Opin. Drug Deliv.* **2005b**, *2*, 335–351.
- 34) Irie, T.; Uekama, K. *J. Pharm. Sci.* **1997**, *86*, 147–162.
- 35) Matsuda, H.; Arima, H. *Adv. Drug Deliv. Rev.* **1999**, *36*, 81–99.
- 36) Munro, I. C.; Newberne, P.M.; Young, R.R.; Bar, A. *Regul. Toxicol. Pharmacol.* **2004**, *39*, S3–S13.
- 37) Gould, S.; Scott, R.C. *Food Chem. Toxicol.* **2005**, *43*, 1451–1459.
- 38) Rajewski, R.A.; Traiger, G.; Bresnahan, J.; Jaberboansari, P.; Stella, V.J. *J. Pharm. Sci.* **1995**, *84*, 927–932.
- 39) Blender, M.L.; Komiyama, M. *Cyclodextrin Chemistry*: Springer-Verlag, Berlin, **1978**.
- 40) Harada, A.; Kamachi, M. *Macromolecules* **1990**, *23*, 2821–2823.
- 41) Harada, A.; Li, J.; Kamachi, M. *Macromolecules* **1993**, *26*, 5698–5703.
- 42) Li, J.; Harada, A.; Kamachi, M. *Polym. J.* **1994**, *26*, 1019–1026.
- 43) Hwang, M. J.; Bae, H.S.; Kim, S. J.; Jeong, B. *Macromolecules*, **2004**, *37*, 8820–8822.
- 44) Harada, A. *Coord. Chem. Rev.* **1996**, *148*, 115–133.
- 45) Harada, A.; Hashidzume, A.; Takashima, Y. *Adv. Polym. Sci.* **2006**, *201*, 1–43.
- 46) Jiao, D.; Scherman, A. *Green Chem.* **2012**, *14*, 2445–2449.
- 47) Mock, W.L.; Irra, T.A.; Wepsiec, J.P.; Manimaran, T.L. *J. Org. Chem.* **1983**, *48*, 3619–3620.
- 48) Schulze, B.; Schubert, U.S. *Chem. Soc. Rev.* **2014**, *43*, 2522–2571.

- 49) Moses, J.E.; Moorhouse, A.D. *Chem. Soc. Rev.* **2007**, 36, 1249.
- 50) Wang, Y.H.; Cong, H.; Zhao, F.F.; Xue, S.F.; Tao, Z.; Zhu, Q.J.; Wei, G. *Catal. Commun.* **2011**, 12, 1127–1130.
- 51) Cong, H.; Zhao, F.F.; Zhang, J.X.; Zeng, X.; Tao, Z.; Xue, S.F.; Zhu, Q.J. *Catal. Commun.* **2009**, 11, 167–170.
- 52) Reddy, K.R.K.K.; Cavallini, T.S.; Demats, D.J.F.; Silva, L.F. *New J. Chem.* **2014**, 38, 2262–2264.
- 53) Cong, H.; Yamato, T.; Tao, Z. *New J. Chem.* **2013**, 37, 3778–3783.
- 54) Basilio, N.; Garcia-Rio, L.; Moreira, J.A.; Pessego, M. *J. Org. Chem.* **2010**, 75, 848–855.
- 55) Klock, C.; Dslouza, R.N.; Nau, W.M. *Org. Lett.* **2009**, 11, 2595–2598.
- 56) Zhao, Y.; Liang, L.L.; Chen, K.; Ji, N.N.; Cheng, X.J.; Xiao, X.; Zhang, Y.Q.; Xue, S.F.; Zhu, Q.J.; Dong, N.; Tao, Z. *Dalton Trans.* **2014**, 43, 929–932.
- 57) Lei, W.H.; Jiang, G.Y.; Zhou, Q.X.; Hou, Y.J.; Zhang, B.W.; Cheng, X.X.; Wang, X.S. *Chem. Phys. Chem.* **2013**, 14, 1003–1008.
- 58) Hu, J.X.; Hu, Y.F.; Xiao, X.; Zhang, Y.Q.; Tao, Z.; Xue, S.F.; Liu, J.X.; Zhu, Q.J. *Eur. J. Inorg. Chem.* **2013**, 3632–3640.
- 59) Gao, Z.W.; Feng, X.; Mu, L.; Ni, X.L.; Liang, L.L.; Xue, S.F.; Tao, Z.; Zeng, X.; Chapman, B.E.; Kuchel, P.W.; Lindoy, L.F.; Wei, G. *Dalton Trans.* **2013**, 42, 2608–2615.
- 60) Hu, Y.F.; Chen, K.; Liu, J.X.; Lin, R.L.; Sun, W.Q.; Xue, S.F.; Zhu, Q.J.; Tao, S. *Polyhedron*, **2012**, 31, 632–637.
- 61) Chen, K.; Feng, X.; Liang, L.L.; Zhang, Y.Q.; Zhu, Q.J.; Xue, S.F.; Tao, S. *Cryst. Growth Des.* **2011**, 11, 5712–5722.
- 62) Zhang, X.X.; Krakowiak, K.E.; Xue, G.P.; Bradshaw, J.S.; Izzat, R.M. *Ind. Eng. Chem. Res.* **2000**, 39, 3516–3520.
- 63) Whang, D.; Heo, J.; Park, J.H.; Kim, K. *Angew. Chem. Int. Ed.* **1998**, 37, 78–80.
- 64) Hoffman, R.; Knoche, W.; Fenn, C.; Buschmann, H.J. *J. Chem. Soc. Faraday Trans.* **1994**, 90, 1507–1518.
- 65) De Lima, S.M.; Gomez, J.A.; Barros, V.P.; Vertuan, G.D.; Assis, M.D.; Graeff, C.F.D.; Demets, G.J.F. *Polyhedron*, **2010**, 29, 3008–3013.
- 66) Lu, X.Y.; Masson, E. *Org. Lett.* **2010**, 12, 2310–2313.
- 67) Koner, A.L.; Marquez, C.; Dickman, M.H.; Nau, W.M. *Angew. Chem. Int. Ed.* **2011**, 50, 545–548.
- 68) Dsouza, R.N.; Pischel, U.; Nau, W.M. *Chem. Rev.* **2011**, 111, 7941–7980.
- 69) Nau, W.M.; Mohanty, J. *Int. J. Photoenergy*, **2005**, 7, 133.
- 70) Parvari, G.; Reany, O.; Keinan, E. *Isr. J. Chem.* **2011**, 51, 646–663.
- 71) Koner, A.L.; Nau, W.M. *Supramol. Chem.* **2007**, 19, 55–66.
- 72) Buschmann, H.J.; Schollmeyer, E. *J. Incl. Phenom. Macrocycl. Chem.* **1997**, 29, 167–174.
- 73) Minami, T.; Esipenko, N.A.; Zhang, B.; Isaacs, L.; Anzenbacher, P. Jr. *Chem. Commun.* **2014**, 50, 61–63.
- 74) Minami, T.; Esipenko, N.A.; Zhang, B.; Isaacs, L.; Nishiyabu, R.; Kubo, Y.; Anzenbacher, P. Jr. *J. Am. Chem. Soc.* **2012**, 134, 20021–20024.
- 75) Lucas, D.; Minami, T.; Iannuzzi, G.; Cao, L.P.; Wittenberg, P.; Anzenbacher, P. Jr.; Isaacs, J. *J. Am. Chem. Soc.* **2011**, 133, 17966–17976.
- 76) Jon, S.Y.; Ko, Y.H.; Park, S.H.; Kim, H.J.; Kim, K. *Chem. Commun.* **2001**, 1938–1939.
- 77) Pattabiraman, M.; Natarajan, A.; Kaanumalle, L.S.; Ramamurthy, V. *Org. Lett.* **2005**, 7, 529–532.
- 78) M. Pattabiraman, Kaanumalle, L.S.; Natarajan, A.; Ramamurthy, V. *Langmuir*, **2006**, 22, 7605–7609.
- 79) Pattabiraman, M.; Natarajan, A.; Kaliappan, R.; Mague, J.T.; Ramamurthy, V. *Chem. Commun.* **2005**, 4542–4544.
- 80) Maddipatla, M.V.S.N.; Kannumalle, L.S.; Natarajan, A.; Pattabiraman, M.; Ramamurthy, V. *Langmuir*, **2007**, 23, 7545–7554.
- 81) Barooah, N.; Pemberton, B.C.; Sivaguru, J. *Org. Lett.* **2008**, 10, 3339–3342.
- 82) Barooah, N.; Pemberton, B.C.; Johnson, A.C.; Sivaguru, J. *Photochem. Photobiol. Sci.* **2008**, 7, 1473–1479.
- 83) Pemberton, B.C.; Barooah, N.; Srivastava, D.K.; Sivaguru, J. *Chem. Commun.* **2010**, 46, 225–227.
- 84) Pemberton, B.C.; Kumarasamy, E.; Jockusch, S.; Srivastava, D.K.; Sivaguru, J. *Can. J. Chem.* **2011**, 89, 310–316.
- 85) Lagona, J.; Mukhopadhyay, P.; Chakrabarti, S.; Isaacs, L. *Angew. Chem. Int. Ed.* **2005**, 44, 4844–4870.
- 86) Masson, E.; Ling, X.; Joseph, R.; Kyeremeh-Mensah, L.; Lu, X. *RSC Adv.* **2012**, 2, 1213–1247.
- 87) Lee, J.W.; Samal, S.; Selvapalam, N.; Kim, H.J.; Kim, K. *Acc. Chem. Res.* **2003**, 36, 621–630.
- 88) Saleh, N.; Konar, A.L.; Nau, W.M. *Angew. Chem. Int. Ed.* **2008**, 120, 5478–5481.
- 89) Isaacs, L. *Chem. Commun.* **2009**, 6, 619–629.
- 90) Olga, A.; Samsoneko, D.G.; Fedom, V.P. *Russ. Chem. Rev.* **2002**, 71, 741–760.

- 91) Whang, D.; Kim, K. *Chem. Commun.* **1997**, 24, 2361–2362.
- 92) Huang, W.H.; Liu, S.; Zavalij, P.Y.; Isaacs, L. *J. Am. Chem. Soc.* **2006**, 128, 14744–14745.
- 93) Huang, W.H.; Liu, S.; Zavalij, P.Y.; Isaacs, L. *J. Am. Chem. Soc.* **2008**, 130, 8446–8454.
- 94) Huang, W.H.; Zavalij, P.Y.; Isaacs, L. *Angew. Chem. Int. Ed.* **2007**, 119, 7569–7571.
- 95) Wagner, B.D.; Stojanovic, N.; Day, A.I.; Blanch, R.J. *J. Phys. Chem. B*, **2003**, 107, 10741–10746.
- 96) Hennig, A.; Bakirci, H.; Nau, W.M. *Nat. Methods*, **2007**, 4, 629–632.
- 97) Bailey, D.M.; Hennig, A.; Uzunova, V.D.; Nau, W.M. *Chem. Eur. J.* **2008**, 14, 6069–6077.
- 98) Yuan, L.; Wang, R.; Macartney, D.H. *Tetrahedron: Asymmetry*, **2007**, 18, 483–487.
- 99) Xiaoyong, L.; Issacs, L. *Org. Lett.* **2015**, 17, 4038–4041
- 100) Huang, W.-H.; Zavalij, P. Y.; Isaacs, L. *Angew. Chem. Int. Ed.* **2007**, 46, 7425–7427.
- 101) Dsugi, N.F.A.; Elbashir, A.A.; Suliman, F.E.O. *Spectrochim. Acta Mol. Biomol. Spectrosc.* **2015**, 151, 360–367.
- 102) Dsugi, N.F.A.; Elbashir, A.A. *Spectrochim. Acta Mol. Biomol. Spectrosc.* **2015**, 137, 804–809.
- 103) Neiryneck, P.; Schimer, J.; Jonkheijm, P.; Milroy, L.G.; Ciglar, P.; Brunsveld, L. *J. Mater. Chem. B* **2015**, 3, 539–545.
- 104) Aime, S.; Gianolio, E.; Uggeri, F.; Tagliapietra, S.; Barge, A.; Cravotto, G. *J. Inorg. Biochem.* **2006**, 100, 931–938.
- 105) Tang, B.; Jia, B.; Cui, G.; Ding, Y. *Anal. Chim. Acta.* **2004**, 516, 221–227.
- 106) Liu, F.; Liang, H.L.; Xu, K.H.; Tong, L.; Tang, B. *Talanta*, **2007**, 74, 140–145.
- 107) Chen, D.; Chen, Z.; Xu, K.; Tang, B. *J. Agric. Food Chem.* **2011**, 59, 4424–4428.
- 108) Sun, T.; Guo, Q.; Zhang, C.; Hao, J.; Xing, P.; Su, J.; Li, S.; Hao, A.; Liu, G. *Langmuir*, **2012**, 28, 8625–8636.
- 109) Holzinger, M.; Singh, M.; Cosnier, S. *Langmuir*, **2012**, 28, 12569–12574.
- 110) Siripornnoppakhun, W.; Niamnont, N.; Krumsri, A.; Tumcharern, G.; Vilaivan, T.; Rashatasakhon, P.; Thayumanavan, S.; Sukwattanasinit, M. *J. Phys. Chem. B*, **2012**, 116, 12268–12274.
- 111) Branna, P.; Rouchal, M.; Pruckova, Z.; Dastychova, L.; Lenobel, R.; Pospisil, T.; Malac, K.; Vicha, R. *Chem. Eur. J.* **2015**, 21, 11712–11718.
- 112) Szejtli, J. *Cyclodextrin Technology*; Davis, J.E.D. (series ed.) Kluwer Acad.; Dordrecht, **1988**.
- 113) Thompson, D.O.; *Critical Reviews in Drug Carrier Systems.* **1997**.
- 114) Muller, B.W.; Brauns, U. *J. Pharm. Sci.* **1986**, 75, 571–572.
- 115) Rao, C.T.; Pitha, J.; Lindberg, B.; Lindberg, J. *Carbohydr. Res.* **1992**, 223, 99–107.
- 116) Loscher, W.; Hoenack, D.; Richter, A.; Schulz, M.; Schuerer, M.; Duesing, R.; Brewster, M.E. *Epilepsia*, **1995**, 36, 255–261.
- 117) Arimori, K.; Iwaoku, R.; Nakano, M.; Uemura, Y.; Otagiri, M.; Uekama, K. *Yakugaku Zasshi*, **1983**, 103, 553–558.
- 118) Viernstein H.; Stumpf, C.; Spigel, P.; Reiter, S. *Arzneim-Forsch*, **1993**, 43, 818–821.
- 119) Stella, V.J.; Lee, H.K.; Thompson, D.O. *Int. J. Pharm.* **1995**, 120, 189–195.
- 120) Jarvinen, T.; Jarvinen, K.; Schwarting, N.; Stella, V.J. *J. Pharm. Sci.* **1995**, 120, 189–195.
- 121) Frijlink, H.W.; Franssen, E.J.F.; Eissens, A.C.; Oosting, R.; Lerk, C.F.; Meijer, D.K.F. *Phar. Res.* **1991**, 8, 380–384.
- 122) Panini, R.; Vandelli, M.A.; Forni, F.; Pradelli, J.M.; Salvioli, G. *Pharmacol. Res.* **1995**, 31, 205–209.
- 123) Studenberg, S.D.; Roy, A.K.; Woolley, J.L. *Pharm. Res.* **1996**, 13, 457.
- 124) Haeberlin, B.; Gengenbacher, T.; Meinzer, A.; Fricker, G. *Int. J. Pharm.* **1996**, 137, 103–110.
- 125) Uekama, K.; Horikawa, T.; Horiuchi, Y.; Hirayama, F. *J. Controlled Release*, **1993**, 25, 99–106.
- 126) Jensen, T.; Xhonneux, B.; Mesens, J.; Borgers, M. *Lens Eye Toxic. Res.* **1990**, 7, 459–468.
- 127) Rajewski, R.A.; Stella, V.J. *J. Pharm. Sci.* **1996**, 85, 1142–1169.
- 128) Jarvinen, K.; Jarvinen, T.; Thompson, D.O.; Stella, V.J. *Curr. Eye Res.* **1994**, 13, 897–905.
- 129) Reer, O.; Bock, T.K.; Muller, B.W. *J. Pharm. Sci.* **1994**, 83, 1345–1349.
- 130) Usayapant, A.; Karara, A.H.; Narurkar, M.M. *Pharm. Res.* **1991**, 8, 1495–1499.
- 131) Loftsson, T.; Fridriksdottir, S.; Thorisdottir, S.; Stefansson, E. *Int. J. Pharm.* **1994**, 104, 181–184.
- 132) Loftsson, T.; Fridriksdottir, S.; Stefansson, E.; Thorisdottir, S. *J. Pharm. Pharmacol.* **1994**, 46, 503–504.
- 133) Marttin, E.; Verhoef, J.C.; Romeijn, S.G.; Merkus, F.W.H. *Pharm. Res.* **1995**, 12, 1151–1157.
- 134) Qiao, W.; Wang, B.; Wang, Y.; Yang, L.; Zhang, Y.; Shao, P.J. *Nanomater.* **2010**, 2010, Article ID 796303, 9 pages.
- 135) Farokhzad, O.C.; Langer, R. *ACS Nano*, **2009**, 3, 16–20.
- 136) Hughes, G.A. *Nanomed. Nanotechnol. Biol. Med.* **2005**, 1, 22–30.
- 137) Ravoo, B.J. *Supramolecular Chemistry*, John Wiley and Sons, **2012**
- 138) Homma, T.; Harano, K.; Isobe, H.; Nakamura, E. *J. Am. Chem. Soc.* **2011**, 133, 6364–6370.
- 139) Voskuhl, J.; Stuart, M.C.A.; Ravoo, B.J. *Chem. Eur. J.* **2010**, 16, 2790–2796.

- 140) Vico, R.V.; Voskuhl, J.; Ravoo, B.J. *Langmuir*, **2010**, 27, 1391–1397.
- 141) Kauscher, U.; Ravoo, B.J. *Beilstein J. Org. Chem.* **2012**, 8, 1543–1551.
- 142) Tao, W.; Liu, Y.; Jiang, B.; Yu, S.; Huang, W.; Zhou, Y.; Yan, D. *J. Am. Chem. Soc.* **2011**, 134, 762–764.
- 143) Zhang, Q.; Re Ko, N.; Jung, K.O. *Chem. Commun.* **2012**, 48, 7542–7552.
- 144) Sun, L.; Liu, W.; Dong, C.M. *Chem. Commun.* **2011**, 47, 11282–11284.
- 145) Yhaya, F.; Lim, J.; Kim, Y.; Liang, M.; Gregory, A.M.; Stenzel, M.H. *Macromolecules*, **2011**, 44, 8433–8445.
- 146) Xiao, W.; Chen, W.H.; Zhang, J.; Li, C.; Zhuo, R.X.; Zhang, X.Z. *J. Phys. Chem. B.* **2011**, 115, 13796–13802.
- 147) Thiele, C.; Auerbach, D.; Jung, G.; Qiong, L.; Schneider, M.; Wenz, G. *Polym. Chem.* **2011**, 2, 209–215.
- 148) Moon, C.; Kwon, Y.M.; Lee, W.K.; Park, Y.J.; Yang, V.C. *J. Controlled Release*, **2007**, 124, 43–50.
- 149) Moon, C.; Kwon, Y.M.; Lee, W.K.; Park, Y.J.; Chang, L.C.; Yang, V.C. *J. Biomed. Mater. Res., Part A.* **2008**, 84A, 238–246.
- 150) Longgui, Z.; Ting, S.; Bin, H.; Zhongwei, G. *Nano-Micro. Lett.* **2014**, 6, 89–107.
- 151) Das, S.; Joseph, M.T.; Sarkar, D. *Langmuir*, **2013**, 29, 1818–1830.
- 152) Ang, C.Y.; Tan, S.Y.; Wang, X.; Zhang, Q.; Khan, M.; Bai, L.; Tamil Selvan, S.; Ma, X.; Zhu, L.; Nguyen, K.T.; Tan, N.S.; Zhao, Y. *J. Mater. Chem. B.* **2014**, 2, 1879–1890.
- 153) Zhang, J.; Ma, P.X. *Angew. Chem. Int. Ed.* **2009**, 48, 964–968.
- 154) Zhang, J.; Feng, K.; Cuddihy, M.; Kotov, N.A.; Ma, P.X. *Soft Matter*, **2010**, 6, 610–617.
- 155) Wang, H.; Wang, S.; Su, H.; Chen, K.J.; Armijo, A.L.; Lin, W.Y.; Wang, Y.; Sun, J.; Kamei, K.I.; Czernin, J.; Radu, C.G.; Tseng, H.R. *Angew. Chem. Int. Ed.* **2009**, 48, 4344–4348.
- 156) Chen, K.J.; Tang, L.; Garcia, M.A.; Wang, H.; Lu, H.; Lin, W.Y.; Hou, S.; Yin, Q.; Shen, C.K.F.; Cheng, J.; Tseng, H.R. *Biomaterials*, **2012**, 33, 1162–1169.
- 157) He, Q.; Shi, J. *J. Mater. Chem.* **2011**, 21, 5845–5855.
- 158) Li, Z.; Barnes, J.C.; Bosoy, A.; Stoddart, J.F.; Zink, J.I. *Chem. Soc. Rev.* **2012**, 41, 2590–2605.
- 159) Tang, F. Q.; Li, L.L.; Chen, D. *Adv. Mater.* **2012**, 24, 1504–1534.
- 160) Zhao, Y.L.; Li, Z.; Kabehie, S.; Botros, Y.Y.; Stoddart, J.F.; Zink, J.I. *J. Am. Chem. Soc.* **2010**, 132, 13016–13025.
- 161) Meng, X.; Xue, M.; Xia, T.; Zhao, Y.L.; Tamanoi, F.; Stoddart, J.F.; Zink, J.I.; Nel, A.E. *J. Am. Chem. Soc.* **2010**, 132, 12690–12697.
- 162) Ma, X.; Zhao, Y.; Ng, K.W.; Zhao, Y. *Chem. Eur. J.* **2013**, 19, 15593–15603.
- 163) Ma, X.; Ong, O.S.; Zhao, Y. *Biomater. Sci.* **2013**, 1, 912–917.
- 164) Ma, X.; The, C.; Zhang, Q.; Borah, P.; Choong, C.; Korzh, V.; Zhao, Y. *Antioxid. Redox Signaling*, **2014**, 21, 707.
- 165) Ma, X.; Nguyen, K.T.; Borah, P.; Ang, C.Y.; Zhao, Y. *Adv. Healthcare Mater.* **2012**, 1, 690–697.
- 166) Thomas, C.R.; Ferris, D.P.; Lee, J.H.; Choi, E.; Cho, M.H.; Kim, E.S.; Stoddart, J.F.; Shin, J.S.; Cheon, J. Zink, J.I. *J. Am. Chem. Soc.* **2010**, 132, 10623–10625.
- 167) Guardado-Alvarez, T.M.; Sudha Devi, L.; Russel, M.M.; Schwartz, B.J.; Zink, J.I. *J. Am. Chem. Soc.* **2013**, 135, 14000–14003.
- 168) Wang, C.; Li, Z.; Cao, D.; Zhao, Y.L.; Gaines, J.W.; Bozdemir, O.A.; Ambrogio, M.W.; Frasconi, M.; Botros, Y.Y.; Zink, J.I.; Stoddart, J.F. *Angew. Chem. Int. Ed.* **2012**, 51, 5460–5465.
- 169) Yan, H.; The, C.; Sreejith, S.; Zhu, L.; Kwok, A.; Fang, W.; Ma, X.; Nguyen, K.T.; Korzh, V.; Zhao, Y. *Angew. Chem. Int. Ed.* **2012**, 51, 8373–8377.
- 170) Luo, Z.; Ding, X.; Hu, Y.; Wu, S.; Xiang, Y.; Zeng, Y.; Zhang, B.; Yan, H.; Zhang, H.; Zhu, L.; Liu, J.; Li, J.; Cai, K.; Zao, Y. *ACS Nano*, **2013**, 7, 10271–10284.
- 171) Porta, F.; Lamers, G.E.M.; Morrhayim, J.; Chatzopoulou, A.; Schaff, M.; den Dulk, H.; Backendorf, C.; Zink, J.I.; Kros, A. *Adv. Healthcare Mater.* **2013**, 2, 281–286.
- 172) Mieszawska, A.J.; Kim, Y.; Gianella, A.; van Rooy, I.; Priem, B.; Labarre, M.P.; Ozcan, C.; Cormode, D.P.; Petrov, A.; Langer, R.; Rarokhzad, O.C.; Fayad, Z.A.; Mulder, W.J.M. *Bioconjugate Chem.* **2013**, 24, 1429–1434.
- 173) Luo, Z.; Cai, K.; Hu, Y.; Li, J.; Ding, X.; Zhang, B.; Xu, D.; Yang, W.; Liu, P. *Adv. Mater.* **2012**, 24, 431–435.
- 174) Moya-Ortega, M.D.; Alvarez-Lorenzo, C.; Concheiro, A.; Loftsson, T. *Int. J. Pharm.* **2012**, 428, 152–163.
- 175) Goncalves, M.; Figueira, P.; Maciel, D.; Rodrigues, J.; Shi, X.; Tomas, H.; Li, Y. *Macromol. Biosci.* **2014**, 14, 110–120.
- 176) Kiyonaka, S.; Sada, K.; Yoshimura, I.; Shinkai, S.; Kato, N.; Hamachi, I. *Nat. Mater.* **2004**, 3 (1), 58–64.

- 177) Lee, S.C.; Kwon, I.K.; Park, K. *Adv. Drug Delivery Rev.* **2013**, 65, 17–20.
- 178) Giraud, M.N.; Guex, A.G.; Tevaearai, H.T. *Cardiol. Res. Pract.* **2012**, 2012, Article ID 971614.
- 179) Harada, A.; Takashima, Y. *Supramolecular Polymer Chemistry*. Wiley-VCH Verlag GmbH & Co. KGaA, **2011**, 29–50.
- 180) Harada, A. *J. Polym. Sci., Part A: Polym. Chem.* **2006**, 44, 5113–5119.
- 181) Rodell, C.B.; Kaminski, A.L.; Burdick, J.A. *Biomacromolecules*, **2013**, 14, 4125–4134.
- 182) Wu, D.Q.; Wang, T.; Lu, B.; Xu, X.D.; Cheng, S.X.; Jiang, X.J.; Zhang, X.Z.; Zhuo, R.X. *Langmuir*, **2008**, 24, 10306–10312.
- 183) Koopmans, C.; Ritter, H. *Macromolecules*, **2008**, 41, 7418–7422.
- 184) Park, K.M.; Yang, J.A.; Jung, H.; Yeom, J.; Park, J.S.; Park, K.H.; Hoffman, A.S.; Hahn, S.K.; Kim, K. *ACS Nano*, **2012**, 6, 2960–2968.
- 185) Nielsen, A.L.; Madsen, F.; Larsen, K.L. *Drug Delivery* **2009**, 16, 92–101.
- 186) Salmaso, S.; Semenzato, A.; Bersani, S.; Matricardi, P.; Rossi, F.; Caliceti, P. *Int. J. Pharm.* **2007**, 345, 42–50.
- 187) Ma, D.; Zhang, L.M. *Biomolecules* **2011**, 12, 3124–3130.
- 188) Peng, K.; Tomatsu, I.; Kros, A. *Chem. Commun.* **2010**, 46, 4094–4096.
- 189) Davis, M.E.; Zuckerman, J.E.; Choi, C.H.J.; Seligson, D.; Tolcher, A.; Alabi, C.A.; Yen, Y.; Heidel, J.D.; Ribas, A. *Nature* **2010**, 464, 1067–1070.
- 190) Kulkarni, A.; Defrees, K.; Hyun, S.H.; Thompson, D.H. *J. Am. Chem. Soc.* **2012**, 134, 7596–7599.
- 191) Tamura, A.; Yui, N. *Biomaterials* **2013**, 34, 2480–2491.
- 192) Ooya, T.; Choi, H.S.; Yamashita, A.; Yui, N.; Sugaya, Y.; Kano, A.; Maruyama, A.; Akita, H.; Ito, R.; Kogure, K.; Harashima, H.J. *J. Am. Chem. Soc.* **2006**, 128, 3852–3853.
- 193) Yamashita, A.; Yui, N.; Ooya, T.; Kano, A.; Maruyama, A.; Akita, H.; Kogure, K.; Harashima, H. *Nat. Protoc.* **2007**, 1, 2861–2869.
- 194) Dong, R.; Zhou, L.; Wu, J.; Tu, C.; Su, Y.; Zhu, B.; Gu, H.; Yan, D.; Zhu, X. *Chem. Commun.* **2011**, 47, 5473–5475.
- 195) Zhang, J.; Sun, H.; Ma, P.X. *ACS Nano* **2014**, 4, 1049–1059.
- 196) Hu, Q.D.; Fan, H.; Ping, Y.; Liang, W.Q.; Tang, G.P.; Li, J. *Chem. Commun.* **2011**, 47, 5572–5574.
- 197) Liu, K.; Wang, H.; Chen, K.J.; Guo, F.; Lin, W.Y.; Chen, Y.C.; Phung, D.L.; Tseng, H.R.; Shen, C.K. *Nanotechnology* **2010**, 21, Article ID 445603 (8pp)
- 198) Xu, L.Q.; Zhang, B.; Wang, R.; Chen, Y.; Neoh, K.K.; Kang, E.T.; Fu, G.D. *Polym. Chem.* **2012**, 3, 2444–2450.
- 199) Wagner B.D.; Fitzpartick, S.J.; Gill, M.A.; MacRae, A.I.; Stojanovic, N.A. *Can. J. Chem.* **2001**, 79, 1101–1104.
- 200) Saleh, N.; Al-Rawashdeh, N.A.F. *J. Fluorosc.* **2006**, 16, 487–493.
- 201) Rankin, M.A.; Wagner, B.D. *Supramol. Chem.* **2004**, 16, 513–519.
- 202) Sinha, M.K.; Raeny, O.; Parvari, G.; Karmakar, A.; Keinan, E. *Chem. Eur. J.* **2010**, 16, 9056–9067.
- 203) Li, C.F.; Du, L.M.; Zhang, H.M. *Spectrochim. Acta Part A: Mol. Biomol. Spectrosc.* **2010a**, 75, 912–917.
- 204) Li, C.F.; Du, L.M.; Wu, W.Y.; Sheng, A.Z. *Talanta*, **2010b**, 80, 1939–1944.
- 205) Zhou, Y.Y.; Yang, J.; Liu, M.; Wang, S.F.; Lu, Q.A. *J. Luminesc.* **2010**, 130, 817–820.
- 206) Del Pozo, M.; Hernandez, L.; Quintana, C.A. *Talanta* **2010**, 81, 1542–1546.
- 207) Sueldo Occello, V.N.; Veglia, A.V. *Anal. Chim. Acta* **2011**, 689, 97–102.
- 208) Haung, Y.; Wang, J.; Xue, S.F.; Tao, Z.; Zhu, Q.J.; Tang, Q. *J. Incl. Phenom. Macrocycl. Chem.* **2012**, 72, 397–404.
- 209) Dong, N.; Cheng, L.N.; Wang, X.L.; Li, Q.; Dai, C.Y.; Tao, Z. *Talanta*, **2011**, 84, 684–689.
- 210) Li, Y.P.; Wu, W.H.; Du, L.M. *Chin. Chem. Lett.* **2009b**, 20, 322–325.
- 211) Wang, G.Q.; Guo, L.; Du, L. M.; Fu, Y.L. *Microchem. J.* **2013c**, 66, 701–709.
- 212) Wu, W.Y.; Yang, J.Y.; Du, L.M.; Wu, H.; Li, C.F. *Spectrochim. Acta Part A* **2011**, 79, 418–422.
- 213) Zhou, Y.; Yu, H.; Zhang, L.; Xu, H.; Wu, L.; Sun, J.; Lu, Q.; Wang, L. *Microchim. Acta* **2009**, 164, 63–68.
- 214) Li, C.; Li, J.; Jia, X. *Org. Biomol. Chem.* **2009a**, 7, 2699–2703.
- 215) Yao, F.; Liu, H.; Wang, G.; Du, L.; Yin, X.; Fu, Y. *J. Environ. Sci.* **2013**, 25, 1245–1251.
- 216) Lee, H.K.; Park, K.M.; Jeon, Y.J.; Kim, D.; Oh, D.H.; Kim, H.S.; Park, C.K.; Kim, K.J. *J. Am. Chem. Soc.* **2005**, 127, 5006–5007.
- 217) Park, K.M.; Lee, D.W.; Sarkar, B.; Jung, H.; Kim, J.; Ko, Y.H.; Lee, K.E.; Jeon, H.; Kim, K. *Small* **2010**, 6, 1430–1441.
- 218) Kim, D.; Kim, E.; Lee, J.; Hong, S.; Sung, W.; Lim, N.; Park, C.G.; Kim, K. *J. Am. Chem. Soc.* **2010**, **132**, 9908–9919.

- 219) Kim, E.; Kim, D.; Jung, H.; Lee, J.; Paul, S.; Selvapalam, A.; Yang, Y.; Lim, N.; Park, C.G.; Kim, K. *Angew. Chem. Int. Ed.* **2010**, 49, 4405–4408.
- 220) Chen, C.J.; Li, D.D.; Wang, H.B.; Zhao, J.; Ji, J. *Polym. Chem.* **2013**, 4, 242–245.
- 221) Wang, Y.X.; Guo, D.S.; Cao, Y.; Liu, Y. *RSC Adv.* **2013**, 3, 8058–8063.
- 222) Loh, X.J.; Tsai, M.H.; Barrio, J.d.; Appel, E.A.; Lee, T.C.; Scherman, O.A. *Polym. Chem.* **2012**, 3, 3180–3188
- 223) Croissant, J.; Zink, J.I. *J. Am. Chem. Soc.* **2012**, 134, 7628–7631.
- 224) Jung, H.; Park, K.M.; Yang, J.A.; Oh, E.J.; Lee, D.W.; Park, K.; Ryu, S.H.; Hahn, S.K.; Kim, K. *Biomaterials* **2011**, 32, 7687–7694.
- 225) Kim, C.; Agasti, S.S.; Zhu, Z.; Isaacs, L.; Rotello, V.M. *Nat. Chem.* **2010**, 2, 962–966.
- 226) Appel, E.A.; Loh, X.J.; Jones, S.T.; Biedermann, F.; Dreiss, C.A.; Schermann, O.A. *J. Am. Chem. Soc.* **2012**, 134, 11767–11773.
- 227) Lei, W.; Zhou, Q.; Jiang, G.; Hou, Y.; Zhang, B.; Cheng, X.; Wang, X. *Chem. Phys. Chem.* **2011**, 12, 2933–2940.
- 228) Jiao, D.; Geng, J.; Loh, X.J.; Das, D.; Lee, T.C.; Scherman, O.A. *Angew. Chem. Int. Ed.* **2012**, 51, 9633–9637.
- 229) Landa, S.; Macháček, V. *Collection Czech. Chem. Commun.* **1933**, 5, 1–5.
- 230) Prelog V, Seiwerth R. *Berichte* **1941**, 74, (10), 1644–1648.
- 231) Prelog V, Seiwerth R. *Berichte* **1941**, 74 (11), 1769–1772.
- 232) Schleyer, P. von R. *J. Am. Chem. Soc.* **1957**, 79(12), 3292–3292.
- 233) Davies W.L.; Grunert R.R.; Haff, R.F.; McGahan J.W.; Neumayer, E.M.; Paulshock, M.; Watts, J.C.; Wood, T.R.; Hermann, E.C.; Hoffmann, C.E. *Science* **1964**, 144, 862–863.
- 234) Eisch, J.J.; Fregene, P.O. *Eur. J. Org. Chem.* **2008**, 26, 4482–4492.
- 235) Shimizhu, K.; Kon, K.; Onodera, W.; Yamazaki, H.; Kondo, J.N. *ACS Catal.* **2013**, 3(1), 112–117.
- 236) Ortega, N.; Feher-Voelger, A.; Brovetto, M.; Padron, J.I.; Martin, V.S.; Martin, T. *Adv. Synth. Catal.* **2011**, 353, 6, 963–972.
- 237) Rohde, J.J.; Pliushchev, M.A.; Sorensen, B.K.; Wodka, D.; Shuai, Q.; Wang, J.; Fung, S.; Monzon, K.M.; Chiou, W.J.; Pan, L.; Deng, X.; Chovan, L.E.; Ramaiya, A.; Mullally, M.; Henry, R.F.; Stolarik, D.F.; Imade, H.M.; Marsh, K.C.; Beno, D.W.A.; Fey, T.A.; Droz, B.A.; Brune, M.E.; Camp, H.S.; Sham, H.L.; Frevert, E.U.; Jacobson, P.B.; Link, J.T. *J. Med. Chem.* **2007**, 50, 149–164.
- 238) Hrdina, R.; Metz, F.M.; Larrosa, M.; Berndt, J.P.; Zhygadlo, Y.; Becker, S.; Becker, J. *Eur. J. Org. Chem.* **2015**, 6231–6236.
- 239) Hashmi, A.; Salathe R.; Frey W. *Chem. Eur. J.* **2006**, 12, 6991–6996.
- 240) Bochmann, M.; Wilkinson, G.; Young, B. *J. Chem. Soc. Dalton Transactions: Inorganic Chemistry (1972-1999)*, **1980**, 1879–1887.
- 241) Cernochova, Y.; Branna, P.; Rouchal, M.; Kulhanek, P.; Kuritka, I.; Vicha, R. *Chem. Eur. J.* **2012**, 18, 13633–13637.
- 242) Amati, A.; Dousaldo, G.; Zhao, L.; Bravo, A.; Fontana, F.; Minisci, F.; Bjorsvik, H. *Org. Proc. Res. Dev.* **1998**, 2 (4), 261–269.
- 243) Sundberg, R.; Dahlhausen, D.; Manikumar, G.; Mavunkel, B.; Biswas, A.; Srinivasan, V.; King, F.; Waid, P. *J. Heterocyclic Chem.* **1988**, 25 (1), 129–137.
- 244) Munoz, J.; Alcazer, J.; Hoz, A.; Diaz-Ortiz, A. *Tetrahedron Lett.* **2011**, 52 (46), 6058–6060.
- 245) Furstner, A.; Weidmann, H. *Synthesis* **1987**, 12, 1071–1075.
- 246) Guthrie, J.; Pike D.; Lee, Y. *Can. J. Chem.* **1992**, 70, 1671–1683.
- 247) Chu, D.; Wang, B. *US2009/197863 A1*, **2009**.
- 248) Osyanin, V.; Purygin, P.; Belousova, Z. *Russ. J. Gen. Chem.* **2005**, 75 (1), 123–129.
- 249) Hao, Y.; Yoo, W.; Myumara, H.; Kobayashi, S. *J. Am. Chem. Soc.* **2012**, 134 (34), 13970–13973.
- 250) Bay, E.; Bak, D.; Timony, P.; Leone-Bay, A. *J. Org. Chem.* **1990**, 55 (10), 3415–3417.
- 251) Coulombel, L.; Weiwer, M.; Dunach, E. *Eur. J. Org. Chem.* **2009**, 33, 5788–5795.
- 252) Bellucci, G.; Chiappe, C.; Marioni, F. *J. Am. Chem. Soc.* **1987**, 109 (2), 515–522.
- 253) Davis, M.; Groshens, T. *Org. Prep. Proc. Int.* **2011**, 43 (3), 314–318.
- 254) Park J.; Wang, Z.U.; Sun, L.B.; Chen, Y.P.; Zhou, H.C. *J. Am. Chem. Soc.* **2012**, 134 (49), pp 20110–20116.
- 255) Boomgaarden, W.; Vogtel, F.; Nieger, M.; Hupfer, H. *Chem. Eur. J.* **1999**, 1, 345–355.
- 256) Mazik, M.; Koenig, A. *J. Org. Chem.* **2006**, 71 (20), 7854–7857.
- 257) Tullberg, E.; Frejd, T. *Synth. Commun.* **2007**, 37 (2), 237–245.
- 258) Dohi, T.; Yamaoka, N.; Itani, I.; Kita, Y. *Aust. J. Chem.* **2011**, 65 (5), 529–535.
- 259) Bedford, R.; Mitchell, C.J.; Webster, R.L. *Chem. Commun.* **2010**, 46, 3095–3097
- 260) Herr, R.R.; Enkoji, T.; Dailey, J.P. *J. Am. Chem. Soc.* **1957**, 79 (15), pp 4229–4232.
- 261) Petrovski, Z.; Romao, C.C.; Afonso, C.A.M. *Synth. Commun.* **2008**, 38 (16), 2761–2767.

- 262) Arslants, E.; Smith-Jones, P.; Ritter, G.; Schmidt, R. *Eur. J. Org. Chem.* **2004**, 19, 3979-3984.
- 263) Rekharsky, M.V.; Mori, T.; Yang, C.; Ko, Y.H.; Selvapalam, N.; Kim, H.; Sobransingh, D.; Kaifer, A.E.; Liu, S.; Isaacs, L.; Chen, W.; Moghabaddam, S.; Gilson, M.K.; Kim, K.; Inoue, Y. *Proc. Natl. Acad. Sci.* **2007**, 104, 20737-20742.
- 264) Feast, W.J.; Lovenich, P.; Puschmann, H.; Taliani, C. *Chem. Commun.* **2001**, 505-506.
- 265) Soomro, S.A.; Benmouna, R.; Berger, R.; Meier, H. *Eur. J. Org. Chem.* **2005**, 16, 3586-3593.
- 266) Rosa, J.C.; Galanakis, D.; Ganellin, C.R.; Dunn, P.M. *J. Med. Chem.*, **1996**, 39 (21), pp 4247-4254.
- 267) Houk, K.N.; Menzer, S.; Newton, S.P.; Raymo, F.M.; Stoddart, J.F.; Williams, D.J. *J. Am. Chem. Soc.*, **1999**, 121 (7), pp 1479-1487.
- 268) Yu, C.; Zhao, B.; Zhao, Y.; Lin, J. *Org. Prep. Proc. Int.* **2010**, 42 (2), 183-185.
- 269) Spiniello, M., White, J.M. *Org. Biomol. Chem.* **2003**, 1, 3094-3101.
- 270) Kitagawa, T.; Idomoto, Y.; Matsubara, H.; Hobara, D.; Kakiuchi, T.; Okazaki, T.; Komatsu, K. *J. Org. Chem.* **2006**, 71 (4), 1362-1369.
- 271) Belser, T.; Stohr, M.; Pfaltz, A. *J. Am. Chem. Soc.* **2005**, 127 (24), pp 8720-8731.

Curriculum Vitae

Personal Details

Name: Shantanu Ganesh Kulkarni
Date of Birth: 31/03/1986
Place of Birth: Kopargaon, India.

Educational Details

2003-2006: B.Sc. (Chemistry) from University of Pune, India.
2006-2008: M.Sc. (Organic Chemistry) from University of Pune, India.
2012 to till date: Ph.D. Tomas Bata University in Zlin, Czech Republic.

Professional Details

- 1) Junior Research Associate- Jubilant Biosys Ltd. Bangalore, India in Medicinal Chemistry department from April 2009 to May 2011.
- 2) Research Associate- Syngene International Ltd. Bangalore, India in Medicinal Chemistry department from June 2011 to August 2012.
- 3) Junior Research Scientist- Syngenta Biosciences Pvt. Ltd., Goa, India in Process Chemistry department from September 2012 to November 2012.

Publications

- 1) M. J. Pawar, A. S. Burungale, S. G. Kulkarni, B. K. Karale: Synthesis, characterization and antimicrobial activity of some pyridine containing pyrazolylchromanones and pyrazolylpyrazolines *Indian Journal of Heterocyclic Chemistry* **2011**, *20*, 225–228.
- 2) S. G. Kulkarni, Z. Prucková, M. Rouchal, L. Dastychová, R. Vícha: Adamantylated tris-imidazolium-based tritopic guests and their binding properties towards cucurbit[7]uril and β -cyclodextrin *Journal of Inclusion Phenomena and Macrocyclic Chemistry* **2016**, *84*, 11–20.
- 3) S. Kulkarni, Z. Prucková, L. Dastychová, M. Rouchal, P. Kulhánek, R. Vícha: Bis-benzimidazolium guests with (Z)-stilbene centerpiece: ^1H NMR evidence for a hindered free rotation of a half of the guest by inclusion complex formation. *manuscript in progress*, **2016**.
- 4) S. Kulkarni, Z. Prucková, L. Dastychová, M. Rouchal, R. Vícha: Bisimidazolium-based guests with diphenylacetylene centerpiece. *manuscript in progress*, **2016**.

Conference

16th Austrian Chemical Days – Osterreichische Chemitage 2015 in Innsbruck, Austria: Poster entitled “Binding properties of novel adamantane based homotritopic guests”: Shantanu Ganesh Kulkarni, Zdenka Pruckova, Michal Rouchal, Lenka Dastychova, Robert Vicha.